CHALMERS
UNIVERSITY OF TECHNOLOGY

On Settlements in Urban Areas with Soft Clay

- As a result of leakage to deep excavations via an underlying permeable layer

Master's thesis in Infrastructure and Environmental Engineering

ALFRED KINDBERG

DEPARTMENT OF ARCHITECTURE AND CIVIL ENGINEERING
DIVISION OF GEOLOGY AND GEOTECHNICS

CHALMERS UNIVERSITY OF TECHNOLOGY
Gothenburg, Sweden 2021
www.chalmers.se

MASTER'S THESIS ACEX30

On Settlements in Urban Areas with Soft Clay

- As a result of leakage to deep excavations via an underlying permeable layer

Master's Thesis in the Master's Programme Infrastructure and Environmental Engineering

ALFRED KINDBERG

Department of Architecture and Civil Engineering

Division of Geology and Geotechnics

CHALMERS UNIVERSITY OF TECHNOLOGY

Göteborg, Sweden 2021

On Settlements in Urban Areas with Soft Clay
- As a result of leakage to deep excavations via an underlying permeable layer

Master's Thesis in the Master's Programme Infrastructure and environmental engineering

ALFRED KINDBERG

Examensarbete ACEX30
Institutionen för arkitektur och samhällsbyggnadsteknik
Chalmers tekniska högskola, 2021

Department of Architecture and Civil Engineering
Division of Geology and Geotechnics
Chalmers University of Technology
SE-412 96 Göteborg
Sweden
Telephone: + 46 (0)31-772 1000

Department of Architecture and Civil Engineering
Göteborg, Sweden, 2021

On Settlements in Urban Areas with Soft Clay
- As a result of leakage to deep excavations via an underlying permeable layer

Master's thesis in the Master's Programme Infrastructure and environmental engineering

ALFRED KINDBERG

Department of Architecture and Civil Engineering
Division of Geology and Geotechnics
Chalmers University of Technology

Abstract

The need of infrastructure, such as tunnels, increases as cities grow and densify. When tunnels are constructed in soil, open cut excavations are often used. During the time when the excavation is open, there will be a hydraulic head difference between the inside and outside of the excavation. Water can then flow into the excavation which in turn results in reduced pore pressures and ground settlements on the outside. The excavation analysed in this project is a part of the West link, a train tunnel that is being built to shorten travel times throughout the Gothenburg region. The soil in the area around the excavation consists of a thick layer of low permeable clay, underlain by a few metres of friction material followed by bedrock. Most of the inflow is expected to occur via the friction layer. The pore pressure reduction will thus initially take place in the friction material and the clay is over time affected by consolidation.

The area which is affected by an eventual pore pressure reduction is potentially very large and it is out of the scope of this study to determine the size of the area. Additionally, it is basically impossible to create a completely trustworthy groundwater model. Instead, the relation between pore pressure reduction, time, and settlement is investigated to give an indication of when problems start to occur. By continuously measuring the pore pressures in the friction layer in the area during the construction time, it is possible to detect any deviations. Hopefully then can prevention measures be taken before significant settlements occur.

In this thesis, a model representative for the site was created in the numerical software Plaxis 2D to study the relation between pore pressure reduction, time, and settlement. The soil characteristics was evaluated from various soil tests which previously had been performed on behalf of Trafikverket. Two different constitutive models were used in Plaxis: Soft Soil and Soft Soil Creep. The latter was proven to represent the expected behaviour of the clay during pore pressure reductions much better than the Soft Soil model. The most significant results in this project is from the Soft Soil Creep model and it shows that the settlements increase exponentially with increasing pore pressure reductions. It takes for example 21 days until the settlements have reached 50 mm after a pore pressure of 60 kPa. The corresponding number for a pore pressure reduction of 10 kPa is 1100 days. There are several uncertainties regarding the results. The results should therefore not be interpreted as facts, but rather give a hint of when settlement issues may arise. The damage to buildings due to settlements can become large. It is therefore important to seal the excavation as good as possible and to prepare solution measures if leakage after all occurs.

Key words: Deep excavations, consolidation, creep, settlements, soft clay, building damage.

Sättningar i urbana områden med lös lera

- På grund av inläckage till djupa schakt via ett underliggande permeabelt lager

Examensarbete inom masterprogrammet infrastruktur och miljöteknik

ALFRED KINDBERG

Institutionen för Arkitektur och samhällsbyggnadsteknik
Avdelningen för Geologi och geoteknik
Chalmers tekniska högskola

Sammanfattning

Behovet av ny infrastruktur, såsom tunnlar, ökar i takt med att städer växer och förtätas. När tunnlar byggs i jord används ofta öppna schakt. Under byggtiden uppstår då en skillnad i vattentryck mellan insidan och utsidan av schaktet. På grund av tryckskillnaden kan vatten flöda in till schaktet vilket i sin tur leder till minskade portryck och därmed sättningar på utsidan. Schaktet som analyseras i detta projekt är en del av Västlänken, en tågtunnel som byggs för att förkorta restiderna i hela Göteborgsregionen. Jorden i området runt schaktet består av ett mäktigt lager lågpermeabel lera som följs av ett tunnare lager friktionsmaterial. I princip allt vatteninflöde förväntas ske via friktionslagret. Portryckssänkningen sker således initialt i friktionslagret och med tiden påverkas leran av konsolidering.

Området som omfattas av en eventuell portryckssänkning är potentiellt mycket stort och det är utanför projektets omfattning att analysera vilket område som påverkas. Dessutom är det i princip omöjligt att skapa en grundvattenmodell som går att lita på fullständigt. Istället så studeras relationen mellan portryckssänkning, tid och sättning för att skapa en bild av när problem kan uppstå. Genom att kontinuerligt mäta portrycken i friktionslagret i området under byggskedet kan eventuella avvikelser identifieras och förhoppningsvis hinner åtgärder vidtas innan några nämnvärda sättningar hinner ske.

I detta projekt skapades en modell över områdets jordlager i den numeriska mjukvaran Plaxis 2D för att studera relationen mellan portryckssänkning, tid och sättning. Jordens egenskaper bestämdes med hjälp av olika typer av undersökningar som tidigare utförts på uppdrag av Trafikverket. Två materialmodeller användes i Plaxis: Soft Soil och Soft Soil Creep. Den sistnämnda visade sig representera lerans förväntade beteende under en portryckssänkning betydligt bättre jämför med Soft Soil modellen. De mest signifikanta resultaten i detta projekt är från Soft Soil Creep modellen och visar att sättningarna ökar exponentiellt vid ökande portryckssänkningar i friktionslagret. Exempelvis så tar det 21 dagar innan marksättningen når 50 mm vid en sänkning med 60 kPa medan motsvarande siffra för en sänkning med 10 kPa är 1100 dagar. Det finns vissa osäkerheter angående resultaten och de bör därmed inte tolkas som exakta fakta, utan snarare ge en överblick om när problem kan uppstå. Byggnadsskador på grund av sättningar kan bli stora. Det är därför både viktigt att täta schaktet så bra som möjligt för att förhindra läckage samt att ha förberett åtgärder om vatten trots allt läcker in.

Nyckelord: Djupa schakt, konsolidering, krypning, sättningar, lös lera, byggnadsskador.

Preface

This Master's thesis was carried out at Chalmers University of Technology at the Division of Geology and Geotechnics during the spring semester of 2021.

I would most of all like to express my gratitude towards my examiner Mats Karlsson for all the valuable support and expertise throughout the entire process. I would also like to thank my supervisors Ayman Abed and Pierre Wikby for additional inputs and advice.

Alfred Kindberg
Göteborg, June 2021

Table of Contents

List of Notations VI
1 Introduction 1
1.1 Aim and objectives 1
1.2 Limitations 1
1.3 Method 2
2 Area Description 3
3 Theoretical Background 5
3.1 Design of a deep excavation and related problems 5
3.1.1 Construction of a tunnel by the cut and cover method 5
3.1.2 Causes of water inflow to a deep excavation 5
3.1.3 Investigation of the relation between pore pressure reductions and settlements 6
3.1.4 Other sources of settlements caused by deep excavations 7
3.2 Soil behaviour due to water inflow to an excavation 8
3.2.1 Consolidation 8
3.2.2 Creep 11
3.3 Building damage due to settlements 12
3.3.1 Building foundations 12
3.3.2 Problems related to settlements caused by reduced pore pressures 13
3.3.3 Possible solutions to settlement issues 16
3.4 Plaxis 18
3.4.1 Constitutive models 18
3.4.1.1 Soft Soil model 18
3.4.1.2 Soft Soil Creep model 20
3.4.2 Parameters and evaluation 21
3.4.2.1 Modified swelling index, κ^* and modified compression index, λ^* 21
3.4.2.2 Modified creep index, μ^* 23
3.4.2.3 Overconsolidation, OCR or POP 23
3.4.2.4 Friction angle, φ and effective cohesion, c'ref 23
3.4.2.5 Coefficient of earth pressure at rest for normally consolidated state, K_0^{NC} 23
3.4.2.6 Permeability, k_x and k_y 23
3.4.2.7 Poisson's ratio for unloading-reloading, ν_{ur} 23
3.4.2.8 Dilatancy angle, ψ 24
3.4.3 Piles in Plaxis 24
4 Method 25

4.1 Site characterization and simplifications 25
4.2 Plaxis calculations and settings 28
4.2.1 Recovery after a pore pressure reduction 29
4.2.2 Analysis of piled buildings 29
4.3 Sensitivity analysis 30
5 Results and Discussion 32
5.1 Main calculations 32
5.2 Recovery after a pore pressure reduction 36
5.3 Analysis of piled buildings 37
5.4 Sensitivity analysis of input parameters 39
5.4.1 Sensitivity to changes of λ* in clay layer 3 and 4 39
5.4.2 Sensitivity to changes of κ* 41
5.4.3 Sensitivity to changes of the POP 42
5.4.4 Sensitivity to changes of permeability in clay layer 1-4 44
5.4.5 Sensitivity to changes of permeability in clay layer 4 46
5.4.6 Sensitivity to changes of c'ref and φ 47
5.4.7 Summary of the sensitivity analysis 48
5.5 Final discussion 48
5.6 Sources of error and drawbacks of the model 49
6 Conclusions 51
6.1 Recommendations for further research 51
7 References 53
8 Appendix 55
Appendix A: Groundwater and soil properties 55
Appendix B: Results 64

List of Notations

Roman letters

c'ref	Effective cohesion
C_c	Compression index
c_k	Change of permeability
C_s	Swelling index
c_u	Undrained shear strength
C_v	Coefficient of consolidation
C_α	Creep index
e	Void ratio
K	Bulk modulus
k	Permeability
K_0^{NC}	Coefficient of earth pressure at rest for normally consolidated state
M	Oedometer modulus
M*	The slope of the line which the top of the ellipse is based on in the Soft Soil and Soft Soil Creep model
M_0	Elastic oedometer modulus
m_v	Coefficient of volume
p'	Mean effective stress
$\dot{p'}$	Mean effective stress increase
p'_{p0}	Initial preconsolidation pressure
p_{eq}'	Current mean effective stress
p_p'	Isotropic preconsolidation pressure
q	Deviatoric stress
T_v	Time factor
u	Pore water pressure
U_v	Degree of consolidation

Greek letters

γ_w	Unit weight of water
μ*	Modified creep index
$\dot{\varepsilon}_v$	Volumetric strain rate
$\dot{\varepsilon}_v^e$	Elastic strains
$\dot{\varepsilon}_v^p$	Plastic strains
κ*	modified swelling index
λ*	modified compression index
ν_{ur}	Poisson's ratio for unloading-reloading
σ	Total stress
σ'	Effective stress
σ'_0	Effective in-situ vertical stress
σ'_c	Apparent preconsolidation pressure
σ'_v	Effective vertical stress

τ	Reference time
φ	Friction angle
ψ	Dilatancy angle

Abbreviations

CAUC	Anisotropically consolidated undrained compression
CPT	Cone penetration test
CRS	Constant rate of strain
$L_{spacing}$	Spacing out-of-plane
T_{skin}	Skin resistance
OCR	Overconsolidation ratio
POP	Pre-overburden pressure
SS	Soft Soil
SSC	Soft Soil Creep

1 Introduction

Deep excavations are a crucial part of modern construction which are used for example when constructing tunnels. When performing deep excavations, it is necessary to lower the groundwater inside the excavation to create workable conditions. The groundwater lowering may cause water inflow to the excavation which in turn may result in pore pressure reductions and settlements outside of the excavation. The effects of the water inflow may be detectable several hundreds of metres away (Cashman & Preene, 2013). Settlements are especially problematic in urban areas because of the large number of structures that could be damaged.

The West link is a train tunnel below Gothenburg scheduled to be completed in 2026 (Trafikverket, 2018). It will be built both in bedrock and in clay. The parts in clay will be constructed using the method of open cut excavations (Trafikverket 2020). One of these excavations will be analysed in this thesis and it is located inside the amusement park Liseberg. The geology in the area makes the topic extra interesting. On top of the bedrock there is a layer of friction material which is followed by a thick layer of soft clay. The depth of the tunnel requires the retaining walls to be installed all the way down to the bedrock. Since the bedrock is overlain by friction material with relatively high permeability, substantial amounts of water could enter the excavation via gaps between the bedrock and retaining wall. The initial pore pressure reduction will therefore most likely occur in the friction layer. The pore pressures in the clay will then strive to equalise and slowly reduce, which causes settlements in the clay because the effective stress increases.

1.1 Aim and objectives

The aim of this project is to investigate the possible effects on the nearby area caused by pore pressure reductions due to the deep excavation in Liseberg. By analysing a real case, it is possible to highlight the challenges and draw conclusions valid for other deep excavations constructed in areas with similar geology.

To accomplish the aim, the objectives of this thesis are as follows:

- Study the mechanisms of settlements due to inflow to deep excavations and also evaluate possible prevention measures to building damage caused by the settlements.
- Create a representative soil profile with appropriate parameters for the Liseberg site.
- Investigate the relationship between pore pressure reduction, time and settlements close to the Liseberg excavation with the numerical software Plaxis 2D.
- Perform a sensitivity analysis to determine which soil parameters are the most important and how they affect the results.

1.2 Limitations

To model a real case is a complex and time-consuming task. The following limitations have therefore been set.

- The calculations in this thesis will only study settlements due to changes in pore pressures because of leakage into the excavation. Other possible causes of settlement, such as wall deflection and internal erosion will just be mentioned briefly. Construction

related topics, for instance stability, hydraulic uplift, forces on construction elements and wall types will not be examined.

- The analysis will be performed for one specific case. The results will therefore not be representable for other excavations even though the theory and the work process more or less could be same depending on the geology.
- Evaluating the area influenced by the pore pressure reduction is beyond the scope and timeframe of this project. Instead, the critical pore pressure reductions considering settlements will be determined. By knowing the critical values, it is possible to have control over the settlements by monitoring the pore pressures in the area around the excavation.
- The model in Plaxis will be simplified from the real case, for example, no buildings will be included in the calculations. Further, the model of the site is based on soil tests performed at a limited number of locations relatively close to the planned excavation. The area possibly affected by the pore pressure reduction is significantly larger and the soil characteristics in parts of the area will therefore differ from the model.
- Not the most advanced constitutive models will be used in Plaxis. Some of the more advanced models would likely give more accurate results but would simultaneously require more effort for evaluating data and understanding the model.

1.3 Method

The initial stage of the project was to briefly investigate the area around the Liseberg excavation to get an overview of the geology and the challenges related to construction of the West link. The sources of information for this primarily were public documents related to the West link. Some of the main findings are presented in Chapter 2 while other subjects are assessed in Chapter 3. When the main subjects had been identified, a more profound literature review was performed by studying various sources, such as books and scientific reports. This literature review can be found in Chapter 3. It covers the design of deep excavations, soil behaviour due to water inflow to excavations, building damage due to settlements and theory regarding Plaxis. The evaluation of soil parameters and the calculation steps in Plaxis are explained in Chapter 4. The main data sources for this were various types of soil test data received from Trafikverket. The results of the Plaxis calculations and discussion about the results are presented in Chapter 5. Finally, conclusions and recommendations for further research can be found in Chapter 6.

2 Area Description

This chapter will provide some background information about the area which this thesis is based on to get a better understanding of why the topics in the method chapter are important. A more detailed description of the soil characteristics and how the values are retrieved will be given in Chapter 4. Simplifications and modifications in the model compared to the real scenario will also be discussed later.

As mentioned in the introduction, the excavation in focus in this thesis is a part of the West link project in Gothenburg. The West link is a train tunnel below the city, planned to be completed in 2026 (Trafikverket, 2018). It is built to provide faster commuting with less need for connections throughout the region. Most of the tunnel will be constructed in bedrock, but some parts will be constructed in clay with open cut excavations (Trafikverket 2020). The analysed excavation is going to be around 25 m deep, 105 m long and 20 m wide. The excavation will be located inside the amusement park Liseberg, close to the station Korsvägen as the red area in Figure 2.1 shows. A few of the nearby buildings will partially or completely be demolished while some issues are solved by reinforcing the foundations (Trafikverket, 2016a).

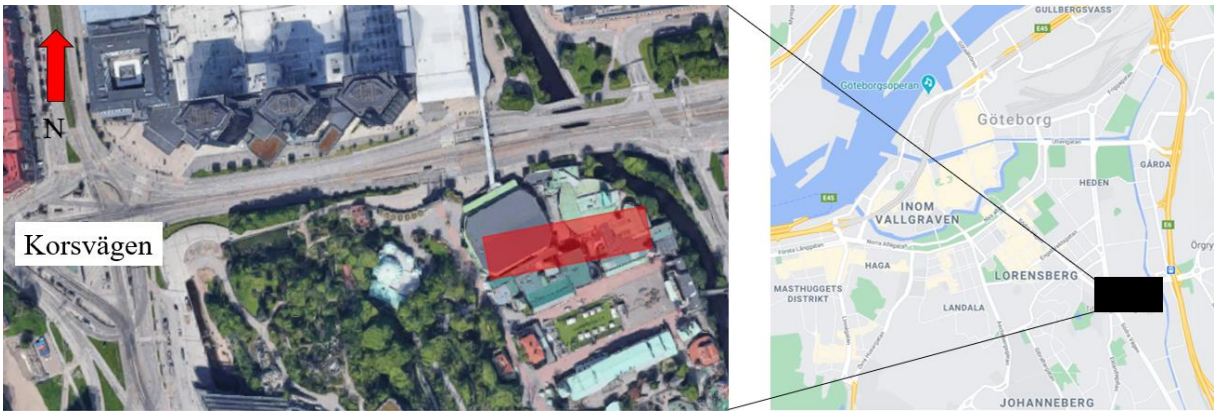

Figure 2.1: Map of where in Gothenburg the excavation will be constructed (Google, 2021).

Just like many other parts of Gothenburg, the level of the bedrock varies a lot in the area. To the west of the excavation there is a hill and the West link tunnel will continue through the bedrock. In the east direction there is clay, but it is another stage of the construction. The soil depth is constantly decreasing from north to south. 250 m to the north of the excavation it is almost 50 m to the bedrock, at the excavation it is just under 30 m of soil and 250 m to the south there is only about 5 m to the bedrock. The stratigraphy is quite typical for Gothenburg with filling material, followed by clay, friction material and bedrock.

The first buildings in the area were raised in the 18th century (Antiquum, 2014). Since then, the area has been heavily exploited with many structures constructed and demolished over the years. Most of the oldest buildings are now gone, but a few remain. Especially these, but also other old buildings are considered to have a high historic and architectural value and should not be damaged. Additionally, in the area there are other sensitive historical values in the shape of statues, green areas and so on. Due to the history, the soil is very disturbed from its natural conditions. Some soil characteristics, such as the thickness of the fill and the overconsolidation ratio may therefore differ considerably when moving short distances. There are furthermore

ongoing settlements at a rate of around 5 mm/year and most of this is due to creep effects (Sundkvist & Wallroth, 2016).

At the location of the excavation, the filling material is on average 2 m thick, the clay is approximately 21 m thick and the friction layer is around 6 m thick. The characteristics of the clay are highly important in the settlement predictions. Most of the clay in the studied area is very soft and homogeneous without any clear layers of other materials. At the depth of around 19 m the clay becomes siltier, with higher unit weight and lower water content as a result. The clay generally is lightly overconsolidated, with the lowest OCR in the middle of the clay layer. The sensitivity is moderate to high, with higher sensitivity at larger depths. The filling material in the area usually consists of different types of soils mixed with old paving stones and remains of old buildings (Högsta & Sanell, 2016). The friction layer mostly contains moraine, but occasionally also pure sand (Sundkvist & Wallroth, 2016). The bedrock consists of tonalite gneiss. Since the excavation is constructed in a valley, the top layer of the bedrock is expected to have a rather high conductivity due to the number of cracks.

The clay has a very low permeability, whereas it is much higher for the fill and the friction material. Because of this, the filling material and the friction layer is referred to as the upper and lower aquifer, respectively. The pore pressures in the upper aquifer are always hydrostatic and the groundwater level is mainly influenced by the weather (Berntson, 1983). Because of weathering from frost and dry periods, the first metres of clay contain many cracks and have the same hydrostatic characteristics as the fill, even though the permeability decreases with depth. This phenomenon usually extends to a depth of around 5 m. The pore pressures in the two aquifers are to a large extent independant of each other. A pore pressure reduction in the lower aquifer will therefore not be visible on groundwater measurements in the upper aquifer. In the lower aquifer, the pore pressures can be both above and below hydrostatic conditions. The groundwater level in the upper aquifer is roughly 1 m below ground. The pore pressures in the lower aquifer are hydrostatic, starting from the ground level. Issues with reduced pore pressures in the upper aquifer are mainly related to rotting of old wooden foundations (Sundkvist & Wallroth, 2016). Reduced pore pressures in the lower aquifer could cause ground settlements and are the main topic of this report.

3 Theoretical Background

This chapter will provide a general understanding of deep excavations in an urban environment, with the special focus on settlements due to reduced pore pressures in the lower aquifer. In the beginning, the basics of deep excavations are described. Further the soil behaviour during a pore pressure reduction is explained as well as how buildings are damaged by settlements and possible solutions to the issues. Finally, the software Plaxis and its input parameters will be discussed.

3.1 Design of a deep excavation and related problems

Deep excavations can have several purposes and can be performed using different construction methods. The excavation analysed in this thesis is a cut and cover tunnel. Therefore, this process will be explained in more detail. Most of the theory is nevertheless applicable to other types of excavations as well.

3.1.1 Construction of a tunnel by the cut and cover method

The parts of the West link built in clay will be constructed by using the cut and cover method (Trafikverket, 2020). The construction materials and exact procedure varies, but the basic process can shortly be described in four steps as illustrated in Figure 3.1. The first step is to install the retaining walls. Depending on the clay depth, the walls are either floating in the clay or pushed all the way down through the friction layer to the bedrock. The latter is true for the excavation analysed in this thesis. Step two is to dig down to the depth the tunnel will be constructed on. If required, additional retaining structure elements are installed in the process, for instance struts and anchors. The third step is to create the tunnel at the bottom of the excavation. The soil material will be filled back into the excavation pit when the tunnel is completed.

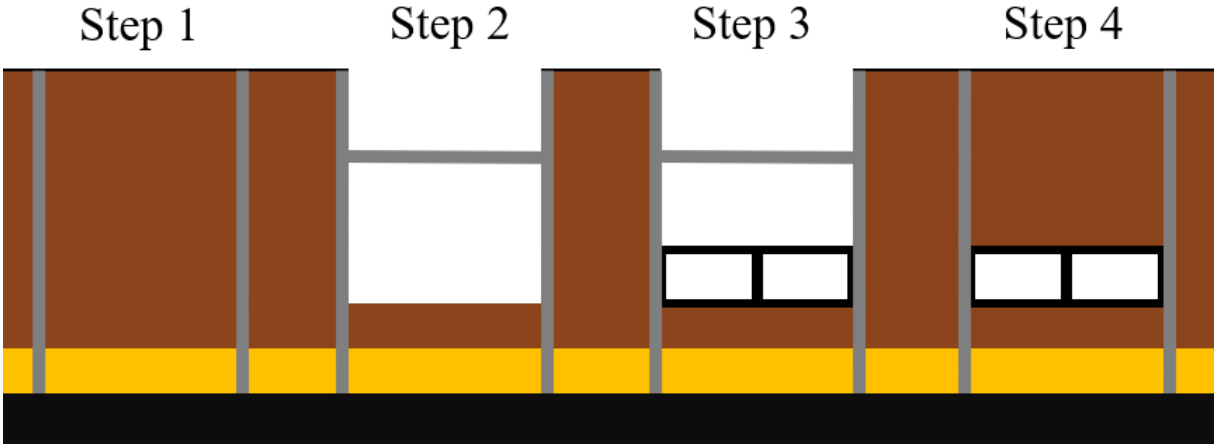

Figure 3.1: Construction steps of a deep excavation in clay, after Trafikverket (2020).

3.1.2 Causes of water inflow to a deep excavation

To be able to work in an excavation it is necessary to keep the pore pressure levels below the bottom of the excavation, otherwise the excavation may be flooded by groundwater (Cashman & Preene, 2013). Additionally, it is often required to reduce the pore pressures even more to prevent hydraulic uplift, a phenomenon where the pore pressures in the friction layer are high and cause failure of the excavation bottom. The reduction of pore pressures creates a hydraulic head difference between the inside and the outside of the pit. If the excavation is completely

sealed this is not a problem. But if not, the pore pressures outside the excavation may be affected since the pressures always strive to equalise. As Figure 3.2a suggests, there are several ways for outside groundwater to enter the excavation (Persson, 2007). The bedrock is rarely precisely horizontal. When installing the retaining walls, which typically are prefabricated with a given width, there will be small gaps between the wall and the bedrock as illustrated in Figure 3.2b. Since the soil on top of the bedrock is friction material with relatively high conductivity, these gaps are enough for significant amounts of water to enter the excavation. Water could also seep through inadequately sealed retaining walls. Since the permeability of the clay at the site studied in this project is very low, it is assumed that any seepage through the walls will occur in the friction layer. In addition, the groundwater can enter via cracks in the bedrock. Grout is often injected to friction layers and bedrock to reduce the leakage, but even with grout, the permeability will be substantially higher than for the clay. Lastly, some water may flow below the grout, and the grout might have local deficiencies.

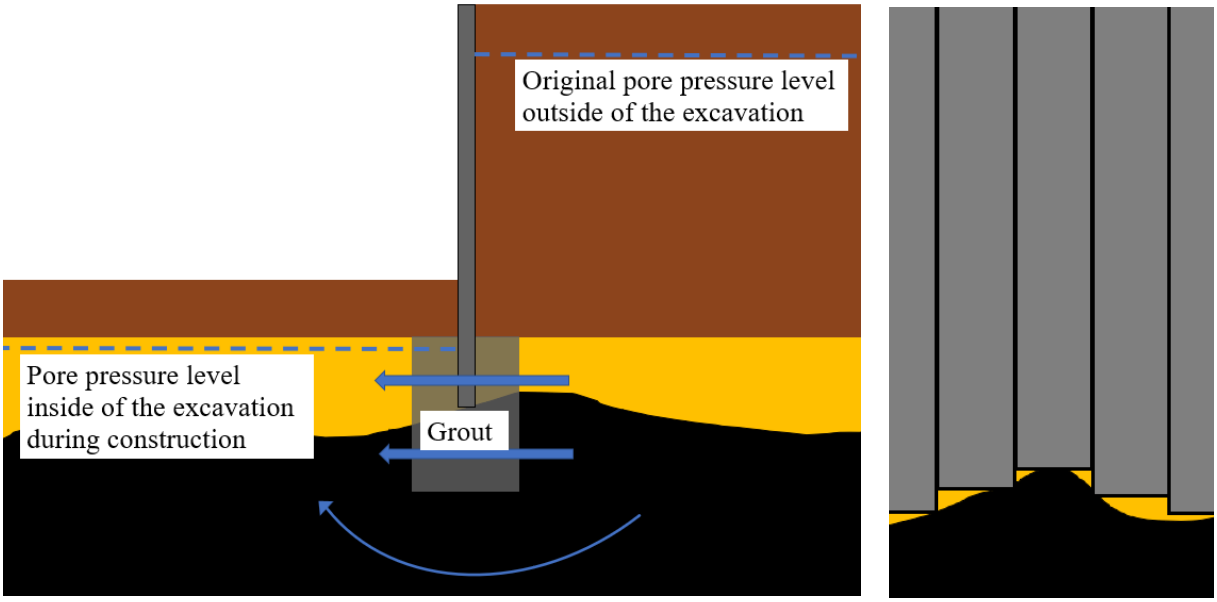

Figure 3.2: a) Water flow into an excavation, after Persson (2007) b) Gap between retaining wall and bedrock, after Ödlund Eriksson (2014).

3.1.3 Investigation of the relation between pore pressure reductions and settlements

The magnitude of the pore pressure reduction and the influenced area are governed by a complex relation of many factors (Fetter, 2014). The most obvious parameter is the amount of water inflow to the excavation. Other factors are for example infiltration rates, topography and hydrologic boundaries in the shape of streams and bedrock. Further, the properties of the bedrock and soil layers do have an impact. Permeability, storativity, thickness and inclination of the soil layers all affect the system. The pore pressure reduction is thus not uniform in the area. Even if it would be possible to create a decent groundwater model of the area, it is beyond the scope of this project. Test pumping in the lower aquifer has been performed at three locations for the West link project, but not very close to the planned excavation in Liseberg (Sundkvist & Wallroth, 2016). The maximum distances to where the pore pressure reductions were detectable varied between 250 and 1000 m.

Instead of relying on a groundwater model, another approach can be taken (Högsta & Sanell, 2016). During the construction phase of the excavation, the pore pressures in the friction layer nearby the excavation are regularly measured and analysed to detect any deviations. By beforehand calculating the expected settlements for given pore pressure reductions in relation to time, it can be determined how large the deviations may be before problems arise. Thus, actions may hopefully be taken before any damage occurs to the nearby buildings. One of the main objectives for this thesis is to perform this type of calculations for the analysed excavation.

3.1.4 Other sources of settlements caused by deep excavations

This thesis will almost entirely focus on the pore pressure reduction and not on the other, more construction related issues. It is nevertheless important to be aware of the other issues to get a broader picture of the challenges of constructing excavations in an urban environment. Korff (2012) mentions vibrations from installation of soil elements, movement of retaining walls and lowering of pore pressures. Cashman & Preene (2013) also includes internal erosion as a source of settlement in certain soils.

It is hard to distinguish the effects of installation works and movement of retaining walls from each other since they often occur simultaneously (Korff, 2012). To complicate things further, the stress on the deep soil below and close to the excavation is reduced when soil inside the excavation is removed. The settlements due to installation works and movement of retaining walls are yet larger than the uplift from unloading. The total settlements from this category are to a large extent correlating with the depth of the excavation. When several studies of hundreds of cases each were summarised, it was concluded that the maximum settlements usually are between 0.2-1% of the excavation depth. The largest settlements occur within 0.75 times the depth, and the settlements become zero at a distance from the excavation of 2-3 times the depth. For the 25 m deep excavation studied in this thesis, this would mean maximum settlements from this category is 5-25 cm. The maximum settlements would be less than 19 m away from the excavation and the total distance influenced would be 50-75 m. Since the West link has a large budget and strict regulations, the settlements should be in the lower range, at least where it is deemed necessary.

Internal erosion is when fine particles in the soil get washed away and leave small voids in the soil. When the voids collapse, it does result in settlements (Cashman & Preene 2013). For this to happen, it is necessary to have an inhomogeneous soil which makes it possible for relatively high flows, but simultaneously the soil shall contain grain sizes small enough to move. An example of this is moraine. It is unlikely that any constant inflows to the excavation analysed in this report would cause large enough velocities for internal erosion to take place. However, as exemplified in the construction of the Göta tunnel in Gothenburg, internal erosion may occur as a result of other construction activities (Persson, 2007). In that case the ground did settle several decimetres close to the excavation and a large share of it is believed to originate from internal erosion. The reason for the high flows were partly because of high water pressures used during drilling of anchors and partly due to infiltration wells used to prevent pore pressure reductions.

3.2 Soil behaviour due to water inflow to an excavation

The settlements in the clay due to inflow to the excavation can be split into two different categories, consolidation and creep. Consolidation will in the studied case occur as a direct result of changes in pore pressures. Creep is going on continuously, regardless of changes in pore pressures. However, when the preconsolidation pressure decreases, the creep rate will drastically increase.

3.2.1 Consolidation

Consolidation is one of the most essential concepts in soil mechanics. The principle is founded on three key parameters: the total stress, σ, the effective stress, σ' and the pore pressures, u. The relationship between them is described by Equation 3.1.

$$\sigma = \sigma' + u \qquad \text{Eq. (3.1)}$$

Knappet and Craig (2012) defines consolidation as "the gradual reduction of volume of a fully saturated soil of low permeability due to the change of effective stress". The most common case of consolidation is when something is constructed on the ground which leads to an increase in the total stress on the soil. When the total stress increases, the entire extra load is initially carried by the water in the soil. This creates excess pore pressures which dissipates with time, which in turn increases the effective stresses and causes deformations. Figure 3.3a visualises this phenomenon. In the case of a pore pressure reduction in an underlying layer, the total stress will instead remain constant while the pore pressures slowly decrease due to flow from the clay to the friction layer. The effective stresses then increase over time as shown in Figure 3.3b.

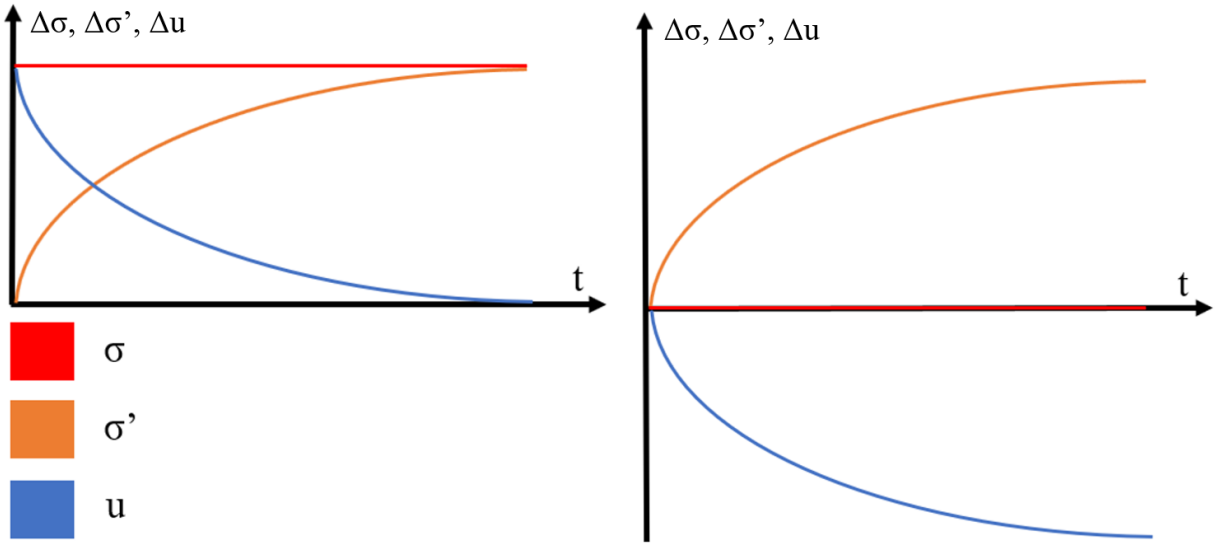

Figure 3.3: a) Consolidation due to external loading. b) Consolidation due to reduced pore pressures.

The time dependency of this behaviour was early investigated by Terzaghi (1925) who derived the one-dimensional vertical consolidation equation. It is stated in Equation 3.2 and is based on the following assumptions:

1. The soil is homogeneous.
2. The soil is fully saturated.

3. The particles of soil and pore fluid are incompressible.
4. Compression and flow are one-dimensional (vertical).
5. The strains are small.
6. Darcy's law is valid at all hydraulic gradients.
7. The permeability is constant.
8. The stiffness is constant.
9. There is a unique relationship, independant of time, between void ratio and vertical effective stress.

$$\frac{\partial \mathrm{u}}{\partial \mathrm{t}} = C_v \left(\frac{\partial^2 u}{\partial z^2} \right) \qquad \text{Eq. (3.2)}$$

Where:

- u are the pore pressures.
- t is the time.
- z is the depth.
- C_v is the coefficient of consolidation, based on Equation 3.3.

$$C_v = \frac{k}{m_v * \gamma_w} \qquad \text{Eq. (3.3)}$$

Where:

- k is the permeability.
- m_v is the coefficient of volume.
- γ_w is the unit weight of water.

Because of assumption 7 and 8, k and m_v are constant during the process, thus C_v is also constant. The solution of Equation 3.2 is complicated and therefore it is customary to use Equation 3.4 to estimate the time dependency of consolidation.

$$T_v = \frac{C_v * t}{d^2} \qquad \text{Eq. (3.4)}$$

Where:

- T_v is the time factor.
- d is the thickness of the soil layer. If the soil can drain in two directions, d is set to half of the thickness.

The share of the total excess pore pressures which have dissipated is called the degree of consolidation, U_v. It is dependant on the drainage path and T_v. Knappett and Craig (2012) illustrates this with three examples of excess pore pressure distributions where the drainage is one-sided, see Figure 3.4. The degree of consolidation at any T_v will be the largest in example 3, followed by example 1 (unless all excess pressures have dissipated, then U_v are the same). This is because the average distance between the excess pore pressures and the draining layer is shortest in example 3 and second shortest in example 1.

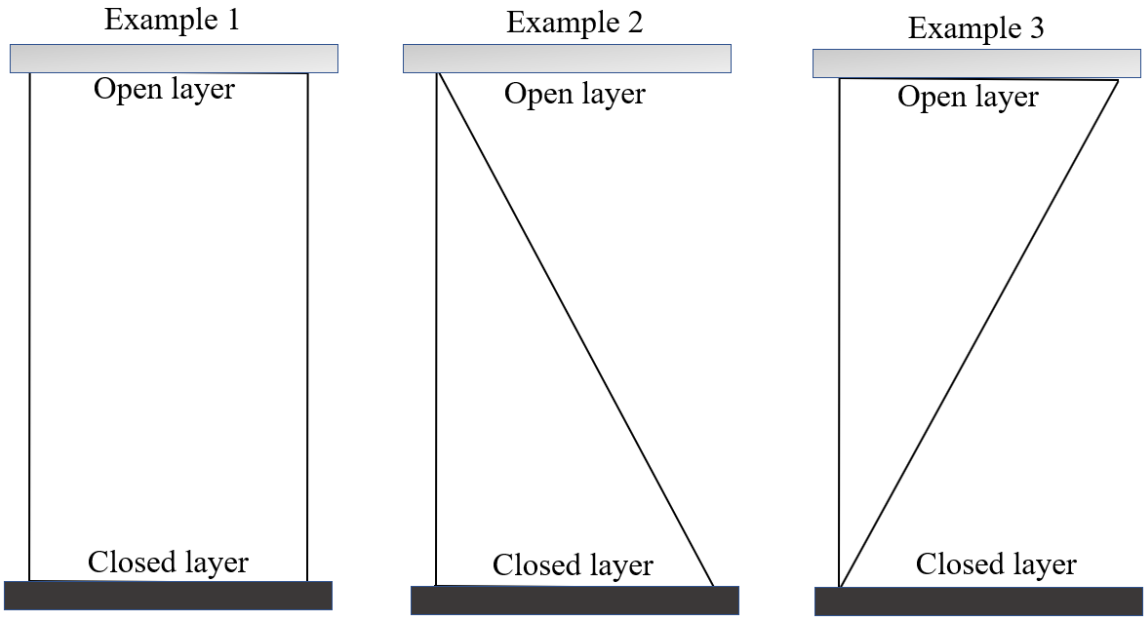

Figure 3.4: Examples of excess pore pressure distributions, after Knappett and Craig (2012).

Figure 3.5 describes a sudden pore pressure reduction in the lower aquifer in a case where the geological conditions are similar to the ones at the studied site. As mentioned in Chapter 2, the conditions of the first 5 metres of soil are always hydrostatic because of cracks in the clay. The pore pressures in the rest of the soil are in this case assumed to be hydrostatic in the beginning. The excess pore pressure distribution will initially look like example 2 above. Unlike the examples above water may drain both towards the upper and the lower layer, but since there are no excess pore pressures at the top, all drainage will occur towards the bottom. The drainage situation will thus be comparable to example 3, but upside down. The time factors shown in the Figure 3.5 are not precise, but a relatively large share of the excess pore pressures will dissipate early during the consolidation process. Early in the consolidation process does however not necessarily mean fast, since it may take over 100 years for all excess pore pressures to equalise in certain conditions (Berntson, 1983). By analysing Figure 3.5 with consideration of Equation 3.1 it is evident that the lower clay layers will experience a larger effective stress increase. The effective stress increase will furthermore occur earlier compared to the upper layers since it is closer to the draining layer.

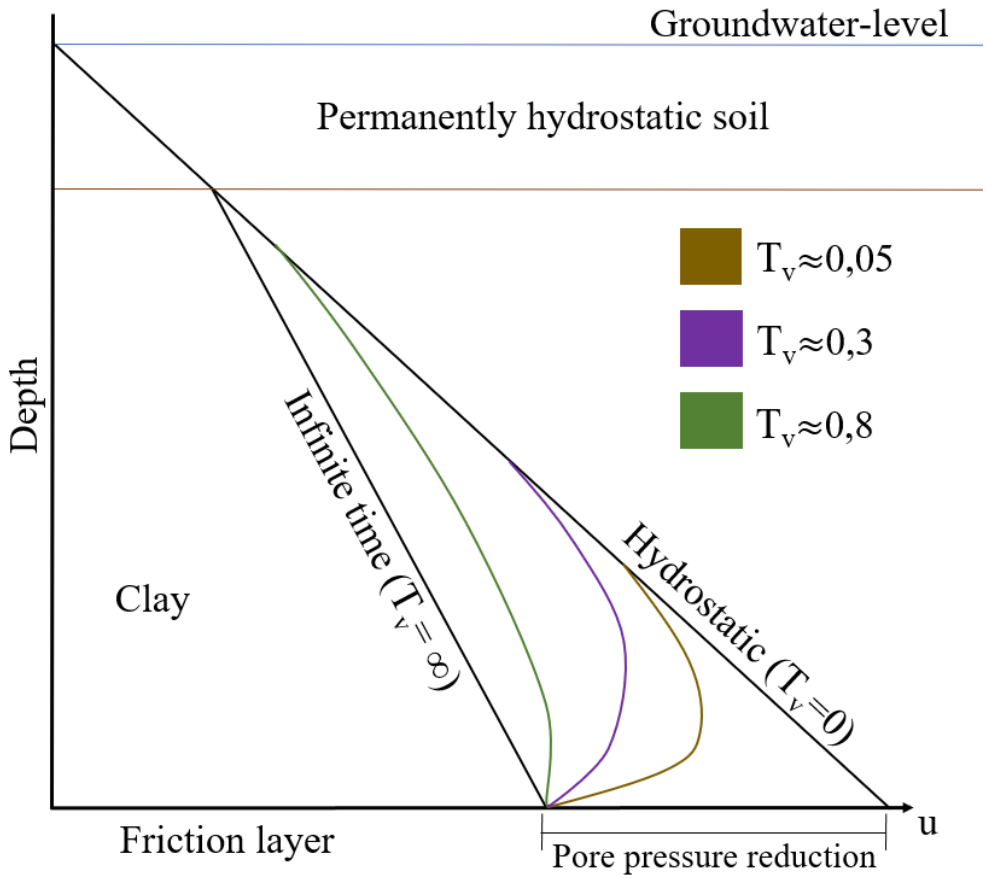

Figure 3.5: Pore pressure profile in a clay with a draining layer below.

Terzaghi's theory has proven to work relatively well for most applications, but it has some weaknesses. Assumption 9 is not correct because of creep effects, explained further in the next section. Consolidation is nor a one-dimensional process in terms of stresses. Biot (1941) did for this reason further develop the consolidation theory to include two and three dimensions. The complete equations and the solutions are long and complicated, but they are based on relatively simple mechanisms. For example, implementing Hooke's law for calculating the strains and possibilities for varying the stresses, strains and permeabilities in different directions. The equations by Biot are the ones implemented in Plaxis consolidation calculations (Bentley, 2021a).

3.2.2 Creep

When all the pore pressures have dissipated after the consolidation process, the clay will continue to deform due to creep, also known as secondary compression (Knappet & Craig, 2012). Creep is when the particles in the soil rearrange and thus reduce the volume of the soil. When the particles rearrange, small excess pore pressures are created which dissipates with time. In fact, creep is occurring in all stress states, but it increases drastically when the in-situ stress becomes closer to the preconsolidation pressure. It starts to become relevant around OCR values of 1.25 (Larsson & Sällfors, 1995). Bjerrum (1967) investigated the relationship between void ratio, overburden pressure and time. In a state of constant pressure, the creep rate will be faster in the beginning and decrease with time, as displayed in Figure 3.6. The figure also shows what happens when the soil is loaded after a long time of constant stress. The reason why the creep rate is faster in the beginning is because the preconsolidation pressure increases when the

soil is deformed from creep. The behaviour is valid for all stress states. However, since the creep is small for OCR values above 1.25, the OCR is mainly affected by creep when the OCR is small. A high initial void ratio further increases the creep. The share of the total deformations creep accounts for are thus very site specific. There are examples where creep stands for over two thirds of the total settlements (Larsson, 1986).

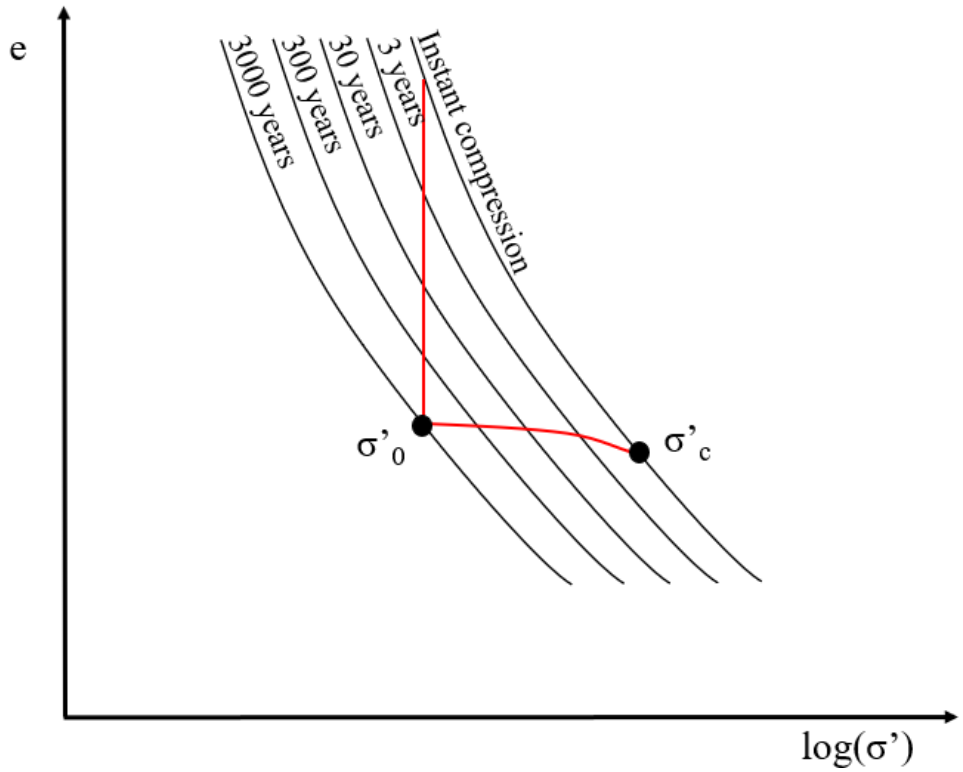

Figure 3.6: Creep during a constant overburden pressure, after Bjerrum (1967).

3.3 Building damage due to settlements

The damage on a building depends to a large extent on the magnitude of settlements and on how the building is founded. To study the damage caused by reduced pore pressures it is important to understand the mechanisms behind why buildings get damaged and how the damage could be reduced.

3.3.1 Building foundations

Many different types of foundations have been used over the years to reduce the settlements and increase the stability of constructions. The design of the foundation depends on many factors, such as the building type, soil properties and the technology available at the time of construction. This section will mention the most common foundation types in Gothenburg. The foundation types can be split into three categories when it comes to settlement predictions (Sundkvist & Wallroth, 2016).

The buildings in the first category are not affected by the pore pressures at all. This includes constructions with end bearing piles, buildings founded directly on bedrock or on friction material on top of the bedrock. The most common type of end bearing piles in Sweden are concrete piles with the dimensions of 235*235 mm or 270*270 mm (Olsson & Holm, 1993).

Piles can also be made of steel. Since the pile materials are very stiff, the increased load from reduced pore pressures should not result in any significant settlements for the buildings.

The second category is foundations very dependant on the pore pressures in the lower aquifer, but only slightly dependant on the pressures in the upper aquifer. Pore pressure reductions in the lower aquifer will cause settlements as described earlier. If the groundwater level in the upper aquifer drops, it increases the effective stress on all the clay below. The settlements from this are yet believed to be small because the magnitudes are relatively small and time spans are relatively short. This group consists of buildings which are founded directly on top of the clay, buildings founded on top of the fill without any wood in the foundation and buildings with cohesion piles. Because all settlements due to reduced pore pressures in the lower aquifer do occur deeper than 5 m, all buildings without cohesion piles in this category will settle with the same rate as the ground level. Structures with cohesion piles will also settle after a pore pressure decrease, but not necessarily as much as the ground. The magnitude of settlement in comparison to the ground is dependant on factors such as the pile type, the depth of the pile and the soil characteristics (Eriksson et al., 2004).

The third category is foundations very affected by pore pressure changes both in the upper and the lower aquifer. Many old and sensitive buildings are founded in the upper aquifer on different types of wooden elements, for example piles made of logs. If the groundwater level drops, the old wood will be exposed to oxygen and start to rot. This leads to transferring of stresses from the pile to the soil which may result in deformations. Because this report only investigates pore pressure reductions in the lower aquifer, these types of foundations will be assumed to settle with the same rate as the ground. This might overpredict the settlements slightly but should not have a major impact on the results since the piles are quite shallow in comparison to where the majority of pore pressure decrease takes place.

3.3.2 Problems related to settlements caused by reduced pore pressures

Building damage can be grouped into three main categories: aesthetic, serviceability and stability (Building Research Establishment, 1995). Aesthetic damage usually consists of superficial cracks in the façade. Serviceability problems include many factors, for instance when the settlements affect the buildings weather protection or cause damage to pipes. Stability issues are when parts the construction are in the risk of collapse, this is yet a very unlikely consequence of a pore pressure reduction.

Cashman & Preene (2013) defines two aspects to look at when estimating damage due to settlements, maximum settlement and building tilt. Settlements solely in the vertical direction do not necessarily cause any problems. The issues start to occur when the building settles unevenly, also known as differential settlements. It is however unlikely to have completely horizontal settlements below buildings without piles, as it requires the soil conditions to be completely homogeneous. If the soil is inhomogeneous, parts of the building may slightly bend upwards or downwards, also known as hogging and sagging, respectively. Another complication is if the surroundings settle at a different rate than the building, resulting in problems with connecting entrances and stairs. The estimated vertical settlements thus are a good hint of the expected damage.

There are several mechanisms causing buildings to tilt due to settlements (Cashman & Preene, 2013). In a homogeneous soil without any piles, the settlements will correlate with the pore pressure reduction curve. This implies that the settlements become larger the closer to the excavation and the nearby buildings will therefore tilt towards it, see Figure 3.7. Moreover, because the gradient is steeper closer to the excavation the buildings might be subjected to hogging.

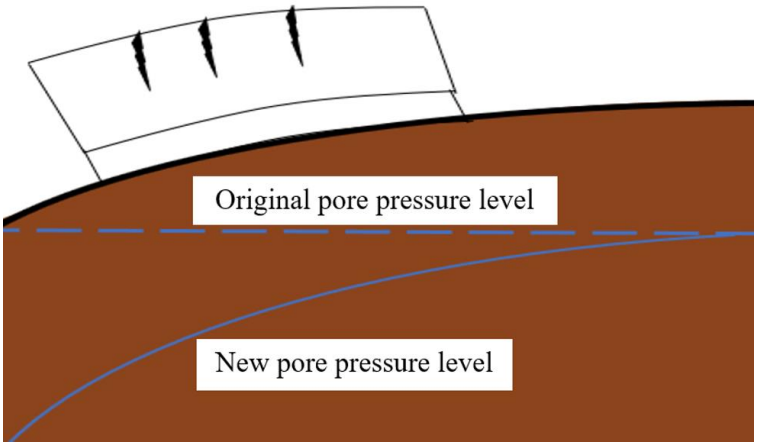

Figure 3.7: Building tilt due to an inclined pore pressure curve, after Cashman & Preene (2013).

The properties in heterogeneous soil can vary in different places below a building. If the construction is not piled, this may cause inclined settlements and building damage, as displayed in Figure 3.8. Depending on how the properties vary this could also result in hogging or sagging.

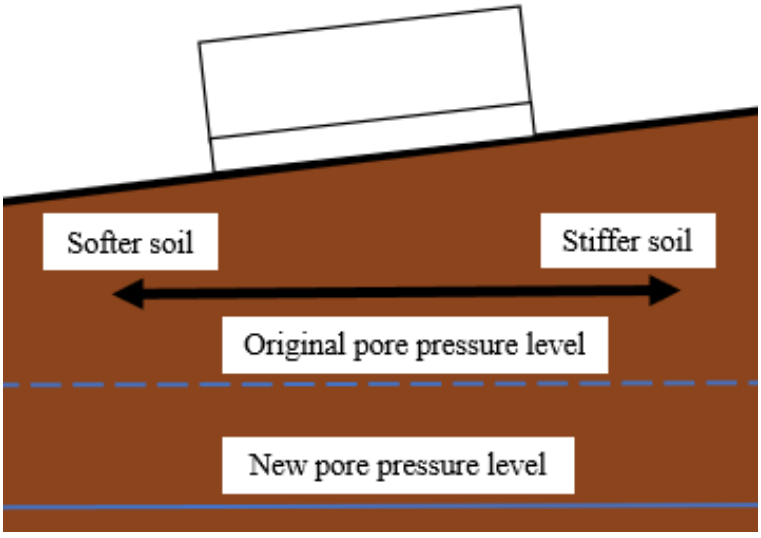

Figure 3.8: Building tilt due to varying soil properties, after Cashman & Preene (2013).

Inclined settlements may also appear next to piled buildings. In the case of end-bearing piles, the settlement of the building will be very small, but any nearby structures without piles will settle. The settlements will be smaller adjacent to the piled building and increase with distance, see Figure 3.9. Note that the inclination does not necessarily have to be linear, so hogging or sagging might therefore occur in this case as well.

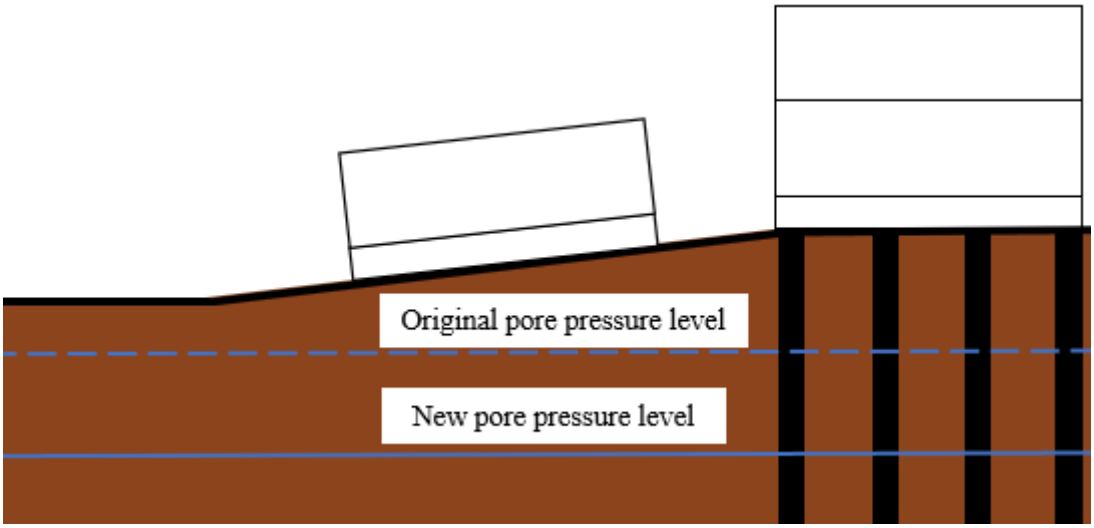

Figure 3.9: Building tilt due to a nearby piled building, after Cashman & Preene (2013).

Many factors influence how sensitive different buildings are and how much settlements may occur before they get damaged. The amount of damage is for example based on the stiffness of the building foundation and the building materials (Korff, 2012). Different degrees of damage may also be tolerable depending on the situation. Attempts have been made to specify when building damage may occur and some of these are presented below. It is yet important to keep in mind that these are not definite values.

Damage by sagging and hogging is determined by something called the deflection ratio. It is the ratio between Δ and L for a building foundation as described in Figure 3.10. Buildings are in general more sensitive to hogging than sagging, and buildings with smaller length to height ratio are more sensitive compared to higher ratios (Bond et al., 2013). To limit the damage to constructions, the following values are suggested:

- Maximum deflection ratio in sagging: 1/2500 if L/H=1.
- Maximum deflection ratio in sagging: 1/1250 if L/H=5.
- Maximum deflection ratio in hogging is 1/5000 if L/H=1.
- Maximum deflection ratio in hogging is 1/2500 if L/H=5.

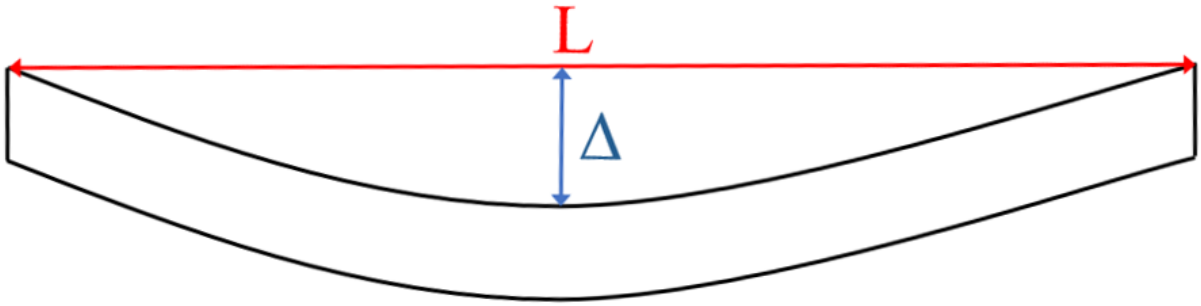

Figure 3.10: Definition of Δ and L during sagging of a building foundation.

In Table 3.1, tentative values of maximum settlement and building tilt for an initial risk assessment are stated, these are suggested by Cashman & Preene (2013). For the construction of the West link, a more detailed analysis of nearby buildings has been performed (Trafikverket, 2017). The acceptable vertical settlements are set between 5 and 20 mm for different structures while the allowable inclinations are 0.1-0.2%.

Table 3.1: Guideline values for estimating building damage due to settlements (Cashman & Preene 2013).

Risk category	Maximum settlement [mm]	Building tilt [%]	Anticipated effects
Negligible	< 10	<0.2	Superficial damage unlikely
Slight	10 – 50	0.2-0.5	Possible superficial damage; unlikely to have structural significance
Moderate	50 – 75	0.5-2	Expected superficial damage and possible structural damage to buildings; possible damage to rigid pipelines
Severe	> 75	>2	Expected structural damage to buildings and expected damage to rigid pipelines or possible damage to other pipelines

3.3.3 Possible solutions to settlement issues

Since the settlements correlate with the pore pressures, one solution is to prevent as much as possible of the pore pressure reduction. This may be done in multiple ways. The pore pressures will be less affected by reducing the water inflow to the excavation. As stated in section 3.1.2, grout is regularly used to reduce the permeability of soil and rock when there is risk of leakage. It is however a challenge to reduce the permeability as much as theoretically is possible since the work must be performed far below ground (Cashman & Preene, 2013). A good site characterization is thus very important to find soil with higher permeability and weakness zones in the bedrock. Several methods may be used for grouting, the more expensive and time-consuming methods often result in better quality and lower permeability. Another solution to prevent pore pressure reductions is artificial infiltration even if it is not always suitable for various reasons. The permeability of the soil which the water is pumped into must be relatively high (Cashman & Preene, 2013). The only possible layer in the case studied in this thesis is therefore the friction layer in the bottom. When performing infiltration, it is important to consider the effects of internal erosion as explained in section 3.1.4. In addition, it is often a quite complicated legal process before permission is granted to infiltrate the groundwater. This is because large areas might be affected by the infiltration, and changes to the natural groundwater state could influence soil living organisms and transport contaminants in the soil. Moreover, by good planning and high efficiency of the construction work it may be feasible to reduce the construction time and consequently reduce the total water inflow and settlement.

Instead of constructing the excavation using the conventional methods described in section 3.1.1, other techniques could be utilised. Shirlaw et al. (2005) mentions several innovative methods to perform deep excavations in clay, one of them is underwater excavations. The

method was in fact originally discussed for parts of the West link project (Trafikverket, 2014). In an underwater excavation, parts or the entire volume of the excavated soil are replaced with water (Shirlaw et al., 2005). It does obviously complicate the construction of the tunnel, but it has several benefits. Thanks to the high water levels inside the excavation, the hydraulic head difference and the water inflow will be much smaller compared to a dry excavation. Additionally, the water acts as a counterforce to movement of the retaining wall and thus reduce the settlements close to the excavation. There are not many documented examples of underwater excavations, but the available case studies show a significant reduction both in total settlements and distance to zero settlement compared to conventional methods (Shirlaw et al., 2005), (Cao et al., 2019), (Li et al., 2020).

If settlements after all occur, it is possible to mitigate some of the damage. It can be done by reinforcing the foundations of old structures, sometimes referred to as underpinning (Thorburn & Littlejohn, 1993). There are a great number of methods available depending on the building characteristics, existing foundation and soil conditions. One of the most common methods that is suitable for deep clay is to construct piles for existing buildings. There is technology available to place piles straight below the floor of a building as long as the ceiling in the bottom level is relatively high, see Figure 3.11a. Sometimes the ceiling is yet too low, or it is undesirable to move things out of the bottom level. In this case, it is possible to extend the current foundation and place a row of piles close to the building. When doing this, it is necessary to place another pile row a bit further away which carries the tension forces created by the imbalance between the building and the first pile row, see Figure 3.11b. An issue with both methods is that the ground around the construction still will settle, potentially causing damage as described previously in Figure 3.9. The method with piles on the side may furthermore result in sagging of the building if the distance between the walls is large.

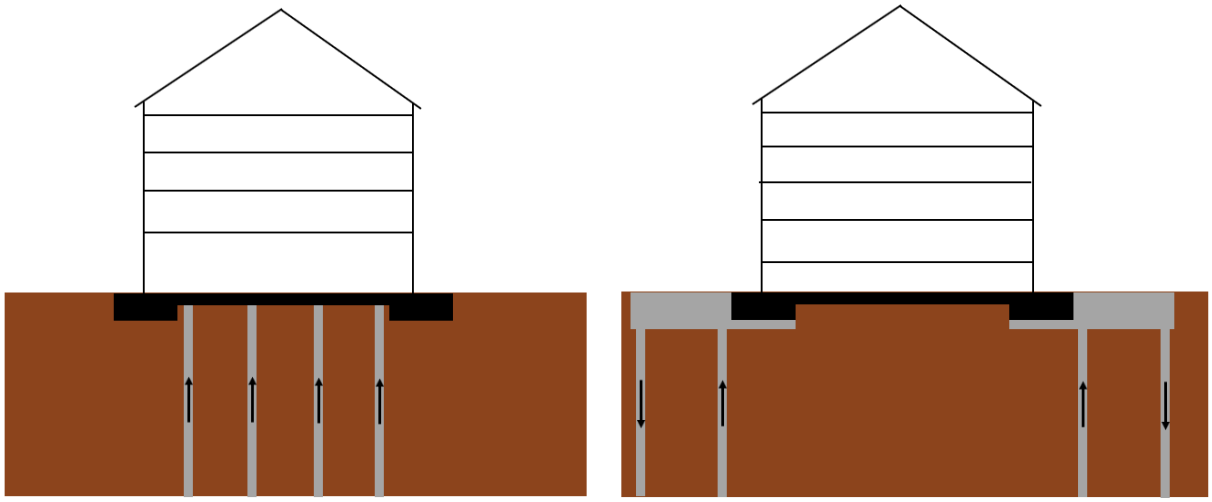

Figure 3.11: a) Reinforcement by piles underneath a building. b) Reinforcement by piles on the side of a building. Inspired by Thorburn & Littlejohn (1993).

Finally, in some cases may the most economical solution simply be to let eventual settlement damage occur and pay for repairment of the constructions afterwards (Powers et al., 2007). This is often true for projects where the overall settlements are estimated to be small, but sometimes also correct for larger settlements. If this approach is taken, it is extra important to detailly

investigate the condition of the buildings at risk to distinguish between old and new damage. For many projects, the West link included it is however unthinkable to consciously let settlement damage occur since the general public would not accept it.

3.4 Plaxis

Plaxis is a finite element software developed specifically for geotechnical engineering (Bentley, 2021b). The program can be used to model basically all geotechnical problems. In this project the 2D version of Plaxis will be used but there is also a 3D version. Most problems are possible to solve by using 2D even though it sometimes requires some modifications. In this project, everything is assumed to be plane strain which means that the modelled cross sections are assumed to be infinetely long in the z-direction. 2D also demands less computing time than 3D problems. The results of an analysis are heavily dependant on the large amount of settings and features available in the program. It is therefore very important to understand how the model works and not to trust the results blindly. Additionally, as with all geotechnical models, the output results will never be of better quality than the input values. The remaining part of this chapter is dedicated to explain some of the most important aspects related to the program and how the input parameters are evaluated.

3.4.1 Constitutive models

In numerical modelling, constitutive models are an essential part. A constitutive model can be seen as a mathemetical formulation of how the soil is affected by stress changes (Karstunen & Amavasai, 2017). All constitutive models have a yield surface or somethng similar to it. The surfaces govern the relation between small and large strains. Examples of this can be seen in the following sections. Other common components of constitutive models are elastic laws, hardening laws and flow rule. These mechanisms control how the yield surface behaves under different scenarios.

There are a number of different constitutive models avalable in Plaxis. Some of the more common are Mohr-Coulomb, Modified Cam-Clay, Hardening Soil, Soft Soil (SS) and Soft Soil Creep (SSC). Initially in this project, the SS model will be used to get a good understanding of the problem. During later stages, SSC is utilised to evaluate the effects of creep. The key aspects of these models are described in the following sections. To get the full details of the model, it is recommended to read the Plaxis material models manual (Bentley, 2021c). Both Mohr-Coulomb and Modified Cam-Clay are relatively simple models and do not capture the soil behaviour well enough. Hardening Soil model is not very suitable for Swedish clays because they are too soft (Karstunen & Amavasai, 2017). There are also more advanced models available, such as Creep-SCLAY1S, that presumably would give more accurate results. The main reason why these are overlooked is because they would require more time for evaluating parameters and understanding the model properly. More effort is instead put into the other parts of the analysis. In addition, the available data is not sufficient to evaluate all required parameters in a correct manner.

3.4.1.1 Soft Soil model

The yield surface in the SS model is isotropic and has the shape of an ellipse in the p'-q space. Changes in stress within the yield surface result in elastic strains, while stress states that would

become outside the surface expands it and causes plastic deformations. The surface is defined according to Equation 3.5 and is displayed in Figure 3.12. The shape and size of the yield surface are founded on two parameters: the preconsolidation pressure and the slope M* (Karstunen & Amavasai, 2017). The preconsolidation pressure determines the size of the ellipse in the p'-direction, referred to as p_0'. The top of the ellipse always follows a straight line with the slope M*, a parameter determined by the program founded on the K_0^{NC} value. The SS model has a separate failure line, which is the line the stresses never can exceed. It is a regular Mohr-Coulomb line, based on the cohesion intercept and the friction angle. The cohesion makes it possible to have tensile stresses which is unrealistic for soils, therefore it is necessary to include a tension cut-off.

$$fc = \frac{q^2}{(M^*)^2} + p'(p' - p_0') \qquad \text{Eq. (3.5)}$$

Where:

- p' is the mean effective stress, $(\sigma_1'+\sigma_2'+\sigma_3')/3$.
- q is the deviatoric stress, $\sigma_1' - \sigma_3'$.
- M* is the slope of the line which the top of the ellipse is based on.
- p_0' is the size of the yield surface.

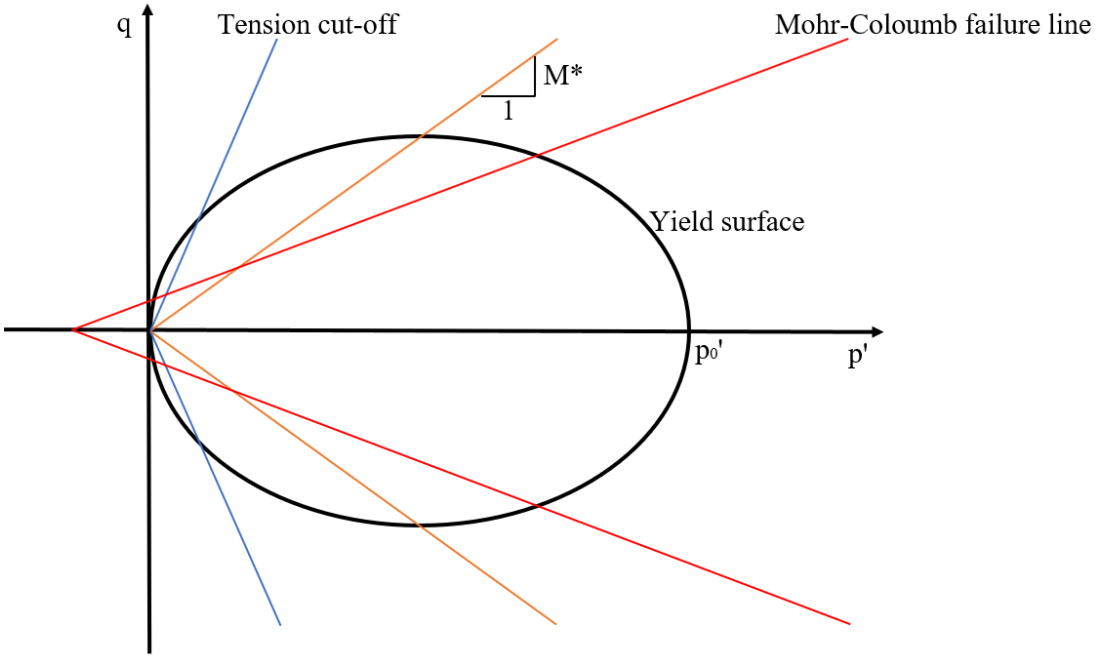

Figure 3.12: Yield surface of the SS model, after Karstunen & Amavasai (2017).

One of the key advantages of the SS model compared to simpler models is that the model is strain-hardening. It means that instead of having linear stiffness like the Mohr-Coulomb model, the elastic modulus for unloading-reloading is higher than the initial one. Since the yield surface is heavily dependant on the preconsolidation pressure it is important to evaluate it carefully. Some of the drawbacks include that the model is not good for heavily overconsolidated clay or unloading problems, but it is not a major issue in this thesis. It does neither take any creep effects into account, because of that the SSC model will also be used.

3.4.1.2 Soft Soil Creep model

The SSC model is developed from the SS model but does also consider the effects of creep. Many of the features and parameters from the SS model are consequently the same, but the creep effect complicates a few things. As mentioned previously in Section 3.2.2, creep does occur in all stress states, even if it is very small for larger values of OCR. Because of this there are no purely elastic region in the SSC model (Bentley, 2021c). The surface between small and large strains is therefore instead referred to as the normal compression surface, displayed in Figure 3.13. The size of the surface is dependant on the preconsolidation pressure and it increases with increasing plastic strains, according to Equation 3.6. The other surface in the figure represents the current mean effective stress state. It has the same shape as the normal compression surface, but the size is instead determined by Equation 3.7. By using the output values from the two equations, the volumetric strain rate, $\dot{\varepsilon}_v$ is calculated by Equation 3.8. Note that this model makes use of a tension cut-off and a Mohr-Coulomb failure line just as the SS model even if it is not included in the figure.

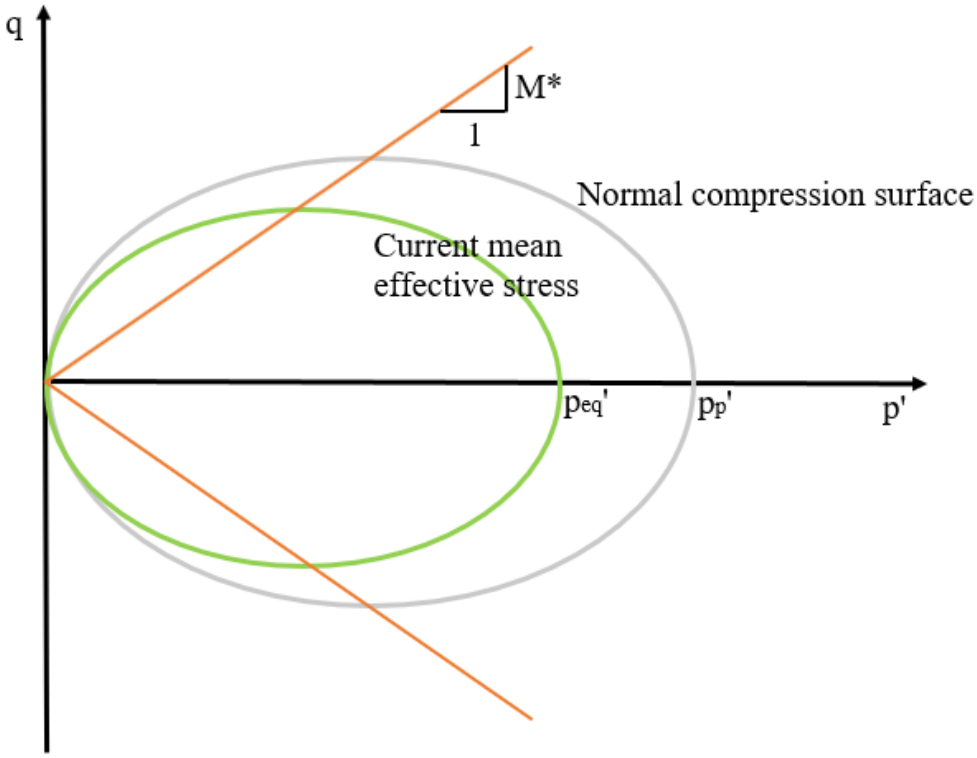

Figure 3.13: Yield surface of the SSC model, inspired by Bentley (2021c).

$$p'_p = p'_{p0} * \exp\left(\frac{\varepsilon^{\cdot p}_v}{\lambda^* - \kappa^*}\right) \quad \text{Eq. (3.6)}$$

$$p'_{eq} = p' + \frac{q^2}{M^* p'} \quad \text{Eq. (3.7)}$$

$$\dot{\varepsilon}_v = \varepsilon^{\cdot e}_v + \varepsilon^{\cdot p}_v = \kappa^* * \frac{\dot{p'}}{p'} + \frac{\mu^*}{\tau}\left(\frac{p_{eq}{}'}{p_p{}'}\right)^{\frac{\lambda^* - \kappa^*}{\mu^*}} \quad \text{Eq. (3.8)}$$

Where:

- $p_p{}'$ is the isotropic preconsolidation pressure.
- p'_{p0} is the initial preconsolidation pressure.
- $p_{eq}{}'$ is the current mean effective stress.
- $\dot{\varepsilon}_v^e$ are the elastic strains.
- $\dot{\varepsilon}_v^p$ are the plastic strains.
- $\dot{p}'$ is the mean effective stress increase.
- κ*, λ* and μ* are the modified swelling index, modified compression index and modified creep index, respectively. These parameters are explained in detail in the following sections.
- τ is the time for a stepwise oedometer test which μ* is evaluated from, usually 1 day.

As Equation 3.8 suggests, there are elastic- and plastic shares of the strains. The elastic strains increase linearly with the stress increase. The plastic strains include both consolidation and creep and depends on the ratio between $p_{eq}{}'$ and $p_p{}'$. The ratio is the inverse of the OCR in the p'-q space. The value of (λ*- κ*)/μ* determines how large impact the OCR has. Since (λ*- κ*)/μ* usually is above 25 and sometimes considerably higher, the model is very sensitive to changes of the OCR, just as the SS model. The major drawbacks of the SSC model are that it predicts too much creep when the OCR is close or equal to 1 and that it often overpredicts the excess pore pressures (Karstunen & Amavasai, 2017).

3.4.2 Parameters and evaluation

This section will explain how the parameters in the used models are obtained for this project. Some of them are model specific, whereas other are more general. Most parameters are evaluated for many soil samples and used to determine the final values for the model, see Chapter 4 for details. The only difference in parameters between the SS model and SSC is the modified creep index, μ*. A few parameters are not mentioned here as they are not considered to be relevant in this project, these are all left at default settings in Plaxis.

3.4.2.1 Modified swelling index, κ* and modified compression index, λ*

To calculate κ* and λ*, CRS-tests are performed on the soil samples. The stress in the form of ln(p') is plotted on the x-axis against vertical strain on the y-axis, see Figure 3.14.

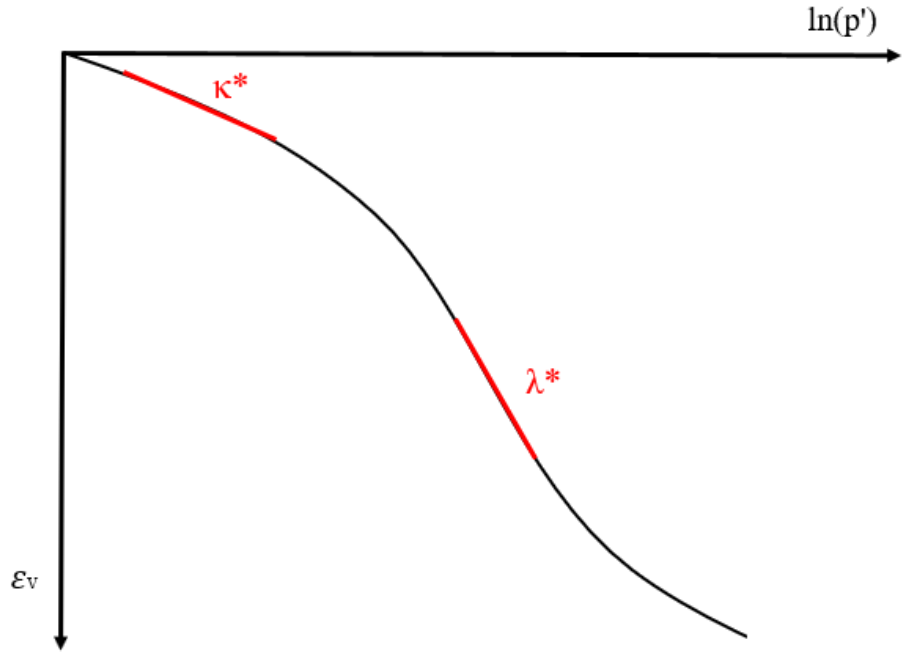

Figure 3.14: Evaluation of κ and λ* from a CRS-test.*

κ* is the inclination of the elastic part and λ* is the inclination of the plastic part. The more common parameters for swelling and compression, C_s and C_c correlates to κ* and λ* as described by Equation 3.9 and 3.10, where e is the void ratio.

$$\lambda^* = \frac{C_C}{2.3(1+e)} \qquad \text{Eq. (3.9)}$$

$$\kappa^* \approx \frac{2C_s}{2.3(1+e)} \qquad \text{Eq. (3.10)}$$

The most realistic values of κ* are obtained from unloading paths which usually have higher stiffness than the initial loading. If the tests have not been unloaded, as the example in Figure 3.14, the values of κ* can be divided by 3-5 based on empirical knowledge. The values of κ* are evaluated by three different methods which are all used to get an indication of the proper κ*. The first is the inclination of the curve in ln(p') scale as in Figure 3.14. κ* is in this case derived at the in-situ pressure because the relationship between stress and strain is most relevant in this point. The second way is via the M_0 parameter which commonly is used in Sweden, it is the inclination of the elastic part of a CRS-curve in linear scale. M_0 is evaluated for the available tests and converted to κ* by Equation 3.11 (Olsson, 2010). Lastly, the bulk modulus, K, is calculated for different values of κ* by Equation 3.12. K relates to the oedometer modulus, M, by Equation 3.13 (Larsson, 2008) where ν_{ur} is Poisson's ratio for unloading-reloading. By these relationships, the values of κ* can be adjusted to make M fit the distribution of M_0.

$$\kappa^* \approx \frac{2\sigma'_v}{M_0} \qquad \text{Eq. (3.11)}$$

$$K = \frac{p'}{\kappa^*} \quad \text{Eq. (3.12)}$$

$$M = \frac{3K(1-\nu_{ur})}{1+\nu_{ur}} \quad \text{Eq. (3.13)}$$

3.4.2.2 Modified creep index, μ*

The modified creep index relates to C_α in the same way as λ* relates to C_c in Equation 3.9. To evaluate the μ* properly, incremental loading oedometer tests shall be performed. In this project there is however no incremental loading oedometer data available. Instead, μ* will be adjusted in Plaxis soil test tool to have the same creep as is observed in the CRS-tests.

3.4.2.3 Overconsolidation, OCR or POP

The input parameter for overconsolidation in Plaxis is either overconsolidation ratio, OCR or pre-overburden pressure, POP. OCR is the ratio between σ'_c and σ'_v. POP is the difference between the pressures. The decision of which to use is made depending on how the values evolve within each soil layer. σ'_c is evaluated from both CRS-tests and CAUC triaxial tests.

3.4.2.4 Friction angle, φ and effective cohesion, c'ref

The friction angle and the effective cohesion are evaluated from CAUC triaxial tests. φ and c'ref are not expected to have any large influence on the results in the type of calculations which is performed in this project.

3.4.2.5 Coefficient of earth pressure at rest for normally consolidated state, K_0^{NC}

K_0^{NC} is the proportion of the vertical effective stresses which applies in the horizontal direction. It may be changed manually but otherwise it is calculated automatically in Plaxis by Equation 3.14, also known as Jaky's formula.

$$K_0^{NC} = 1 - sin\varphi \quad \text{Eq. (3.14)}$$

3.4.2.6 Permeability, k_x and k_y

The permeability of the soil is obtained from CRS-tests. It is possible to set different permeabilities in different directions in Plaxis, hence k_x and k_y. The permeability is however determined to be the same in all directions in Swedish soft clays (Larsson, 1981). The permeability of a soil decreases during compression. This phenomenon can be included in Plaxis calculations by the input parameter called change of permeability, c_k. The magnitude of compression in this project is nevertheless expected to be too small to have a major impact on the permeability and therefore the permeability is assumed to be constant.

3.4.2.7 Poisson's ratio for unloading-reloading, ν_{ur}

ν_{ur} is usually between 0.1 and 0.2 for soft soils but it is not of much significance unless there is a situation of unloading (Bentley, 2021c). Often the automatic value of 0.15 is not changed but if it is considered important can a more representative value of ν_{ur} be obtained by unloading and reloading drained triaxial tests.

3.4.2.8 Dilatancy angle, ψ

The dilatancy angle should always be set at 0º in the Soft Soil models to not have any plastic volumetric strains at failure (Karstunen & Amavasai, 2017).

3.4.3 Piles in Plaxis

As explained in Section 3.3.2, piles are an important aspect to analyse when dealing with pore pressure reductions in an urban environment. A truly 2D model would not be able to predict the soil behaviour around piles since most elements are set to be infinetely long in the z-direction. This problem is solved in Plaxis by something called embedded beam rows (Bentley, 2021c). In an embedded beam row, the required properties for the piles may be set, such as stiffness, width, weight and spacing between them. Since the piles are put "on top" of the soil, the unit weight for the pile should be subtracted by the soil weight (Plaxis, 2012). The output results are given as the average deformations in the z-direction and it is also possible to see the settlement of the individual piles. Both end bearing and cohesion piles can be modelled by adjusting the values of skin friction and base resistance. Figure 3.15 displays how the modelled embedded beam row looks in plaxis and how it would look from above.

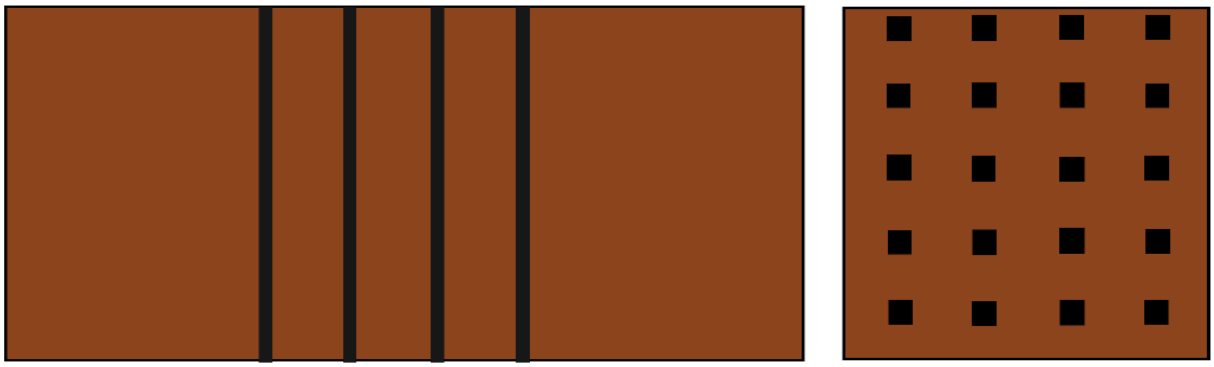

Figure 3.15: Piles in plaxis: a) in 2D view. b) from above.

4 Method

This chapter will describe the soil properties in detail and the used sources of data. It will also explain the different types of analysis performed in Plaxis with corresponding stages, as well as the general settings used and the reasoning behind it.

4.1 Site characterization and simplifications

All data analysed in this project are a part of the site investigations for the West link tunnel. Some of the parameters were already evaluated and are available as public data (Sweco, 2014). Most of the essential parameters for Plaxis can however not be obtained from it. Trafikverket therefore provided a lot of raw data to be used in the analysis. The final values used in the model are mostly from the raw data, but occasionally complemented and adjusted based on the public data and previous knowledge of the local geology. In addition to that, a couple of simplifications are made. All of this is explained in detail below.

Figure 4.1 displays the different locations which the used data was taken from for this project. There are some additional boreholes in the area which are used for the West link project. Those boreholes do however not contain all types of tests and it was for this project considered sufficient to use the four boreholes with complete data. Laboratory tests have been performed on various depths in the four boreholes KK5074, KA5008, KA5031 and KA5040. This included direct shear tests, CAUC triaxial tests, CRS-tests and investigations of unit weight, water content and sensitivity. Triaxial test data was available for 2-4 different depths for each borehole, a total of 13 samples. CRS-data was available for the same points as the triaxial data as well as an additional 10 points, of which 3 were in silty material and could not be evaluated properly. CPT also had been performed in three of the boreholes, but the only data received from it was a graph of how the undrained shear strength changes with depth. All 20 CRS-tests in clay were used to estimate the POP, κ^* and λ^*. From the samples with triaxial data c'ref, φ and additional POP values were evaluated.

The pore pressures have been measured at several locations and depths over time periods of up to 8 years. The pressures fluctuate a bit over time. The maximum and minimum pore pressures for each measurement point in the fill, clay and friction material are displayed in Figure A.1-A.3 in Appendix A. The groundwater level in the upper aquifer is on average 1 m below ground. The pore pressures in the lower aquifer are approximately hydrostatic with a pressure level equivalent to the ground level. The pore pressures in the most upper layers of the clay corresponds to the levels in the upper aquifer while the pore pressure levels in the lower layers are closer to the pressure levels in the lower aquifer. A linear trend can be seen, with zero pore pressures at 1 m depth, and 230 kPa at 23 m depth, which is the bottom of the clay layer.

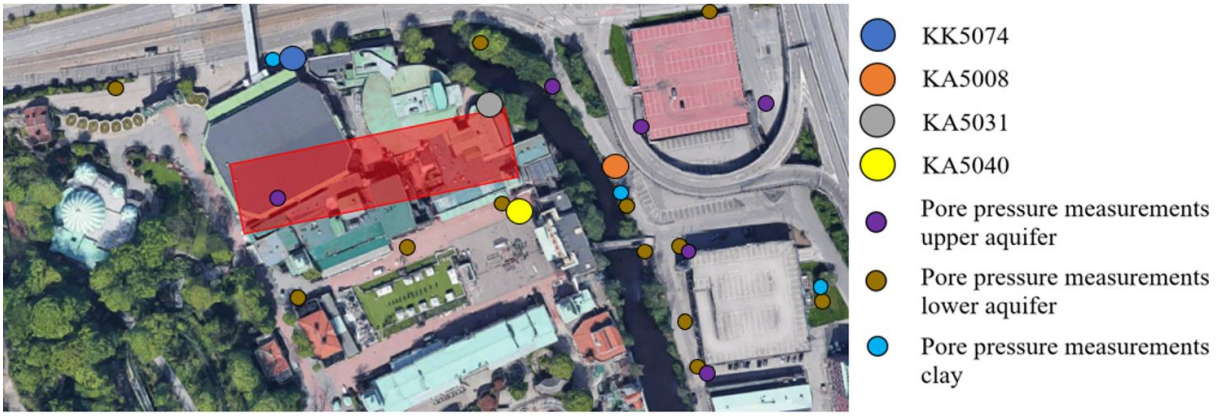

Figure 4.1: Map of the boreholes used in this project (Google, 2021).

Several simplifications have been made to make it possible to assess the problem within the time frame of this project. Because of the potentially large area affected by the pore pressure reduction it is not possible to investigate all of it. For this reason, the entire area is assumed to be homogeneous with soil properties obtained from the test locations in Figure 4.1 above. Despite the relatively short distances between the boreholes, some of the soil parameters do vary significantly. The chosen values for the main part of the analysis are selected to what is believed to represent the reality as good as possible, slightly towards the conservative side when there are large uncertainties. By analysing the soil parameters, the clay has been split into 4 layers. The parameters are summarised in Table 4.1 and some explanations to the values are given below it. The parameters which are not explained are not considered of any major importance and are taken directly from the general values in the area stated by Trafikverket (2016b). In the sensitivity analysis, the impact of the uncertainties regarding the most important input parameters will be evaluated.

The saturated unit weight is 18 kN/m^3 for the fill and 19 kN/m^3 in the friction layer (Trafikverket, 2016b). The unsaturated unit weight is 11 kN/m^3 for both materials. The friction angle in the fill is 35º and in the friction layer it is 39º. The permeability in the friction layer in the studied area is varying between 10^{-7} and 10^{-4} m/s (Sundkvist & Wallroth, 2016). This span is very large, but the exact permeability is not of any importance in the Plaxis calculations as long as it is substantially higher than the clay and allows it to drain freely. The permeability is therefore simply set at 1 m/day which roughly equals 10^{-5} m/s. There is no information available on permeability in the fill and the clay with dry crust properties. It should however not influence the result and it is therefore chosen to be the same as in the friction layer. Any deformations in the friction material are assumed to be insignificantly small compared to the clay. The elastic modulus is therefore set to the very high number of $100*10^6$ kPa. The elastic modulus for the fill is set to 10^3 kPa and the deformation parameters in the dry crust clay is assumed to be the same as the rest of the upper clay layer.

Table 4.1: Parameters for the clay layers.

Depth [m]	Soil	Unit weight [kN/m^3]	κ*[-]	λ*[-]	μ*[-]	POP [kPa]	φ [^{o}]	c'ref [kPa]	Permeability [m/s]
2-5	Dry crust	15 (5)	0.03	0.17	-	15	30	2.4	1.15*10^-5
5-11	Clay 1	15 (5)	0.03	0.17	0.0048	15	30	2.4	2.5*10^-9
11-16	Clay 2	15 (5)	0.03	0.26	0.0052	15	30	3.0	2.5*10^-9
16-19	Clay 3	15 (5)	0.03	0.4	0.0072	15	30	3.6	2.5*10^-9
19-23	Clay 4 (silty)	19 (9)	0.03	0.4	0.0072	24	30	3.6	2.5*10^-9

The laboratory analysis states that the clay starts to become silty at 18 or 21 m depth in the different boreholes. This correlates well with the measured unit weight, displayed in Figure A.4 in Appendix A. The depth of the transition from clay to friction material is set to 23 m based on the undrained shear strength from the CPT, seen in Figure A.5 in Appendix A. From the CPT graph it is only possible to distinguish any major difference in stiffness before the friction layer in one of the boreholes. Several of the CRS-tests yet indicate of having properties more like friction material already at 18 or 21 m depth. A possible reason for this might be that there are very thin layers of silt and the CRS-tests happened to be performed in these layers. The particle arrangement in the tests with silty clay may also have been disturbed when the samples were obtained. Despite that a few samples having properties like friction material, λ* could be evaluated from 4 tests at 18 and 21 m depth. The values of λ* vary a lot and the largest values seem unrealistically high. Due to all the uncertainties, λ* is chosen to be constant from 16 to 23 m depth with a value close to the average of the tests, see Figure A.6 in Appendix A.

The trend values of κ* which are evaluated by the three methods as described in section 3.4.2.1 are equal to 0.04, 0.068 and 0.07, see Figure A.7 and A.8 in Appendix A. The large spread of κ* makes it hard to draw many conclusions. As mentioned previously, κ* is usually too high when evaluated from the initial compression of a CRS-test. To choose a reasonable κ* but remain on the conservative side, the trend values are divided by 2. κ* used in the analysis is therefore set to 0.03.

The graphs from Plaxis soil test tool used to determine μ* are displayed in Figure A.9-A.11 in Appendix A. By the same reasoning as with λ*, μ* is assumed to be the same in clay 3 and 4. The CRS-curves for each soil layer were normalized against σ'_c to make them comparable, and μ* was chosen based on the observed creep. The curves of μ* seen in the figures was also slightly adjusted based on the background creep of 5 mm/year. The difference between the original μ* and the adjusted value is yet small and within the error margin of interpretation of the graphs.

Figure A.12 in Appendix A displays how the POP was chosen. Based on previous knowledge of the region and on the fact that some of the tests seem to have been disturbed, the trend of σ'_c is set at the upper limit of the values for the clay on 8-18 m depth. When calculating σ'_v which is used for determining the POP, the pore pressures in the entire soil are assumed to be

hydrostatic from 1 m depth. The pore pressures are in reality a bit larger towards the bottom of the clay layer as explained before. This is a conservative simplification since it makes the σ'_v slightly larger and thus the POP smaller. The error is however small and combined with uncertainties regarding exact pore pressures, unit weight and interpretation of the data, the error is considered insignificant.

The permeability of the clay is set to $2.5*10^{-9}$ m/s based on the values in Figure A.13 in Appendix A. The measurements in the silty clay have considerably lower permeability than the rest of the clay. The reason for this might be that the natural structure of the silty clay was disturbed when the tests were obtained. However, the permeability could be lower in this type of soil because of the particle arrangement. To be conservative it is assumed that the permeability is the same as in the rest of the clay.

The triaxial data can be found in Figure A.14-A.17 in Appendix A. By normalizing the p'-q graphs against σ'_c, it can be determined that the curves from the depths 15 m and below look relatively similar. The data on shallower clay is more irregular and at least some tests appear to be disturbed. By ignoring the outliers, a vague trend may be seen. The values of c'ref obtained from the tests are very high for being Gothenburg clay. The effective cohesion and friction angle should not have a major impact on the results of the settlement analysis. However, to be on the safe side, the general values for soft clay in Sweden are instead used in the calculations, specifically $c'ref = 0.1*c_u$ and $\varphi=30^o$. The values of c_u are also obtained from the triaxial tests.

4.2 Plaxis calculations and settings

To model the problem in Plaxis, the soil is divided into layers with characteristics as explained above. Since this study only considers the effects of a pore pressure reduction from the deep excavation and not any effects of the excavation itself, the model is quite simple with no additional structures. To simulate the relation between pore pressures in the clay and the other layers, the water conditions in clay layer 1-4 are set to be interpolated during all phases. Pore pressure reductions in the friction layer of 10, 20, 40 and 60 kPa will be analysed for time spans of up to 10 000 days. The most interesting time spans to analyse are however considerably shorter and within the construction time of a couple of years. The pore pressure reduction in all calculations is assumed to occur over 2.5 days. The calculation type in the initial phase is K0 procedure because there are no inclined soil layers. In all other phases the calculation type is consolidation.

All calculations are made with 15-noded elements. A brief mesh sensitivity analysis was performed to investigate the effects of the mesh quality. No significant difference was seen when the mesh quality was higher than "fine". To ensure accurate results in all calculations, the mesh quality is nevertheless set to "very fine". The size of the model is not relevant for the main part of the calculations since the model is homogeneous and only considers 2D consolidation. The groundwater flow boundaries are closed in the x-direction and open in the y-direction to allow the water to flow away. The deformation boundaries are free at y-maximum and fully fixed at y-minimum. In the x-direction they are normally fixed to prevent interaction with the soil.

All calculations for clay layer 1-4 are performed with both SS and SSC model. In the calculations using SSC, the background creep rate is subtracted from the results given in Plaxis. The background creep in each case is determined by running the model for the same periods without any stress changes. The constitutive model for the fill and the friction layer is Mohr-Coulomb. In the clay with dry crust properties, the SS model is used for all calculations since no pore pressure change occurs and any background creep is not relevant since it would be subtracted anyway.

4.2.1 Recovery after a pore pressure reduction

Since the pore pressures in the clay are time dependant, it is interesting to analyse how the soil behaves after the pore pressures in the friction layer returns to normal. This is done by reducing the pore pressures in the friction material for 300 days and then restoring them back to the initial conditions. The results from this analysis may not be the most accurate because the constitutive models are not optimal for this type of calculations. ν_{ur} also has a slight influence on the results and it is assumed to be the default value of 0.15. The analysis should still give a good hint of the soil behaviour.

4.2.2 Analysis of piled buildings

To analyse how piled buildings influence the area, it is examined in Plaxis. Because of the relatively shallow soil depth in the area, it is assumed that all piled buildings are connected to the friction layer or the bedrock. Because this analysis mainly is performed to assess the magnitude of the problem, it was decided to only do the most of calculations for one case and adjust the time to assess different maximum settlements. The chosen case is a pore pressure reduction of 40 kPa with the SS model. Maximum settlements of 0.05-0.3 m are tested. The effects of other pore pressure reductions and differences between the models is also briefly investigated. The simulation of a piled building in the Plaxis model is displayed in Figure 4.2. It consists of 7 embedded beam rows, 3 meters apart with an overlying plate which is 20 m wide. The model is in total 180 m wide to ensure that no mesh related errors occur. Since it is out of the scope to study buildings in detail, many of the input values are taken directly from a report studying embedded pile rows in Plaxis (Plaxis, 2012). Some of the parameters are adjusted to correctly resemble typical Swedish concrete piles. All input values can be seen in Table 4.2. The plate on top is also made of concrete and is assumed to be weightless to not disturb the stress state. The input values for the plate are displayed in Table 4.3. Both the piles and the plate are supposed to be over dimensioned and only deform elastic.

Table 4.2: Input values for the embedded beam rows.

Elastic modulus	$20*10^6$ kPa
Unit weight	10 kN/m^3 (25-15, since the soil weight is subtracted)
Beam type	Massive square beam
Width	0.27 m
$L_{spacing}$	3 m
Axial skin resistance	Linear
T_{skin} top, max	10 kN/m
T_{skin} bottom, max	100 kN/m
Base resistance	1000 kN

Table 4.3: Input values for the plate.

Elastic modulus	$20*10^6$ kPa
Flexural rigidity	$20*10^6$ kN/m
Weight	0

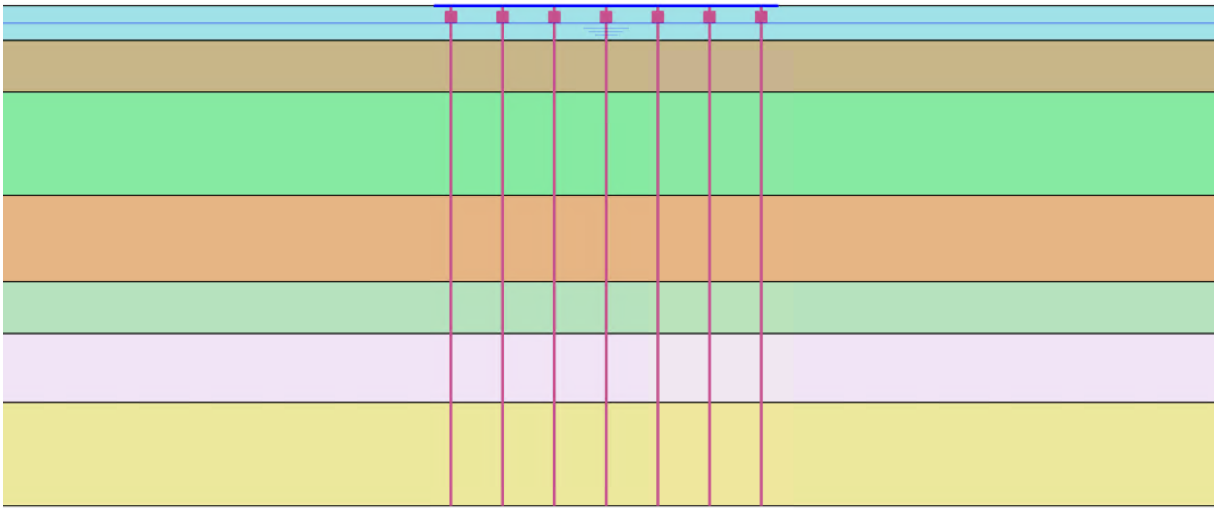

Figure 4.2: Plaxis model with piles.

4.3 Sensitivity analysis

The sensitivity analysis is performed to investigate how large impact various parameters in clay layer 1-4 have on the results. The values in the sensitivity analysis are chosen to represent what is believed to be the plausible minimum and maximum values. These values are based on the magnitude of uncertainty in each input parameter. The selected variations are displayed in Table 4.4 and the reasoning behind the magnitude of variation is given below. Some parameters affect the background creep rate. In these occasions μ* will not be adjusted to fit the background creep, but the new background creep will be subtracted from the results.

Table 4.4: Summary of tested deviations in the sensitivity analysis.

Parameter	Original value	Worst plausable case	Best plausable case
λ* clay layer 3 and 4	0.4	0.6	0.2
κ*	0.03	0.45	0.15
POP	15 and 24 kPa	Original -5 kPa and -10 kPa	Original +5 kPa and +10 kPa
Permeability all clay	$2.5*10^{-9}$ m/s	$4*10^{-9}$ m/s	$1*10^{-9}$ m/s
Permeability silty clay	$2.5*10^{-9}$ m/s	$10*10^{-9}$ m/s	$0.4*10^{-9}$ m/s
c'ref and φ	$0.1*c_u$ and 30°	-	2-13 m depth: 7 kPa and 35° 13-23 m depth: 13 kPa and 28°

The uncertainties regarding the depth of transition between clay and silty clay as well as the properties for these layers are quite large. To cover most of the possibilities, λ* will be varied to 0.2 and 0.6 in both clay layer 3 and 4. The values of λ* in clay layers 1 and 2 are relatively regular in all tests and will not be changed.

In the main analysis, the obtained value of κ* was divided by 2 because it was evaluated from the initial loading of CRS-tests and not from unloading-reloading. It was still a rather

conservative approach and in the sensitivity analysis, the evaluated κ* will be divided by 4 instead, making it equal to 0.015. Due to the large spread of κ* the actual value could also be higher than 0.03. For this reason, the effect of having a κ* of 0.045 is investigated.

Since the used constitutive models are very sensitive to changes in POP, it is very important to investigate the impact of the uncertainties related to it. Small inaccuracies in unit weight, pore pressures, exact depth of tests and interpretation of the CRS-data may result in rather large errors. Therefore, the POP will be varied to both +/-5 and +/-10 kPa in the sensitivity analysis.

Most of the values of permeability in the clay layer vary between $1*10^{-9}$ m/s and $4*10^{-9}$ m/s, see Figure A.13 in Appendix A. The possible effects of these deviations will be analysed. As mentioned previously there is an additional uncertainty regarding the permeability in the silty clay. The measured permeability for the silty clay is on average only $0.4*10^{-9}$ m/s and indicates lower permeability in the layer. Another possibility is that the overall permeability in the silty layer is equal or higher compared to the rest of the clay. This could happen if silt is grouped into thin layers and the measured soil did not contain any layer, or if the layers were disturbed when the samples were obtained. The effect of a permeability of $10*10^{-9}$ in the silty clay will therefore be tested.

The values of c'ref evaluated from the triaxial tests are very high, therefore were instead more general values of c'ref and φ used in the main analysis. In the sensitivity analysis, the influence of using the evaluated values will be studied. They are according to Figure A.15 and A.16 in Appendix A: c'ref=7 kPa and φ=35º for depths less than 13 m and c'ref=13 kPa and φ=28º below 13 m.

5 Results and Discussion

This chapter will present the results of the Plaxis calculations performed as described in Chapter 4. The results and the discussion around it are presented together to make it easier to follow the process. A few sources of error are also discussed along with the results to bring the discussion forward. Some more general discussion points and sources of error will be assessed at the end of the chapter.

5.1 Main calculations

Figure 5.1 displays how the settlements at ground level, with and without creep, develop over time for the different pore pressure reductions. For more detailed graphs, see Figure B.1-B.5 in Appendix B where the same results are displayed with other scales on the axis. The background creep, which already is subtracted from the results in Figure 5.1, is shown in Figure B.6 in Appendix B.

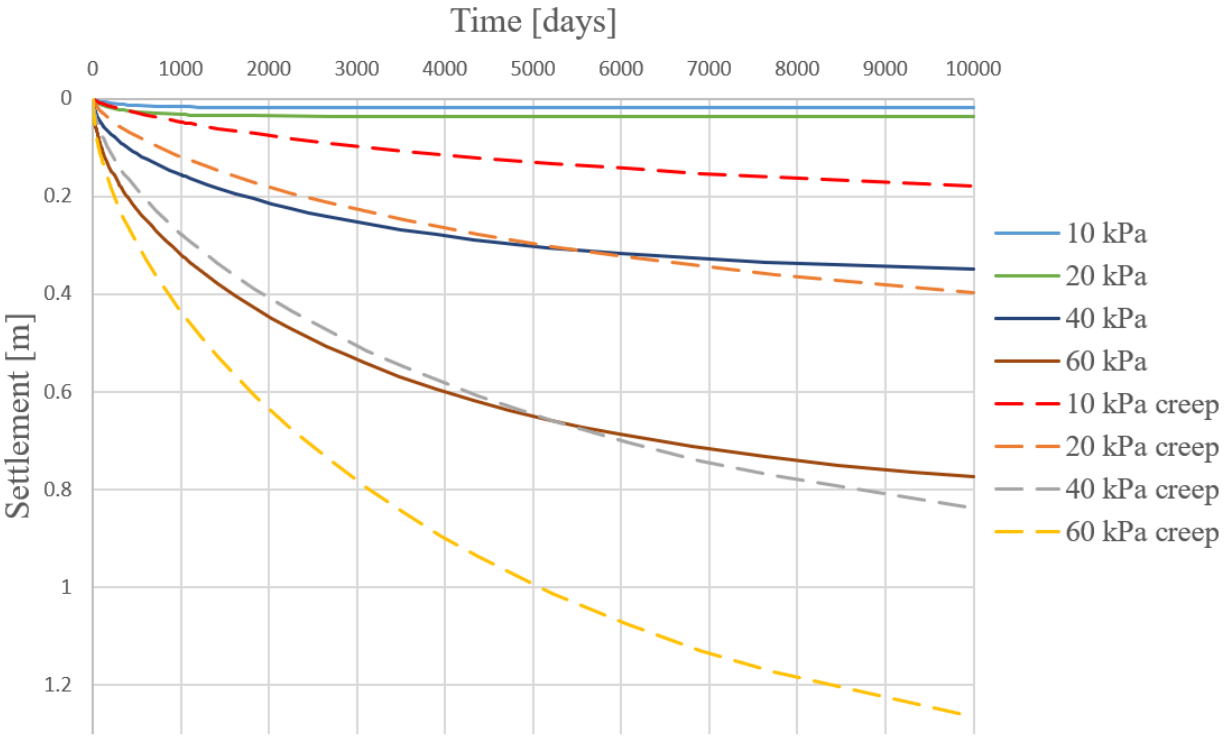

Figure 5.1: Settlement development over 10 000 days for various pore pressure reductions.

Creep effects have a significant impact on all the results. The differences between the model with and without creep becomes extra apparent for the pore pressure reductions of 10 and 20 kPa. When using the SS model, no plastic deformations will occur until the preconsolidation pressure is reached. A reduction of 10 kPa without creep will thus not cause any plastic deformations at all since the POP is above 10 kPa for all clay layers. In the case of a 20 kPa reduction without creep, no plastic deformations occur in clay layer 4. The final pore pressure reduction at the bottom of clay layer 3 is however equal to 15.6 kPa in comparison to a POP of 15 kPa. The plastic deformations after a 20 kPa reduction are very small since the effective stress just exceed the preconsolidation pressure by a maximum of 0.6 kPa. It can yet be concluded that 20 kPa roughly is the tipping point for the possibilities of having plastic strains in the SS model. With the model accounting for creep, larger deformations start to occur before

the preconsolidation pressure is reached. As seen in the cases of 10 and 20 kPa reductions with creep, small changes in effective stress have a very large impact on the deformations over time when the POP in the clay is small. This behaviour clearly resembles reality in a better way than the SS model, considering the theory of creep. The difference in settlements between the models is much smaller for the cases of 40 and 60 kPa pore pressure reductions because relatively large plastic strains take place in the SS model. The differences between the models should be smaller the larger the pore pressure reduction is.

Creep does not have as large of an impact when considering shorter time periods, which are more likely to be the problem when constructing deep excavations. Figure 5.2 and 5.3 display the relationship between depth, settlements and excess pore pressures for different times after a pore pressure reduction of 40 kPa. Figure 5.2 is with the SS model and Figure 5.3 is with the SSC model. Similar graphs for other pore pressure reductions are displayed in Figure B.7-B.12 in Appendix B.

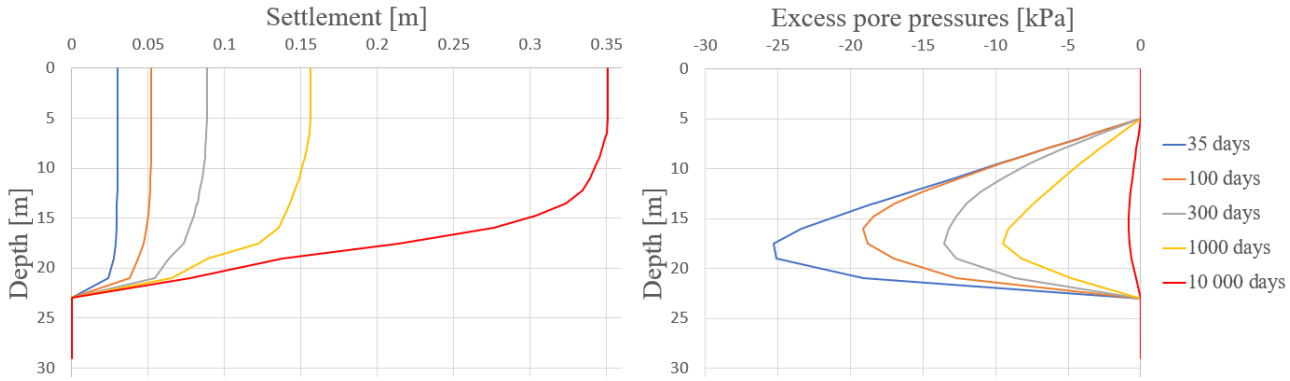

Figure 5.2: Settlements and excess pore pressures for various times after a pore pressure reduction of 40 kPa without creep.

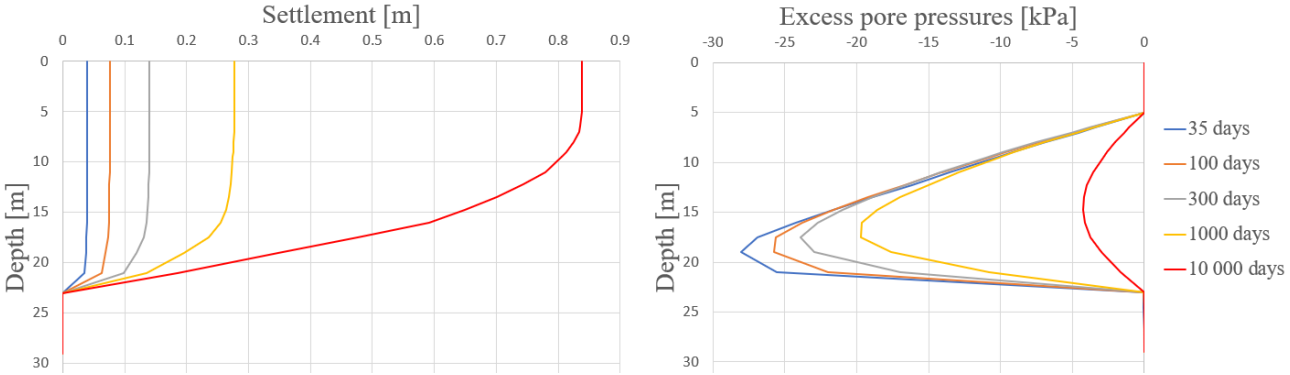

Figure 5.3: Settlements and excess pore pressures for various times after a pore pressure reduction of 40 kPa with creep.

The differences between the pore pressure distributions in the two models are rather large. By studying Figure 5.2 and 5.3, it becomes clear that both the maximum and the average excess pore pressures at all stages are considerably larger in the SSC model. Moreover, the difference in percent become larger over time. A large reason why the differences are larger in the long term likely is because the creep induces extra excess pore pressures which require time to dissipate, and thus the effective stress increase also is delayed. For example, after 1000 days and a 40 kPa pore pressure reduction with the SSC model, the pore pressures are still almost equal to the initial pressures down to 12 m depth. At 12 m depth without creep, more than half

of the excess pore pressures have already dissipated after 1000 days. The same trend can also be seen for the other pore pressure reductions. After a 10 kPa reduction with creep, the excess pore pressures in the upper layer will even increase for up to 300 days due to the creep.

It is totally reasonable that there are larger excess pore pressures when creep is considered. The SSC model is however known to predict too large excess pore pressures due to the creep. These issues might be even more substantial with large excess pore pressures after the pore pressure reduction. If this is the case, it is possible that the settlements are underpredicted with the SSC model, especially for short time periods when less of the excess pore pressures have dissipated. Another issue with the SSC model is that the creep needs some time to set up properly in the beginning. When looking at the background creep, the creep rate is initially too slow, and it takes around 200 days until the creep rate is as it should be. The same thing likely occurs in the stages when the pore pressures reduce and thus could the SSC model predict too little creep in the early stages for this reason as well. This issue could be solved by running the model for a time before the pore pressure reductions take place. It would however create other problems since the background creep increases the preconsolidation pressure in the soil.

Another aspect is that all deformations cause excess pore pressures. This becomes very apparent when analysing some of the excess pore pressure curves without creep, see for example Figure 5.4.

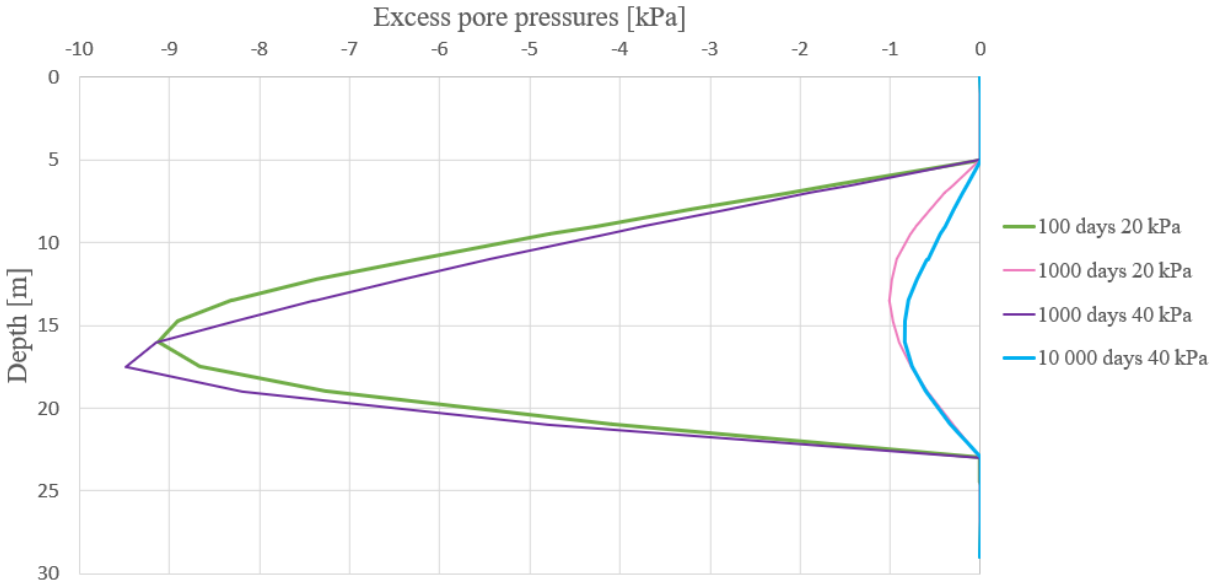

Figure 5.4: Examples of excess pore pressure distributions with the SS model.

The curve 100 days after a reduction of 20 kPa looks very similar to the one 1000 days after a reduction of 40 kPa. Simultaneously, the excess pore pressure distribution 1000 days after a reduction of 20 kPa is fairly similar to the distribution 10 000 days after a 40 kPa reduction. It does in other words take almost 10 times longer for roughly the same pore pressure reduction to occur when the settlements are much larger. This is an extreme case since 20 kPa is on the boundary to having plastic strains, but it proves that deformations have a large effect on the excess pore pressures.

It is further interesting to analyse how the settlements are distributed in the soil. As expected, the settlements will initially take place in the bottom of the clay and move upwards with time,

just as the pore pressure reduction. Settlements on smaller depths occur earlier with the SS model because the excess pore pressures dissipate faster. Most of the pore pressures will dissipate within 1000 days for the pore pressure reductions of 10 and 20 kPa. The larger reductions require much more time, both because more water must leave the clay and because larger deformations cause additional excess pore pressures as just described. With the SSC model, the settlement distribution looks very similar for all investigated times and pore pressure reductions. The changes in pore pressures and settlements above 15 m depth are very small for all times up to 1000 days. The properties of the shallower layers are thus concluded to not be very important, at least for the larger pore pressure reductions since they are very unlikely to occur for longer time periods than 1000 days.

The final settlement distribution towards the depth after 10 000 days is approximately the same for all cases except for 10 and 20 kPa reductions without creep. It is again because the settlements after small pore pressure reductions in the SS model are purely elastic and not affected by λ^* which is larger at larger depths. In all the other cases, over 2/3 of the settlements after 10 000 days do occur at 16-23 m depth. The share of settlements below 16 m seem to be a bit higher for larger pore pressure reductions. It is probably because the total excess pore pressures are larger, and therefore a higher share of the pore pressure reduction in the shallower soil occur later than 10 000 days.

Another notable result from the pore pressure graphs is that the excess pore pressures which are close to the friction layer in clay 4 equalise relatively fast. Already after 35 days, the maximum excess pore pressures has decreased by at least 28% in all cases. The settlement rates are yet not that much faster in the beginning thanks to the higher POP in clay 4. If the POP had been lower, much larger settlements would occur at the early stages for most cases.

By the definitions from Table 3.1, buildings could be moderately damaged by settlements above 50 mm and severely damaged once the settlements pass 75 mm. Of the two used models, the SSC model is believed to achieve the most accurate results. With this model, it takes 1100 days to reach settlements of 50 mm after a 10 kPa reduction. The corresponding times for 20, 40 and 60 kPa are 260, 51 and 21 days, respectively. It is however not certain that the largest pore pressure reductions are the largest risk factors. In the case of a pore pressure reduction of for instance 60 kPa, actions will likely be taken almost immediately. Meanwhile, a pore pressure reduction of 10 kPa would possibly not be seen as a large issue and could even be mistaken as a natural fluctuation. If the finished tunnel for some reason would leak and cause a permanent reduction of 10 kPa, the settlement over 10 000 days reaches 18 cm.

5.2 Recovery after a pore pressure reduction

Figure 5.5 displays how the settlements at the ground level recover if the pore pressures in the friction layer go back to the original levels after 300 days of reduction.

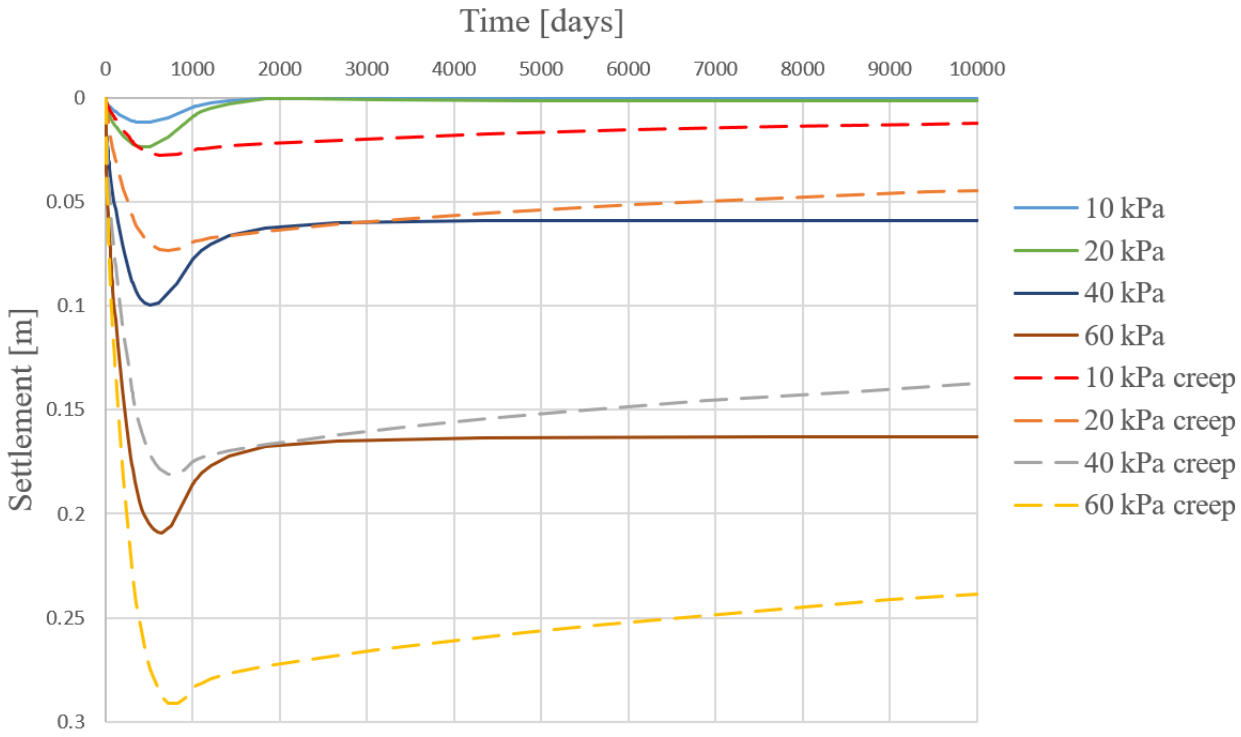

Figure 5.5: Recovery of settlements after a pore pressure reduction during 300 days.

Because of the characteristics of the SS model, all elastic deformations will recover if the pore pressures go back to normal. This is evident in the cases with pore reductions of 10 and 20 kPa. For the pore pressure reduction of 40 kPa does 41% of the maximum settlement recover and the corresponding value for a 60 kPa reduction is 22%. The soil continues to settle between 100 and 350 days after the pore pressures in the friction layer returns to normal. The reason for the delay is because it takes time for the increased pressures to reach the clay further away from the friction layer. Thus, the pressures at certain depths will continue to decrease for a period after 300 days. The time it takes until the ground level starts to move upwards because the pore pressures in most of the clay start to increase again is dependant on how affected the pore pressures are. After a reduction of 60 kPa, more water has left the clay and therefore it takes more time for the pore pressures to return compared to the other reductions. The same trend is seen when analysing the time it takes until steady state is reached after the reduction.

At first glance of the settlements with creep in Figure 5.5, it looks like the settlements recover over a very long period. This is partially correct, but the reason why the ground surface seems to rise is because the background creep is subtracted. When the creep rate increases due to the pore pressure reduction, the overconsolidation ratio does also increase. The creep rate will therefore be smaller than the initial background creep for a long time after the pore pressures have returned to normal in the friction layer. Larger pore pressure reductions result in larger changes to the overconsolidation ratio, and the creep rate is more affected over time. The percentage of the settlements which recover after 10 000 days are much larger for smaller pore pressure reductions. For example, 55% of the settlements do recover after a pore pressure

reduction of 10 kPa, but only 16% after a reduction of 60 kPa. Smaller pore pressure reductions should result in more recoverable settlement since a larger share of the deformations are elastic. The difference is yet not as significant as in the example since the settlements continue to recover after 10 000 days. Considering short term building damage, the recovery of settlements predicted by the SSC model should not have much effect since the damage already has occurred when the settlements start to recover. Having less settlements in the long term are however beneficial, especially if the buildings must be repaired after the pore pressure reduction.

The number of days until settlements of 50 mm have occurred with the SSC model were stated in the previous section. These numbers are still correct, but it is important to remember that it is not the same thing as the maximum tolerable days of the pore pressure reduction to avoid settlements above 50 mm. For the case of a 300-day pore pressure reduction with SSC, the maximum settlements due to the pressure reduction are around 30% higher than the settlements after 300 days. The difference between the maximum settlements and the settlements at the end of the pore pressure reduction should yet be smaller when the pore pressures are reduced for shorter periods. This is because the affected pore pressures after shorter times are in the clay closer to the friction layer.

5.3 Analysis of piled buildings

The settlement distribution at the ground level for different maximum settlements close to a building piled to the bedrock is displayed in Figure 5.6. The calculations are performed as described in Section 4.2.2.

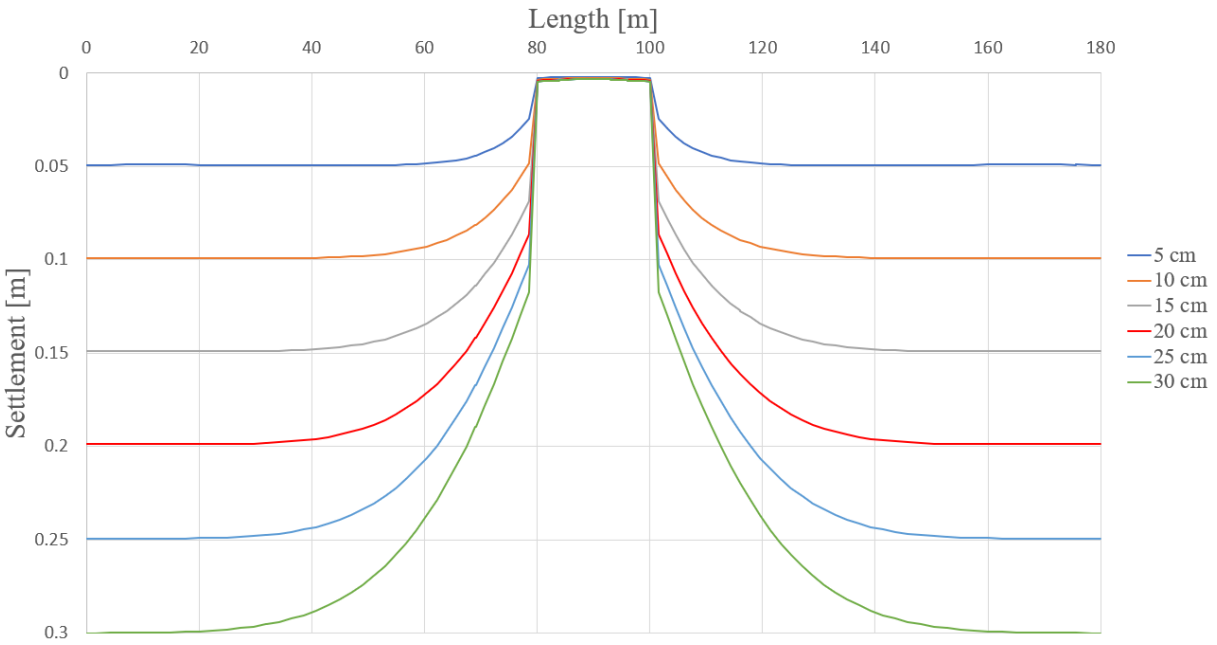

Figure 5.6: Settlements at the ground level close to a building piled to the bedrock.

A similar pattern can be seen for all investigated values of maximum settlements. To begin with, the building itself does barely settle at all because the piles are very stiff and are assumed to only deform elastic. The soil immediately to the side of the building do settle for 39-49% of the maximum settlement, with lower shares for larger settlements. The settlement profile after the immediate settlement is relatively linear for a distance of 5.9 to 14.3 m. This is where the inclination of the ground surface is the largest. After the steepest part, the size of the settlements

continues to increase, but with decreasing rate until the settlements are equal to the maximum settlements. Buildings in this range could potentially be subjected to sagging. The largest deflection ratios for the ground surface are about the same as the critical ratio of 1/2500. The deflection ratio for the building foundations is however most likely smaller since the foundations should be stiffer than the filling material and not bend as much.

Table 5.1 summarises the meaningful results for each studied value of maximum settlement. The distance to the point which has 0.2% inclination is included because it is the smallest inclination where problems related to inclined settlements might occur according to Table 3.1. The total distance influenced is defined as the point where the settlements are 0.5 cm less than the maximum settlement.

Table 5.1: Key results related to problems with settlements close to piled buildings.

Maximum settlement [cm]	Immediate settlement [cm]	Maximum inclination [%]	Length steepest part [m]	Distance to 0.2% inclination [m]	Total distance influenced [m]
5	2.45	0.21	5.9	6	12.6
10	4.81	0.33	7.7	9	23.2
15	6.88	0.42	9.3	13	31.0
20	8.61	0.51	10.9	16	39.2
25	10.23	0.58	12.6	23	43.6
30	11.72	0.65	14.3	27	48.0

If the immediate settlements close to the buildings are as large as the model suggests, it will be a problem for piled buildings since the connecting entrances move several centimetres further down. The problems should nevertheless be relatively easy and cheap to fix compared to the problems for buildings without piles. All the issues associated with inclined settlements do increase with increasing maximum settlements. By reviewing Table 3.1, it can be determined that the size of the maximum settlements generally should be a much bigger issue than the inclined settlements. For example, the expected damage is severe already at 10 cm of maximum settlements, while the overall maximum inclination of 0.65% is in the lower range of moderate damage. The type of damage from maximum and inclined settlements could still be different and therefore it is still relevant to consider the effects of piled buildings when investigating settlements in urban areas.

The analysis of piled buildings was only performed for the case of a pore pressure reduction of 40 kPa without creep. The effects of other pore pressure reductions and the differences compared to the SSC model were also briefly examined. The characteristics of the inclined settlements seem to mainly be influenced by how the settlements are distributed within the soil. When more of the settlements take place at larger depths, the immediate settlements adjacent to the buildings and the maximum inclinations are a bit larger, while the influenced area is smaller. The differences are yet not large enough to affect any of the conclusions.

5.4 Sensitivity analysis of input parameters

This section is going to present the results of the sensitivity analysis which are performed as described in Section 4.3. A positive change in settlement means that the settlements are larger than before. It is unfeasible to comment every single result because the effect of changes to each parameter is tested with and without creep for four different pore pressure reductions during five different time periods. The obtained results can sometimes also be a combination of many different factors. Only the most interesting results and the most influential factors are therefore discussed. The most important findings of the sensitivity analysis are summarised at the end.

5.4.1 Sensitivity to changes of λ* in clay layer 3 and 4

Figure 5.7 and 5.8 display how the settlements change compared to the original calculations when λ* is modified to 0.2 and 0.6 in clay layer 3 and 4.

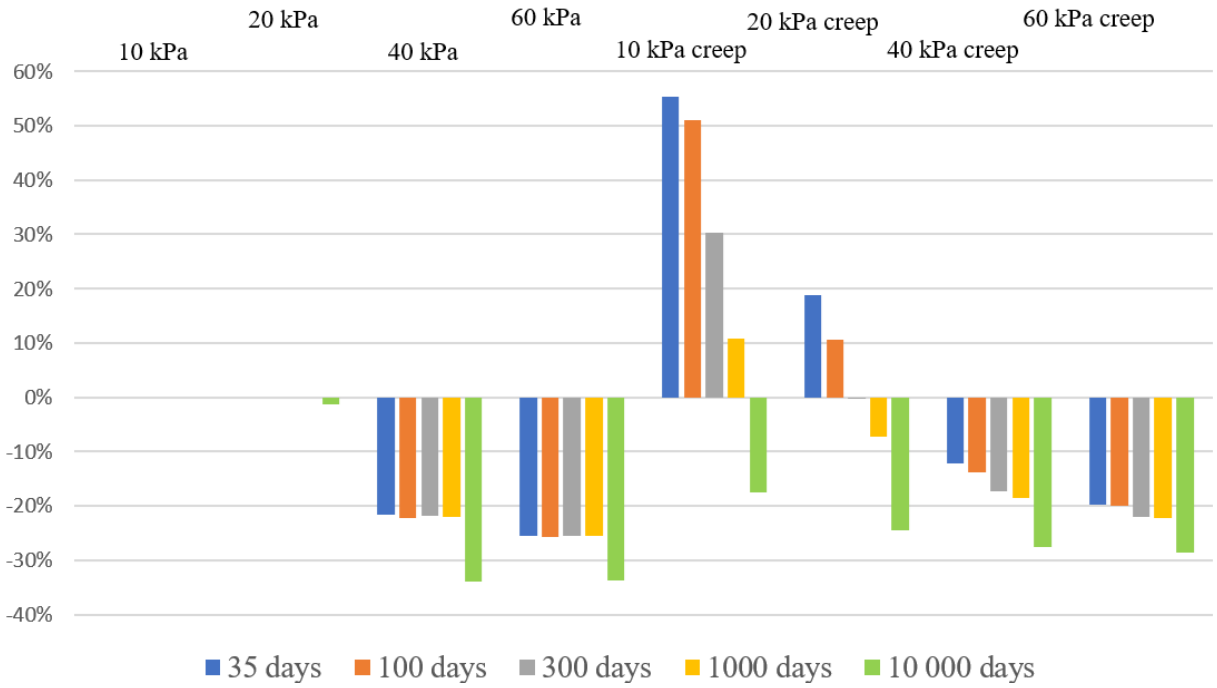

Figure 5.7: Change of settlements when λ is set to 0.2 in clay layer 3-4, compared to the original case.*

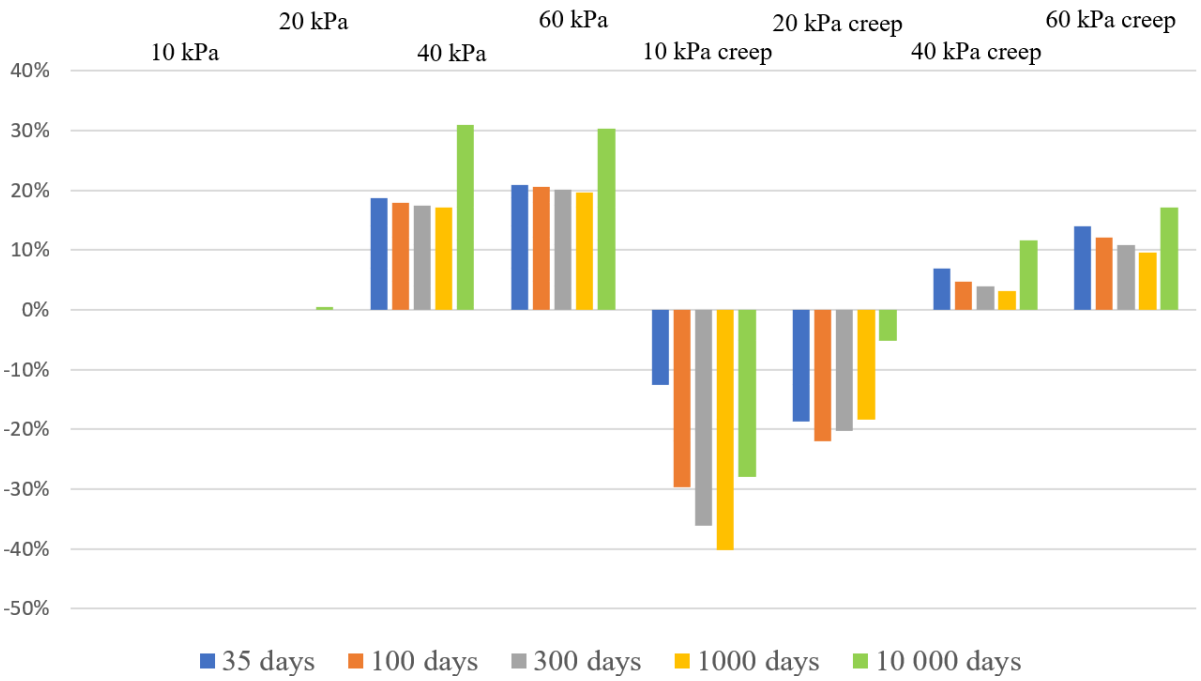

Figure 5.8: Change of settlements when λ is set to 0.6 in clay layer 3-4, compared to the original case.*

With the SS model, changes of λ* do not affect the results for pore pressure reductions of 10 and 20 kPa. This is unrealistic but expected since no plastic deformations occur when the stress is smaller than the preconsolidation pressure. Because plastic strains start to occur at pore pressure reductions of 20 kPa, the influence of λ* should increase gradually when the pore pressure reduction becomes larger than 20 kPa. Changes of λ* will however not affect the results much more than it does for the reduction of 60 kPa since almost all the deformations already are plastic at that stage.

The results for small pore pressure reductions with creep are completely opposite to what is expected for most time spans. The reason for this is most likely that changes to λ* drastically influence how the creep model behaves due to the characteristics of Equation 3.8. The error seems to be smaller for larger pore pressure reductions where the settlements are less affected by the creep, but it is nevertheless uncertain how large the error becomes. This issue could potentially be reduced by to readjusting μ* to have the same background creep as before.

Because of the uncertainties regarding the creep rate, it is hard to draw any definitive conclusions of how important λ* is in the SSC model. λ* should have a larger impact on the larger pore pressure reductions since the effective stress is higher compared to the preconsolidation pressure. It is also hard to tell if λ* should have the most impact in short or long term. A larger proportion of the excess pore pressure dissipation occurs in clay layer 3 and 4 during shorter time spans compared to clay layer 3 and 4. On the other hand, the stress state is further away from the preconsolidation pressure in the early stages and more of the deformations are elastic. The actual influence of λ* with the SSC model should at least not exceed the influence λ* has on the SS model for the larger pore pressure reductions. This is because some of the strains are due to creep in the SSC model.

5.4.2 Sensitivity to changes of κ*

Figure 5.9 and 5.10 display how the settlements are altered compared to the original calculations when κ* is changed to 0.015 and 0.045.

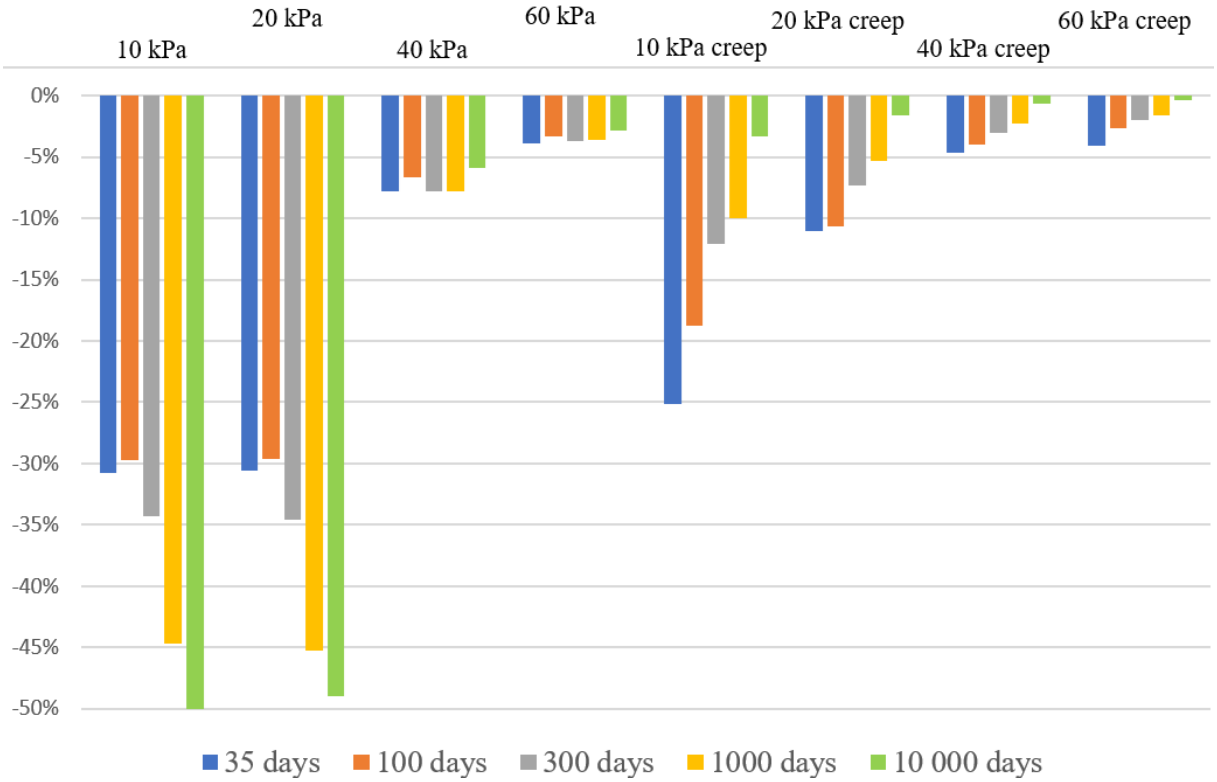

Figure 5.9: Change of settlements when κ is set to 0.015 in clay layer 1-4, compared to the original case.*

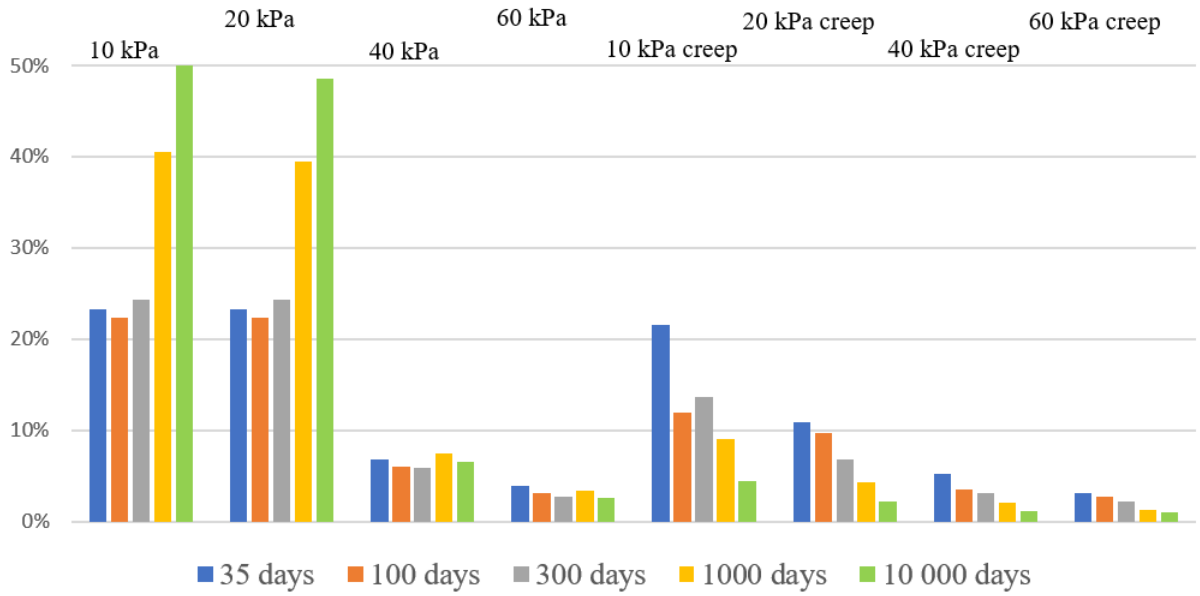

Figure 5.10: Change of settlements when κ is set to 0.045 in clay layer 1-4, compared to the original case.*

It is evident from the figures that κ* has a large impact on small pore pressure reductions but not so much on the larger reductions, just as expected. For the small pore pressure reductions of 10 and 20 kPa with the SS model, the changes are much larger in the long term. This should be because in the short term, the change of κ* affect the excess pore pressures since the deformations are different from before. In the long term, all excess pore pressures have time to

dissipate and the settlements change as much as κ* is changed, +/- 50%. With the SSC model, κ* influences the settlement more in short time periods than during longer periods. This is because a larger share of the strains are elastic in the beginning when the ratio between the effective stress and preconsolidation pressure is smaller.

5.4.3 Sensitivity to changes of the POP

Figure 5.11-5.14 display how the settlements change compared to the original calculations when the POP is decreased and increased by 5 and 10 kPa.

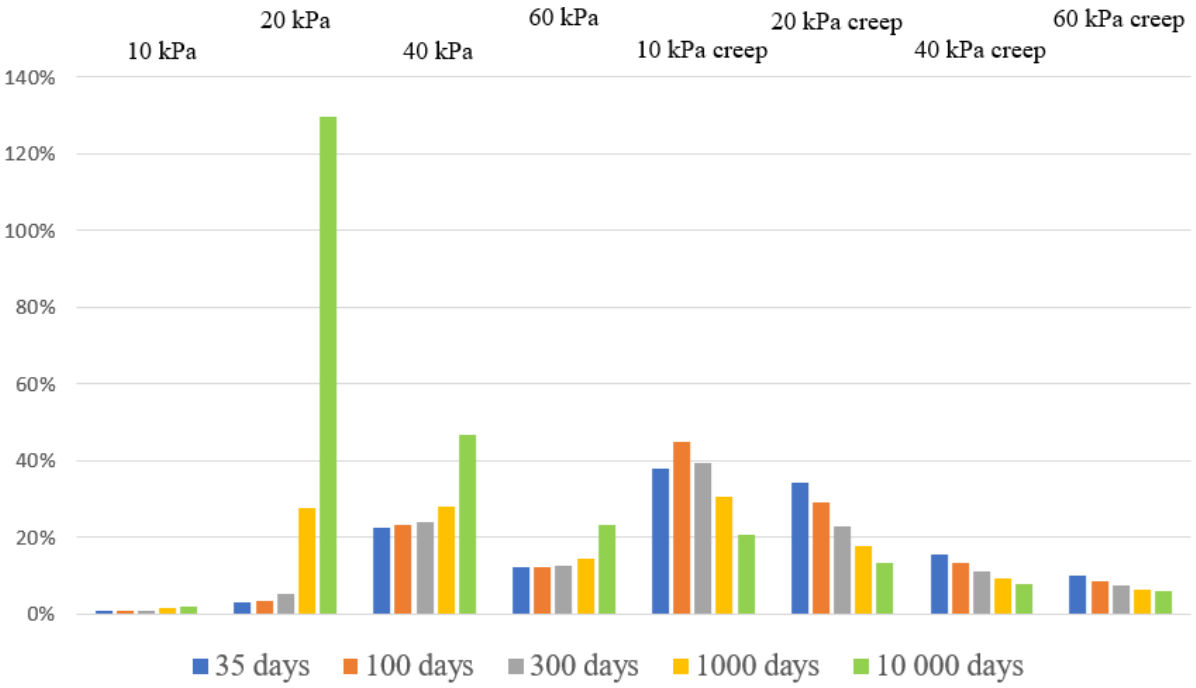

Figure 5.11: Change of settlements when the POP is decreased by 5 kPa in clay layer 1-4, compared to the original case.

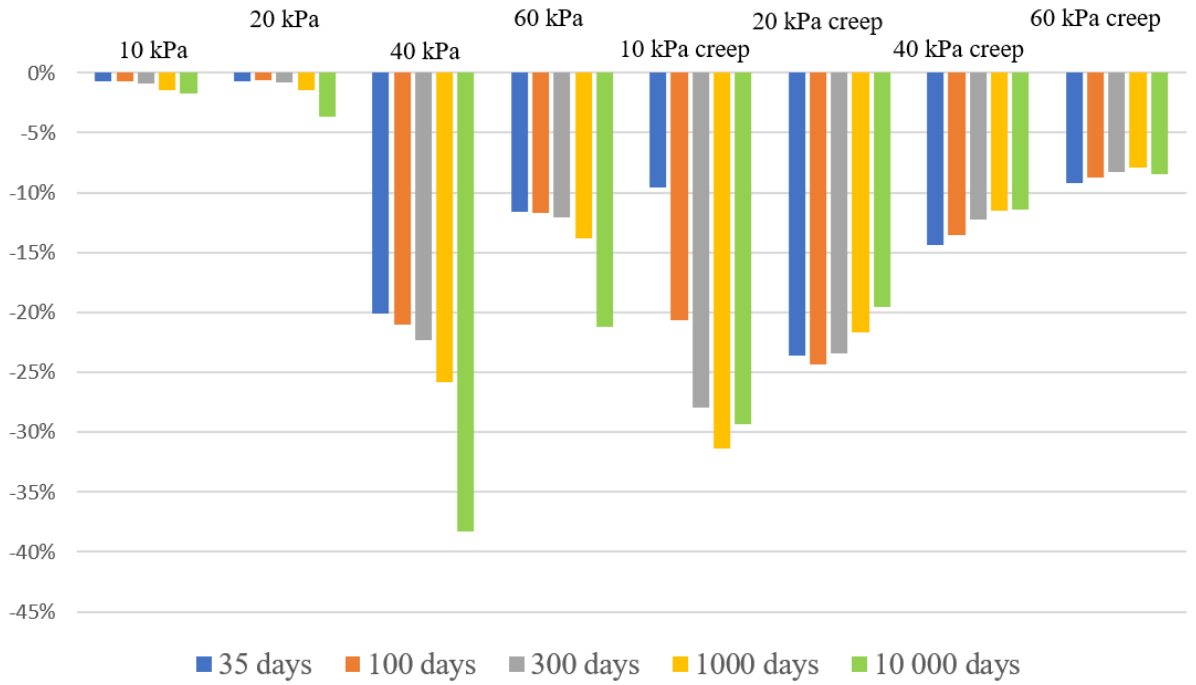

Figure 5.12: Change of settlements when the POP is increased by 5 kPa in clay layer 1-4, compared to the original case.

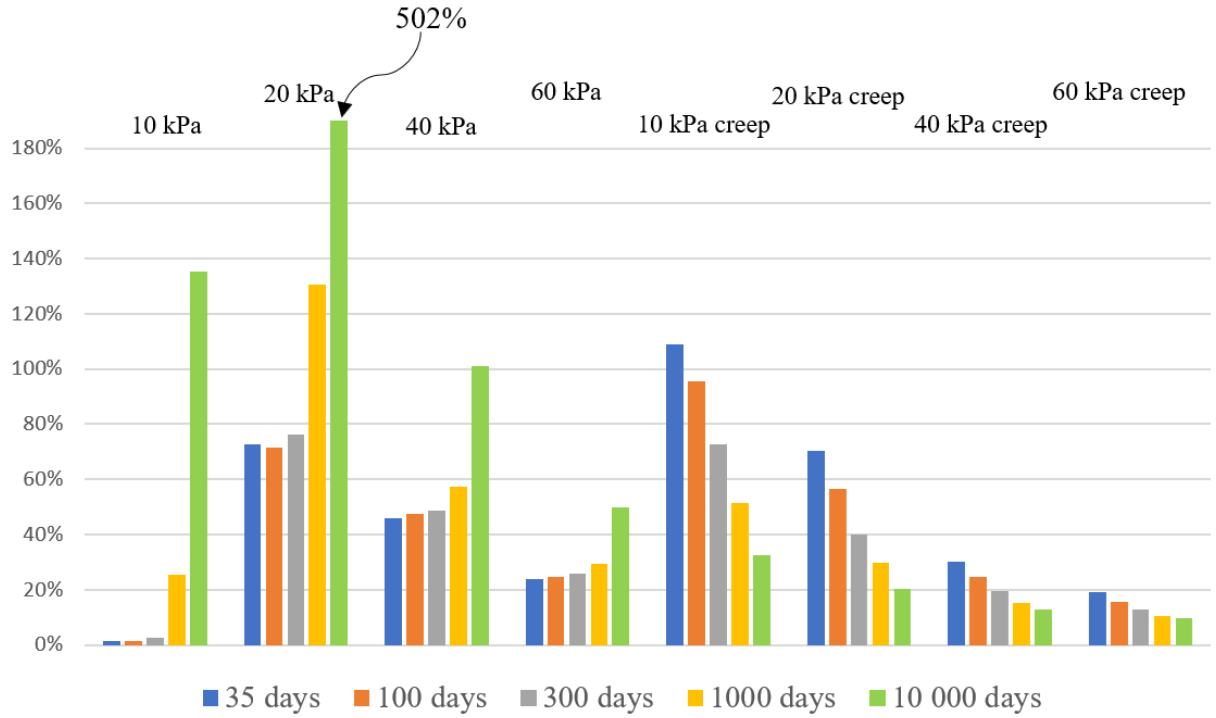

Figure 5.13: Change of settlements when the POP is decreased by 10 kPa in clay layer 1-4, compared to the original case.

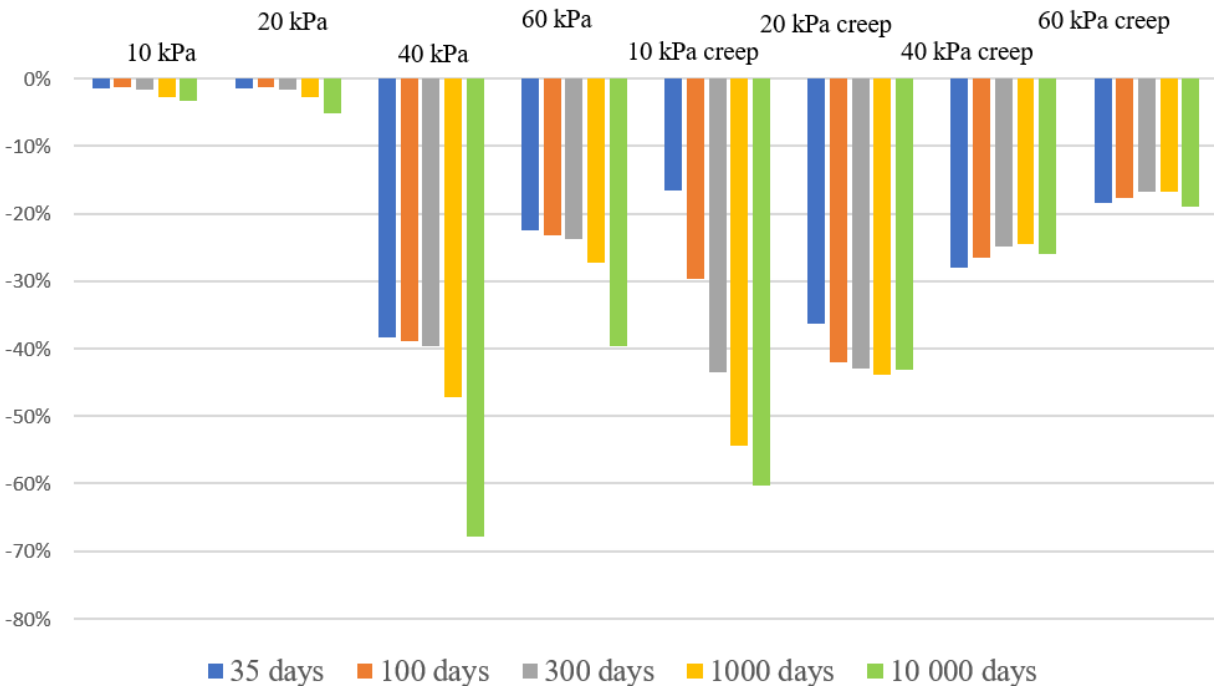

Figure 5.14: Change of settlements when the POP is increased by 10 kPa in clay layer 1-4, compared to the original case.

The characteristics of the SS model are once again very clear when the POP is varied. Since the pore pressure reduction of 20 kPa was on the boundary of having plastic strains before, the difference when reducing the POP is immense. A POP reduction of 5 kPa increases the long term settlements by 129% and a POP reduction of 10 kPa increases the long term settlements by 502%. The changes in the short term are much smaller because of a combination of two factors. In the early stages, less of the excess pore pressures have dissipated and the stress state

in most of the clay will still be below the preconsolidation pressure. The increased deformations do further decrease the rate of consolidation since more excess pore pressures are created when the soil deforms. When the POP is increased, the largest difference in settlement is instead seen when the pore pressure reduction is 40 kPa. This is because 40 kPa is the case where the largest share of the plastic deformations becomes elastic if POP increases.

Changes to the POP in the SSC model are also very substantial. The largest changes in settlements are however not as extreme since there is not a distinct boundary between elastic and plastic strains as it is in the SS model. The impact of changes to the POP are larger when the pore pressure reductions are smaller. This relates to how Equation 3.8 is structured. The significance of changes to the ratio between the effective stress and the preconsolidation pressure is larger when the effective stress is smaller. Further, the difference in settlements compared to the original case generally reduces over time. A possible explanation to this may have to do with the fact that the creep affects the preconsolidation pressure. If the POP is decreased, the creep rate will be much faster in the beginning. The preconsolidation pressure will therefore also increase faster in the beginning, and over time it will approach the preconsolidation pressure in the original calculations. If the POP instead is increased, the opposite will happen and the preconsolidation pressure approaches the original values from above.

5.4.4 Sensitivity to changes of permeability in clay layer 1-4

Figure 5.15 and 5.16 display the change in settlements compared to the original calculations when the permeability is varied to $1*10^{-9}$ m/s and $4*10^{-9}$ m/s for all clay layers.

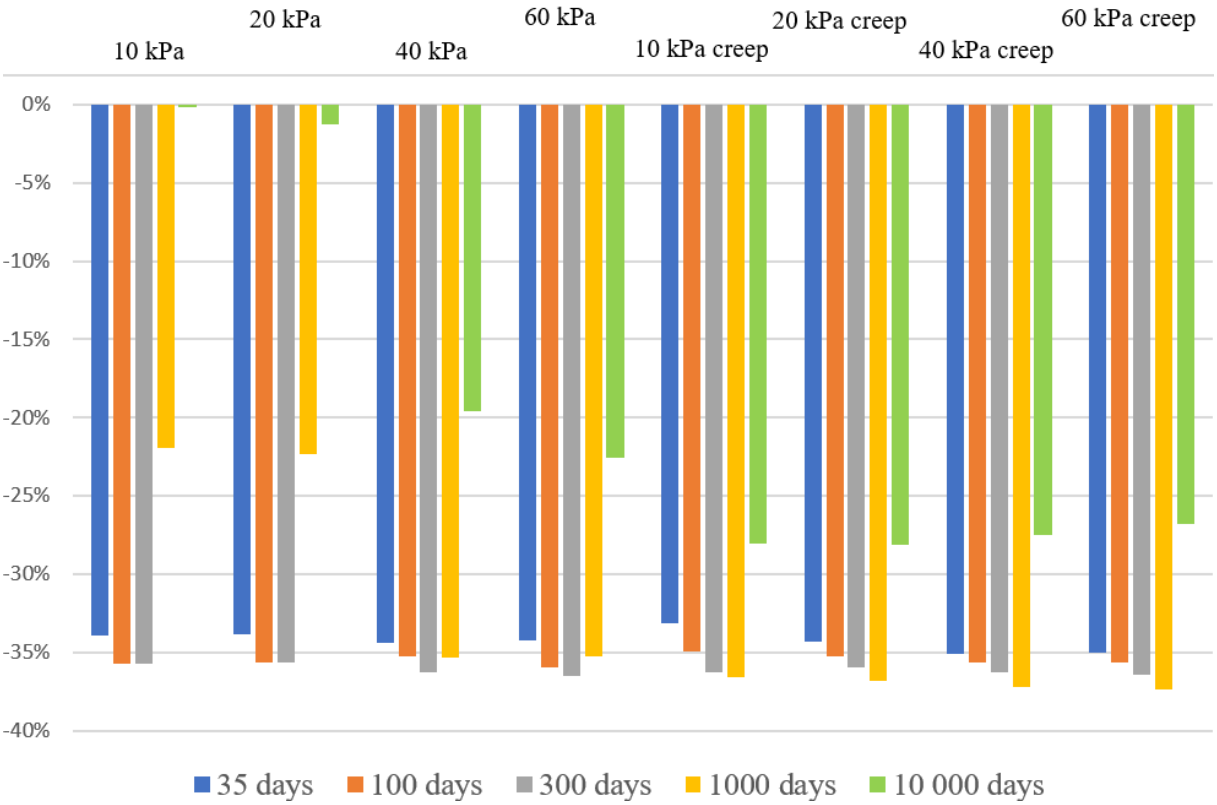

Figure 5.15: Change of settlements when the permeability is set to $1*10^{-9}$ m/s in clay layer 1-4, compared to the original case.

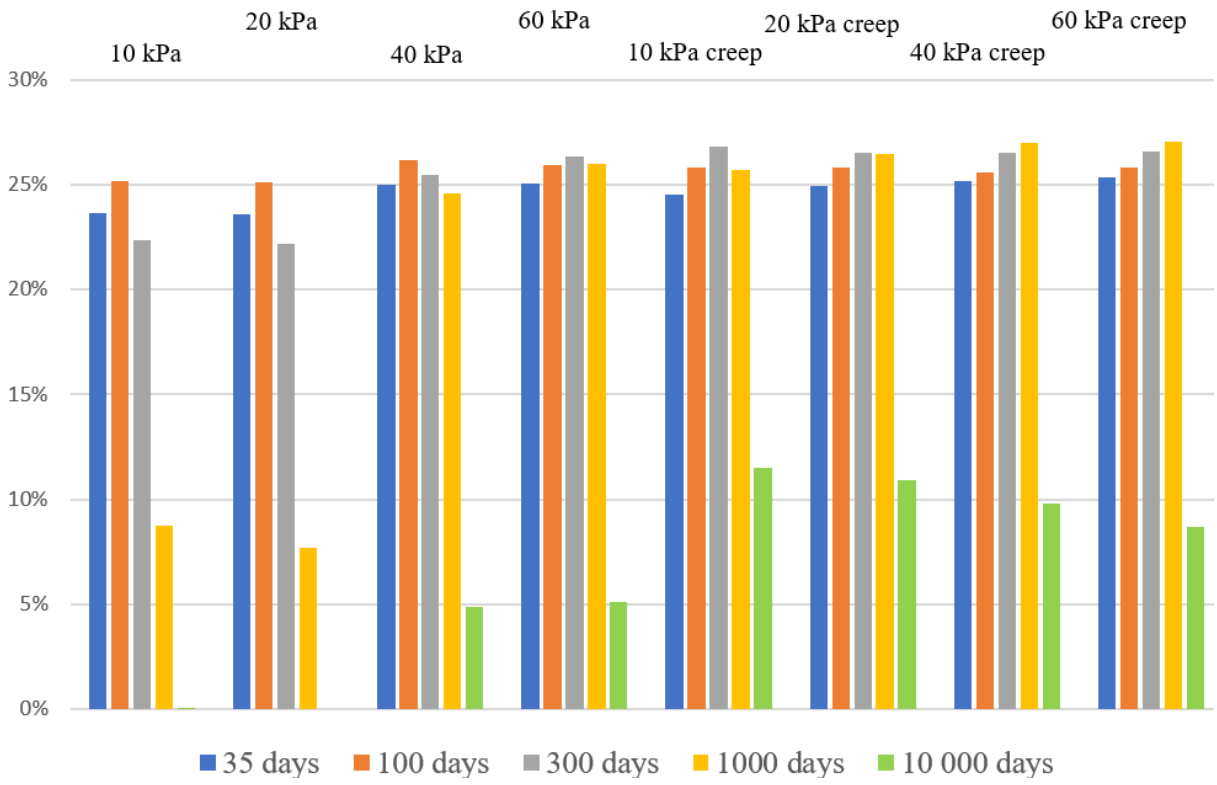

*Figure 5.16: Change of settlements when the permeability is set to 4*10^{-9} m/s in clay layer 1-4, compared to the original case.*

It may not be a surprise, but it is evident from the figures that the permeability is very important in a consolidation analysis. The differences in settlement for periods of 300 days and less are very similar in all analysed pore pressure reductions in both models. Permeability of 1*10^{-9} m/s results in settlement reductions of around 35% while permeability of 4*10^{-9} m/s causes the settlements to increase by roughly 25%. The difference compared to the original case is smaller when considering longer time periods. During 10 and 20 kPa reductions without creep, the change in settlement decreases already after 1000 days since the pore pressures dissipate more slowly towards the end when the hydraulic head difference is small. After 10 000 days there are no differences at all because the excess pore pressures have dissipated regardless of the permeability. When the permeability is 4*10^{-9} m/s, all pore pressures dissipate after 10 000 days for reductions of 40 and 60 kPa with the SS model. The settlements after an infinite time are thus only 5% higher than calculated after 10 000 days in the original model. The differences in settlements after 10 000 days with the SSC model are smaller than the shorter times since the hydraulic head difference becomes smaller with time, but the differences are still quite large. The settlements after 10 000 days are reduced by about 27% when the permeability is reduced and increased by 10% when the permeability is increased.

5.4.5 Sensitivity to changes of permeability in clay layer 4

Figure 5.17 and 5.18 display the results of having permeabilities of $0.4*10^{-9}$ m/s and $10*10^{-9}$ m/s in clay layer 4 when compared to the original calculations.

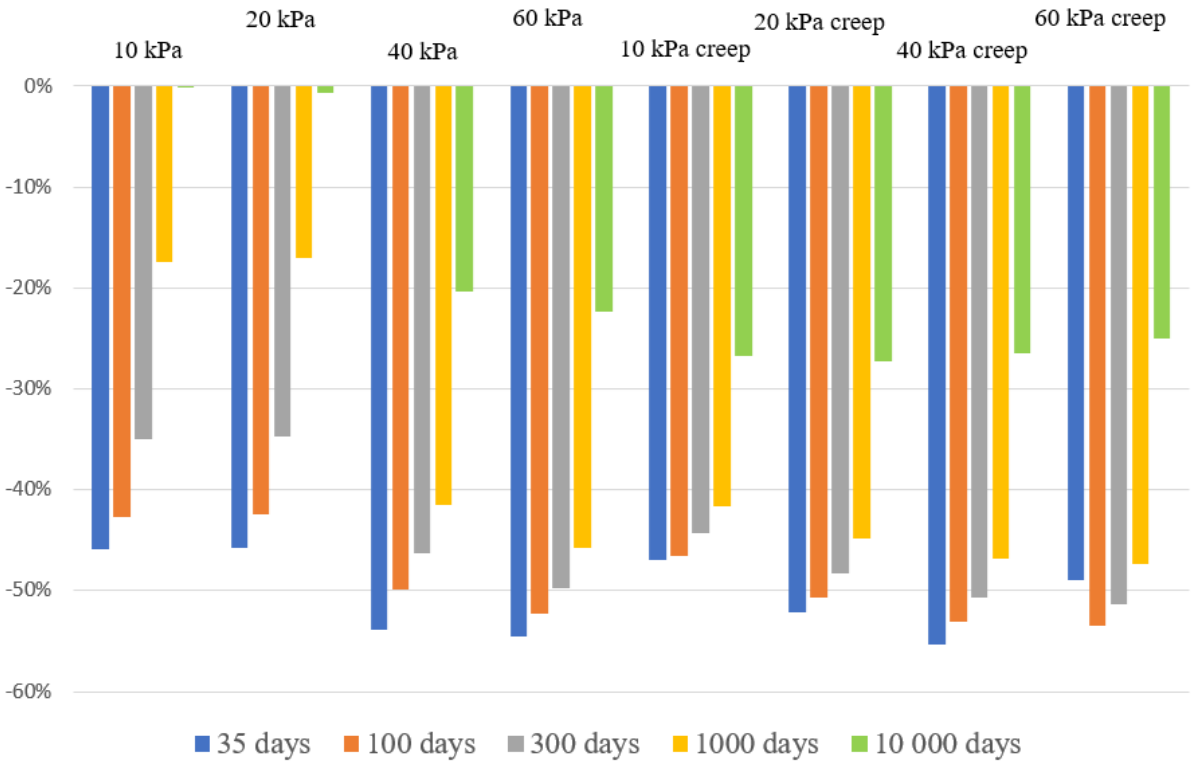

Figure 5.17: Change of settlements when the permeability is set to $0.4*10^{-9}$ m/s in clay layer 4, compared to the original case.

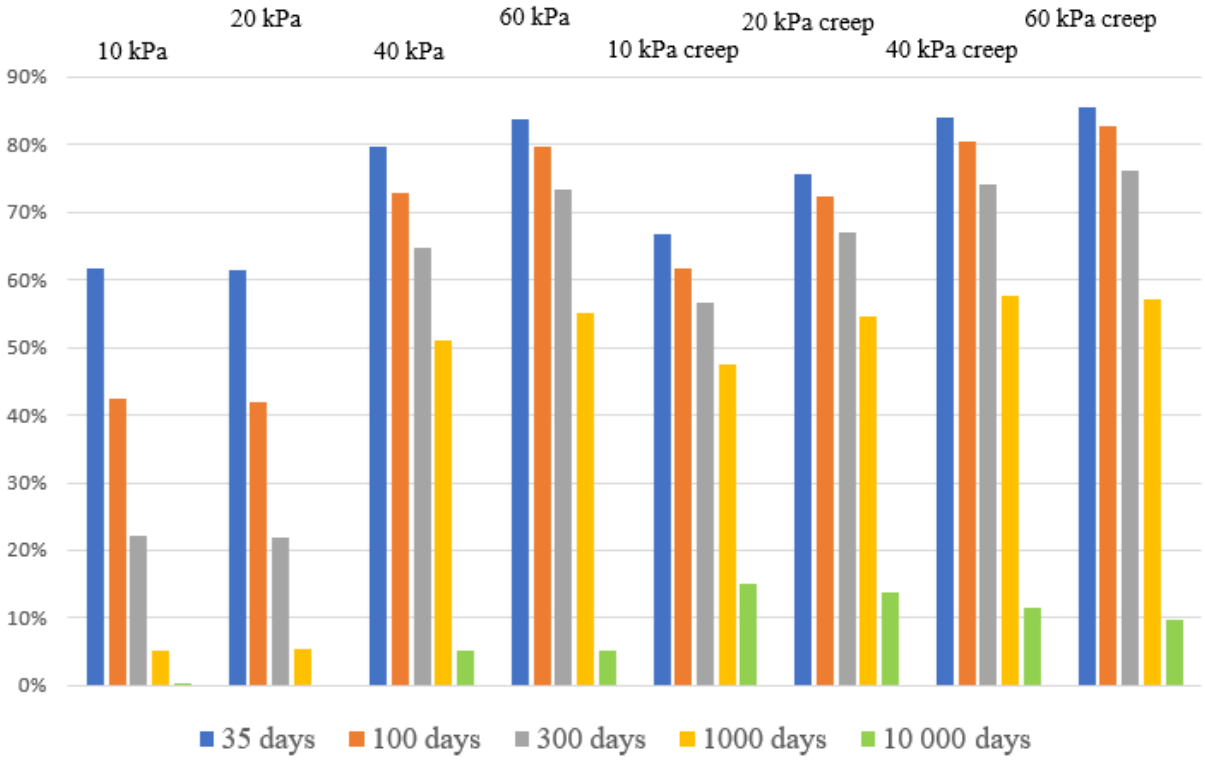

Figure 5.18: Change of settlements when the permeability is set to $10*10^{-9}$ m/s in clay layer 4, compared to the original case.

The change of permeability in clay layer 4 affects the settlements more in short time periods than for longer times. In the early stages, the settlements are almost exclusively occurring in the deeper soil. The magnitude of settlements in the short term therefore changes drastically when the permeability of clay layer 4 changes. The settlements 35 days after the pore pressure reduction are on average reduced by 50% when the permeability in clay 4 is set to $0.4*10^{-9}$ m/s. The corresponding value when the permeability is set to $10*10^{-9}$ m/s is equal to an increase of 70%. The influence of the permeability in clay 4 decreases when more time passes. The main reason for this is likely that much of the excess pore pressures in clay 4 have dissipated regardless of the permeability and the settlements in the other clay layers have more influence on the results. The water flowing out from clay layers 1-3 still must pass layer 4 and the effect of changed permeability in clay layer 4 is therefore apparent in most cases even after 10 000 days.

The uncertainties regarding the values tested in this analysis are perhaps even larger than for the other parameters, particularly the maximum value. It is nevertheless important to consider that a relatively thin layer with different permeability can have a very large impact on the results.

5.4.6 Sensitivity to changes of c'ref and φ

Figure 5.19 displays the difference in settlements compared to the original case when c'ref=7 kPa and φ=35º for depths less than 13 m and c'ref=13 kPa and φ=28º below 13 m.

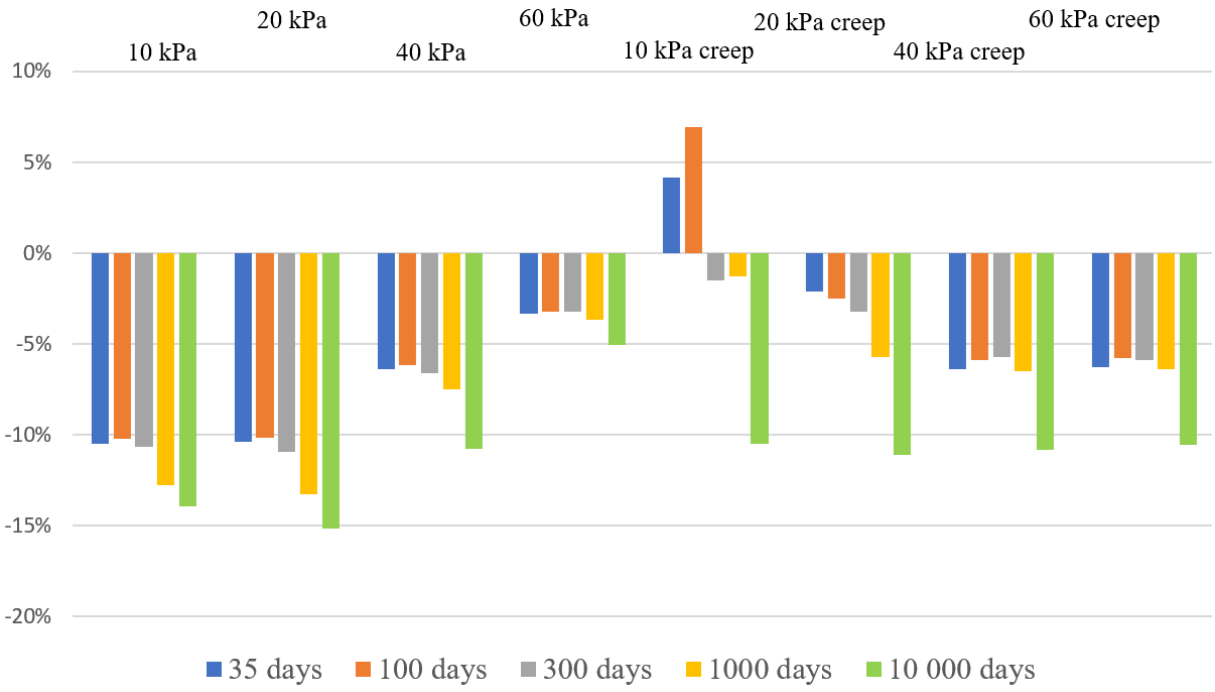

Figure 5.19: Change of settlements when c'ref=7 kPa and φ=35º for depths less than 13 m and c'ref=13 kPa and φ=28º below 13 m, compared to the original case.

The results show that c'ref and φ do not have a very large impact on the results. The settlements are calculated to be around 10% less for the rather extreme case which is tested in this analysis. The parameters might be a bit higher than the ones used for the main analysis, but c'ref is most likely closer to the original values than the ones tested here. Further, the results with creep and

a 10 kPa reduction look a bit weird. It probably has to do with the altered background creep. If deemed necessary, new triaxial tests should be conducted where the samples are analysed the same day as they are retrieved to prevent disturbance. It may yet not be very important for the settlement analysis since many of the other uncertainties affect the results much more.

5.4.7 Summary of the sensitivity analysis

Except for the changes to c'ref and φ, all changes to input parameters evaluated in the sensitivity analysis have an impact of at least 25% when compared to the original calculations for some instance of constitutive model, pore pressure reduction and time. The changes of permeability affect all cases substantially while the impact of all other changes vary drastically for the different cases investigated. Because of the large quantity of results, it is hard to draw many conclusions without generalising too much. Overall, there were no giant surprises in the results. λ* has most influence on higher pore pressure reductions while κ* has a larger impact on the smaller reductions. Changes to the POP alter the results the most when the stress state in the original calculations was close to the preconsolidation pressure. Most of the changes to λ*, κ* and POP have a larger impact on the SS model compared to SSC. Changes to the permeability, both in all clay layers and solely in layer 4 have a very large impact in the short term but it reduces over time.

It was originally in this project planned to perform calculations on the worst- and best-case scenarios where all uncertainties were combined. The idea was however abandoned. Partly because of how λ* changes the SSC model and partly because most of the investigated parameter changes already are rather extreme cases and unlikely to be correct. The probability is unimaginably small that every single parameter is the worst or best plausible case. The results would thus not really mean anything and only give a false picture that the accuracy of the original calculations is lower than it actually is.

5.5 Final discussion

All the data used in the calculations are retrieved from a relatively small area and even within the area there are large uncertainties regarding certain parameters. Meanwhile, the pore pressures could be affected several hundreds of metres away due to inflow to the excavation. It would thus not make much sense to speculate about eventual damage or solutions for any individual buildings in the vicinity without investigating the groundwater paths. The fact that the area around the excavation is densely built up is enough of a reason to try to limit the water inflow to the excavation as much as possible.

The approach of regularly measuring the pore pressures in the area to detect eventual reductions should work relatively well, but there are a few points to keep in mind. To fully utilize the method, it would be necessary to analyse a much larger area and split it up based on the soil characteristics. Unless any kind of test pumping is performed before the excavation is constructed, it is especially important to have many pore pressure measurement points. This is because the flow paths in the friction layer could cause the pore pressures to reduce faster in certain parts of the area. Since the results of a settlement analysis inevitably will be subjected to some uncertainties, the results should in practice not be interpreted as facts. It should rather

give a hint of when problems may occur and when for example infiltration systems should be activated.

Much of the focus in this report has been on relatively large pore pressure reductions and long time spans because it is when settlement problems arise. It is completely necessary to study this before constructing an excavation, but it is important to remember that the actual pore pressure reductions in most cases will be small if things are done correctly. The maximum acceptable settlements caused by the West link construction are for example between 5 and 20 mm for different buildings. It is more likely that the actual settlements are in this order of magnitude than in decimetres. It can also be noted that the limiting values for the West link are very strict while considering that it corresponds to only 1-4 years of background creep at the studied location. It is certainly good that underground constructions do not cause damage to the buildings in the area, but perhaps the most economical solution would be to allow somewhat higher settlements.

5.6 Sources of error and drawbacks of the model

Many of the sources of error originate from the uncertainties regarding the input parameters and are assessed in the sensitivity analysis. A few are also mentioned as a part of the discussion. Most other uncertainties and errors should have a relatively small influence on the results but are nevertheless good to be aware of.

As previously discussed, there are large uncertainties concerning the properties and depth of the silty clay layer close to the friction layer. In the main analysis, λ^* was set to be constant from 16-23 m depth to account for all uncertainties as good as possible. Some of the CRS-tests however indicate that the soil at 18 and 21 m depth is very stiff, but also has low permeability. If this is correct, the settlements at the early stages will be very small because it takes time until the pore pressure reduction reaches the softer clay.

The values of μ^* are based on CRS-tests and a report which states that the background creep is roughly 5 mm/year in the area. Neither of these sources are very precise and not the optimal way of retrieving μ^*.

Some of the data received from the laboratory testing is deviating from what is expected from the clay in the area. A likely reason for this is that the soil samples had been disturbed before testing. A few tests with obvious errors were in this project excluded from the final selection of parameters, but tests which only were slightly disturbed may have been included. Wrongly calibrated laboratory equipment could also cause consistent errors to the data. The eventual errors from this category should yet be comparably small compared to the other uncertainties. The errors could even be assumed to fit within the boundaries of the sensitivity analysis since the values in that analysis probably are quite conservative.

The pore pressures in this study are assumed to be hydrostatic down to 5 m depth in all the calculations based on a previous study of the geology in the Gothenburg area. The pore pressure measurements prove that this roughly is the case at the site, but the hydrostatic range could still be a couple of metres up or down from 5 m. The impact of this should be relatively small, but

it would slightly change the initial excess pore pressure distribution and thus have a small effect on the settlements.

A few additional noteworthy simplifications were made to simplify the Plaxis model. The transitions between different soil layers are obviously not instant in reality as they are in the model. It would be unreasonable to split the soil into too many layers, but some errors will naturally arise where the soil is split up. Further, all the soil data come from soil tests which are performed at locations where there are no buildings. The stress state and soil properties below certain buildings could be affected both by the weight of the buildings and the installation of eventual piles. Another simplification is that it takes 2.5 days for the pore pressures in the friction layer to change from one level to another. The duration of the reduction phase should influence the excess pore pressure distribution and the settlements in the early stages.

6 Conclusions

The analysis made in this thesis confirm that pore pressure reductions in the friction layer due to inflow to excavations can cause large settlements. It is therefore very important to put much effort into sealing the excavation properly before water is pumped away. Even if much effort is made to seal the excavation, there is still a risk of leakage through deficiencies in the grout. The pore pressures in the area should therefore be measured continuously during the construction of the excavation, just as they will do during the West link project. It is further essential to prepare solutions if the pore pressures after all reduce, such as infiltration wells and reinforcing the foundations of eventual sensitive buildings in the risk zone.

When comparing the two constitutive models, Soft Soil model and Soft Soil Creep model, it is evident that creep effects have a large impact on the settlements. The weaknesses of the Soft Soil model become even more apparent during small pore pressure reductions and when the pre-overburden pressure is varied in the sensitivity analysis. Because the Soft Soil model does not predict any large deformations before the effective stress reaches the preconsolidation pressure, it is concluded that the Soft Soil Creep model is the preferable of the two in this type of analysis.

The results show that the settlements increase exponentially when the pore pressure reduction increases. Pore pressure reductions of for example 60 kPa may cause damage to buildings within a week. Even a relatively small pore pressure reduction of 10 kPa is however able to cause severe settlements in the long term. Settlements will furthermore continue to occur for a period after the pore pressures in the friction layer return to normal. It is therefore even more important to act as soon as possible after a pore pressure reduction is detected. Some of the settlements will recover once the pore pressures go back to normal. The share of the settlements which recovers is smaller when more plastic deformations take place and thus large pore pressure reductions are more critical in that way.

Most of the settlements resulting from a pore pressure reduction will occur in the deep clay, close to the friction layer where the initial pore pressure reduction takes place. In the long term, more than 2/3 of the settlements will occur at depths of 16-23 m and the share is even higher for shorter time periods. The properties of these layers are therefore more important to investigate compared to the shallower layers.

Buildings which are piled to the bedrock will not be subjected to any settlements. Piled buildings will yet cause the nearby soil to settle unevenly which in turn may cause damage to adjacent buildings without piles. The issues resulting from the magnitude of vertical settlements are however believed to be larger than the problems caused by inclined settlements.

6.1 Recommendations for further research

This thesis has solely focused on the effects of a pore pressure reduction in the friction layer due to inflow to the excavation in Liseberg. There are several other aspects to the construction of the excavation that could be studied in detail. Creating a groundwater model of the area around the excavation would open up several new possibilities for the analysis. First of all, the relationship between inflow to the excavation and pore pressure reductions would be interesting

to examine to get a better understanding of the situation. A groundwater model could further predict how far away settlements may occur and if there are any directions where the pore pressures are reduced more. By knowing this, it would make more sense to investigate a larger area and divide it into sections based on varying soil properties. By narrowing down the problems to certain sections, the potential damage to specific buildings could also be investigated more in detail where there is a risk of large settlements. It is however important to remember that it is practically impossible to create an exact groundwater model. It should therefore be seen as a complement to the type of calculations performed in this project.

It would further be interesting to include more construction related challenges in the model. For example, the interaction between movement of the retaining walls and settlements. The installation of certain structural elements could also affect the pore pressures around the excavation and complicate the settlement predictions.

The results in this thesis are subjected to a number of uncertainties regarding the input parameters and how well the constitutive models are able to predict the true soil behaviour. Additional soil data, both in terms of quantity and quality could be analysed to refine the calculations. Incremental loading oedometer tests and unloading-reloading CRS-tests should preferably be performed to achieve more accurate values of $\mu^*$and κ^*. The same calculations could also be made with another constitutive model, for example Creep-SCLAY1S, or even with another software.

7 References

Antiquum. (2014). *Fördjupad kulturmiljöbeskrivning för Korsvägen med omgivning.*

Bentley. (2021a). *Plaxis Scientific Manual.*

Bentley. (2021b). *Plaxis General Information Manual.*

Bentley. (2021c). *PLAXIS Material Models Manual.*

Berntson, J. (1983). *Portrycksvariationer i leror i Göteborgsregionen.* Linköping.

Biot, M. *General Theory of Three-Dimensional Consolidation.* Journal of Applied Physics.

Bjerrum, L. *Engineering geology of Norwegian normally-consolidated marine clays as related to settlements of buildings.*

Bond, A., Schuppener, B., Scarpelli, G., & Orr, T. (2013). *Eurocode 7: Geotechnical Design Worked examples.*

Building Research Establishment. (1995). *Assessment of damage in low-rise buildings with particular reference to progressive foundation movement.* Watford.

Cao, C., Shi, C., Liu, L., Liu, J., Lei, M., Lin, Y., Ye, Y. (2019). *Novel Excavation and Construction Method for a Deep Shaft Excavation in Ultrathick Aquifers.*

Cashman, P., & Preene, M. (2012). *Groundwater lowering in construction: A practical guide to dewatering*. Spon press.

Eriksson, P., Jandeby, L., Olsson, T., & Svensson, T. (2004). *Kohesionspålar.* Linköping.

Fetter, C. (2014). *Applied Hydrogeology*.

Google. (2021) *Google Maps.* Retrieved 2021-02-17 from www.google.com/maps

Högsta, U., & Sanell, K. (2016). *Västlänken och Olskroken planskildhet, Ansökan om tillstånd enligt miljöbalken, PM Geoteknik Sättningar* .

Karstunen, M., & Amavasai, A. (2017). *BEST SOIL: Soft soil modelling and parameter determination.*

Korff, M. (2012) *Response of piled buildings to the construction of deep excavations.*

Knappet J.A, & Craig R.F. (2012). *Craig's soil mechanics*. New York: Spon press.

Larsson, R. (1981). *Drained behavior of Swedish clays.* Linköping.

Larsson, R. (2008). *Jords egenskaper.* Linköping.

Larsson, R., & Sällfors, G. (1995). *Sättningsegenskaper i lös lera på grund av geologisk avsättning och "åldring"* . Linköping.

Li, B., Jia, C., Wang, G., Ren, J., Lu, G., Liu, N. (2020) *Numerical Analysis on the Performance of the Underwater Excavation.*

Olsson, C., & Holm, G. (1993). *Pålgrundläggning.* Linköping: AB Svensk Byggtjänst.

Olsson, M. (2010). *Calculating long-termsettlement in soft clays– with special focus on the Gothenburg region.* Linköping.

Persson, J. (2007). *Hydrogeological Methods in Geotechnical Engineering; Applied to settlements caused by underground construction.*

Plaxis. (2012). *Embedded Pile Row in Plaxis 2D.*

Powers, P., Corwin, A., Schmall, P., & Kaeck, W. (2007). *Construction Dewatering and Groundwater Control - New Methods and Applications*.

Shirlaw, J., Tan T., Tong K. (2005). *Deep excavations in Singapore marine clay.*

Sundkvist, U., & Wallroth, T. (2016). *Ansökan om tillstånd enligt miljöbalken för anläggandet av Västlänken och Olskroken planskildhet, PM Hydrogeologi.* Göteborg.

Sweco. (2014). *PM Geoteknik Västlänken, Station Korsvägen, Geoteknisk utredning för detaljplan.*

Sällfors, G. (2013). *Geoteknik - jordmateriallära*. Göteborg.

Terzaghi, K. *Principles of soil mechanics. IV. Settlement and consolidation of clay*. Engineering News-Record, 95

Trafikverket. (2014). *Järnvägsplaner Olskroken planskildhet och Västlänken, Byggbeskrivning.*

Trafikverket. (2016a). *Tekniskt PM Geoteknik.*

Trafikverket. (2016b). *Bilaga 3 Geotekniska parametrar.*

Trafikverket. (2017). *Gränsvärden för deformationer.*

Trafikverket. (2018). *Om Västlänken.* Retrieved 2021-03-20 from https://www.trafikverket.se/nara-dig/Vastra-gotaland/vi-bygger-och-forbattrar/Vastlanken---smidigare-pendling-och-effektivare-trafik/Om-Vastlanken/

Trafikverket. (2020). *Att bygga i lera.* Retrieved 2021-03-29 from https://www.trafikverket.se/nara-dig/Vastra-gotaland/vi-bygger-och-forbattrar/Vastlanken---smidigare-pendling-och-effektivare-trafik/Om-Vastlanken/sa-bygger-vi-vastlanken/att-bygga-i-lera/

Ödlund Eriksson, L. (2014) *Soil Rock Interfaces: Problem Identification and Conceptualisation for Sealing Strategies.*

8 Appendix

Appendix A: Groundwater and soil properties

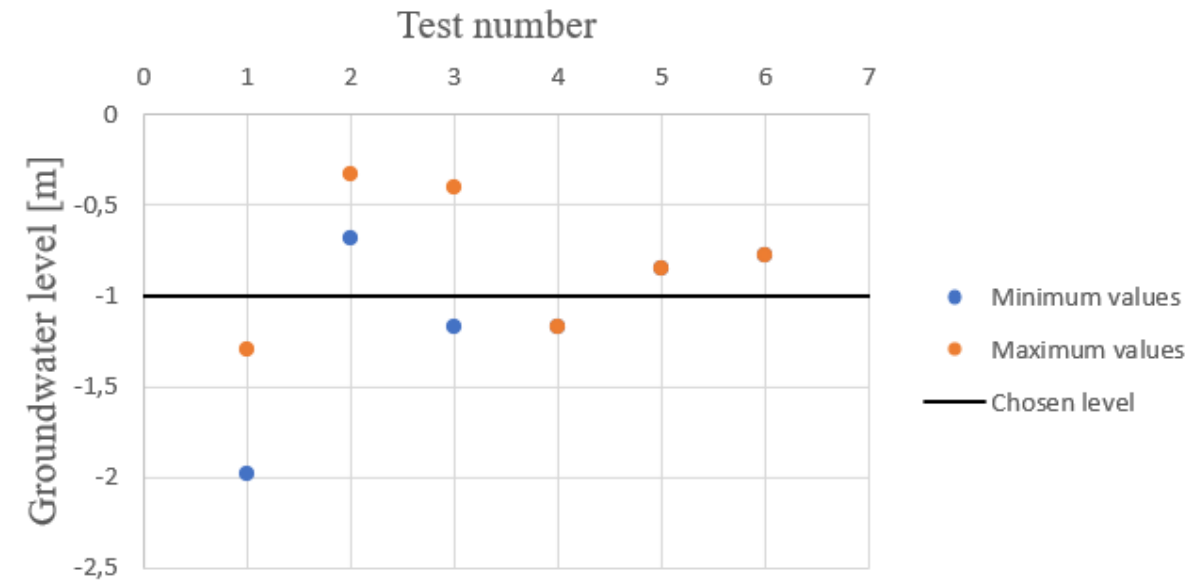

Figure A.1: Groundwater level in the upper aquifer, note that three of the wells only contains one measurement.

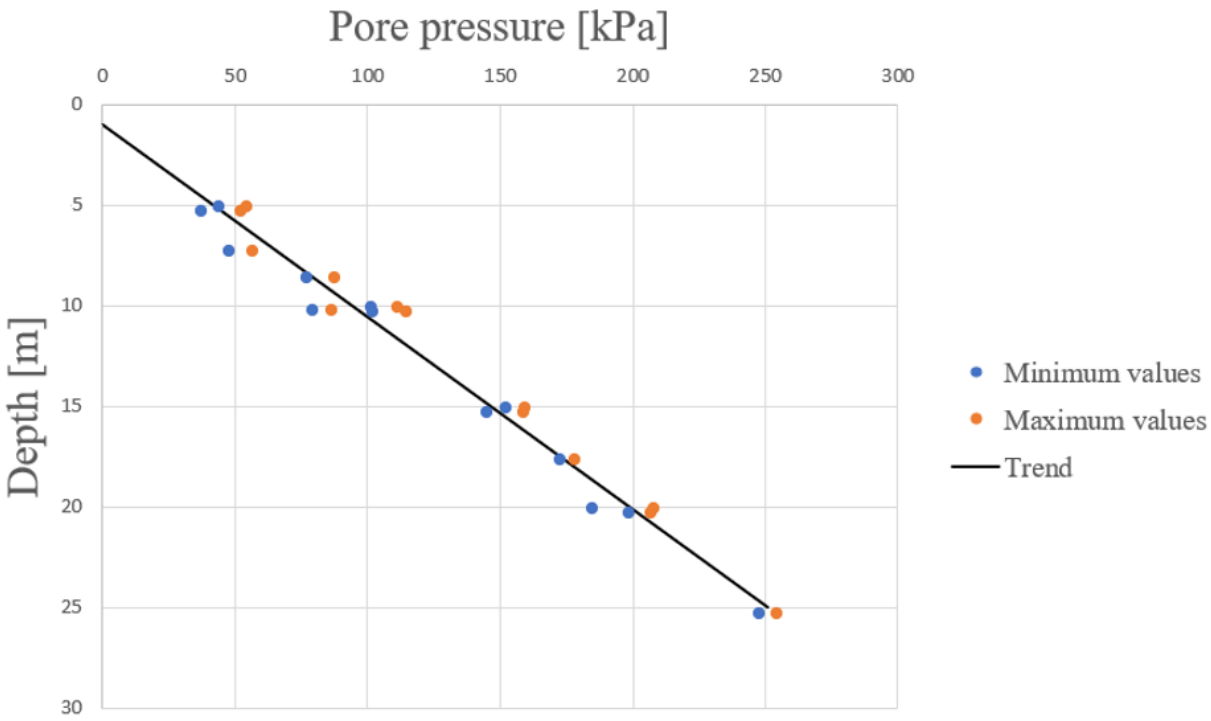

Figure A.2: Pore pressures in the clay layer.

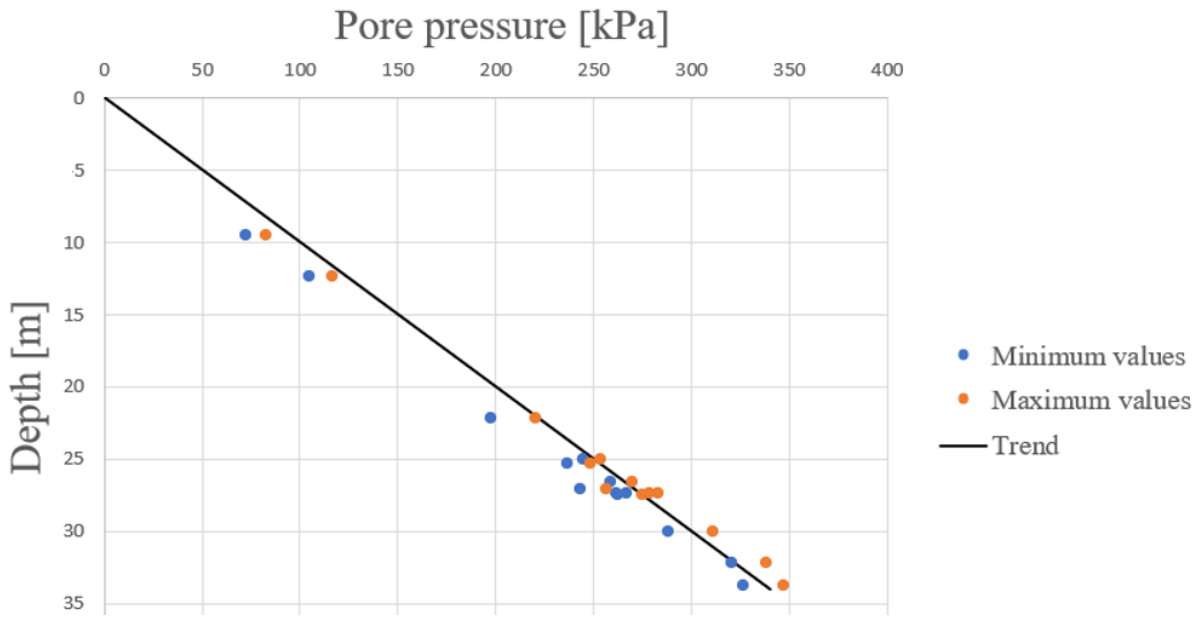

Figure A.3: Pore pressures in the friction layer.

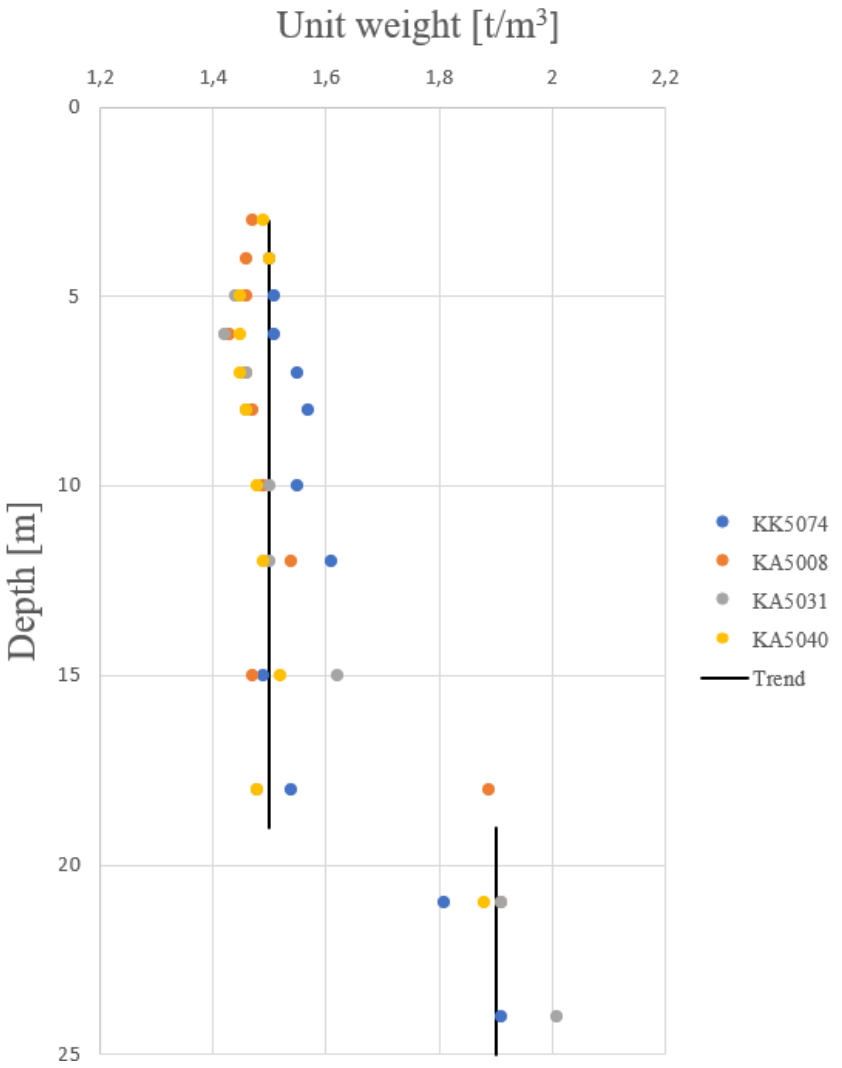

Figure A.4: Unit weight of the clay. Note that the trend and especially the decision to change from 1.5 t/m³ to 1.9t/m³ at 19 m depth is supplemented by the public data from Sweco (2014).

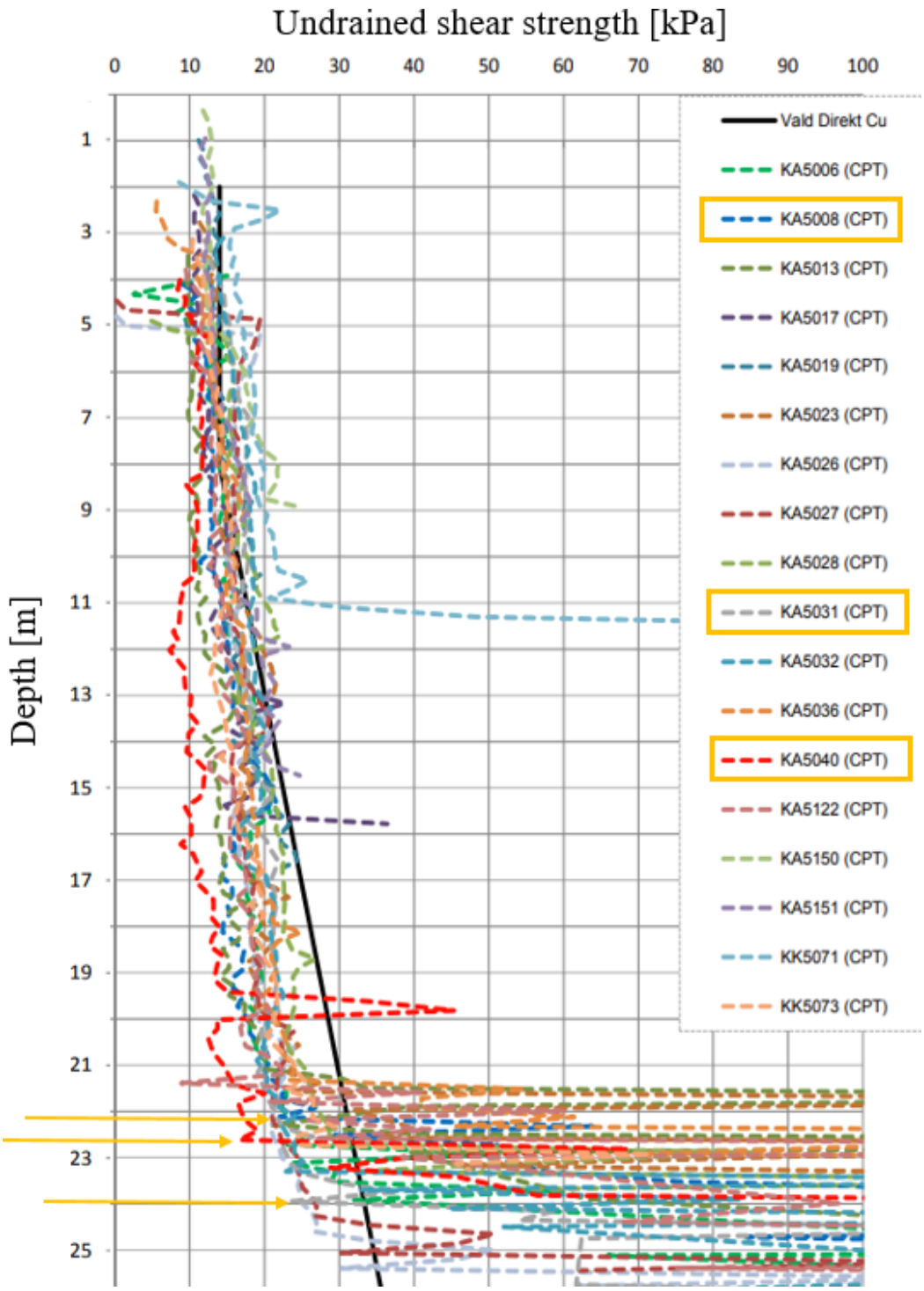

Figure A.5: Undrained shear strength from CPT. The decided depth of the friction layer is selected from KA5008, KA5031 and KA5040.

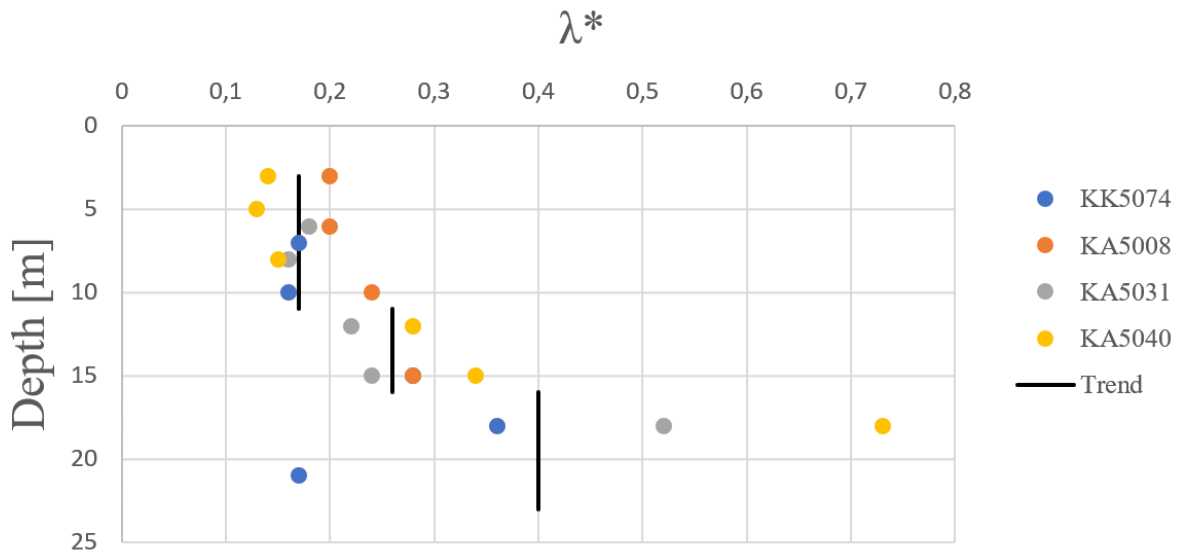

Figure A.6: Evaluated values of λ.*

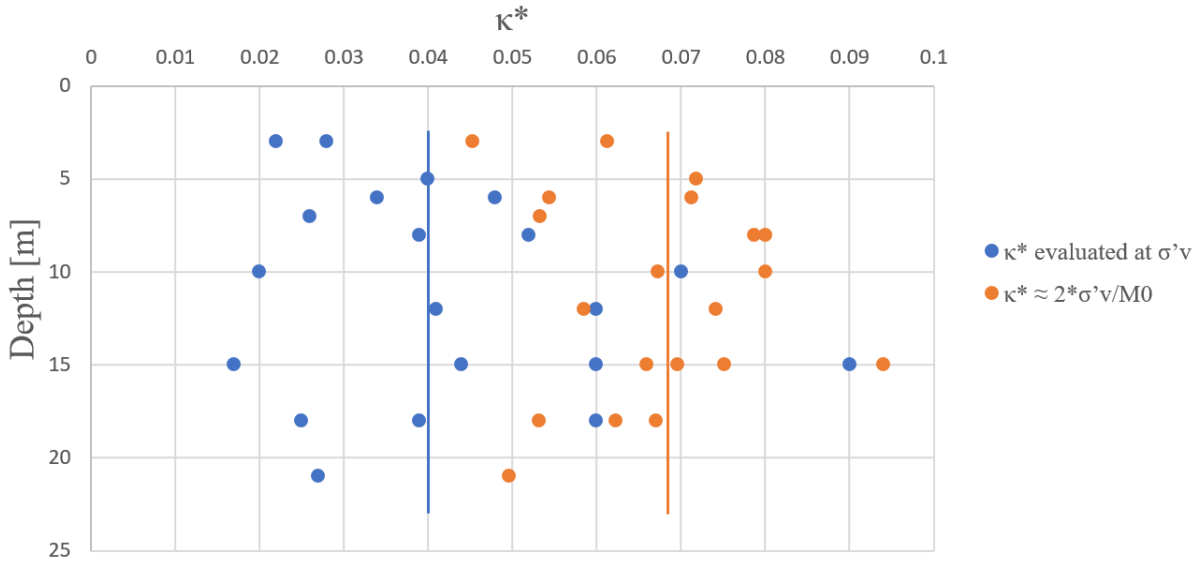

Figure A.7: κ values evaluated at at the preconsolidation pressure from CRS-tests in ln(p') scale, and κ* from Equation 3.11.*

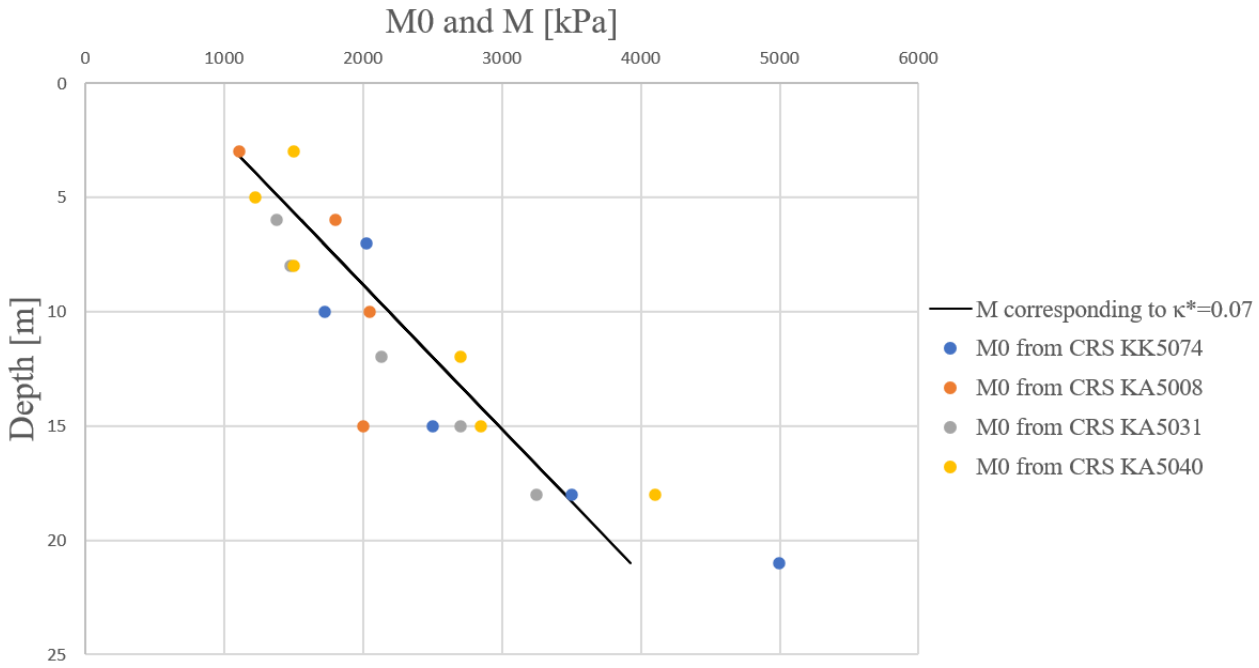

Figure A.8: M_0 from CRS-test in linear scale and M evaluated via the bulk modulus, K.

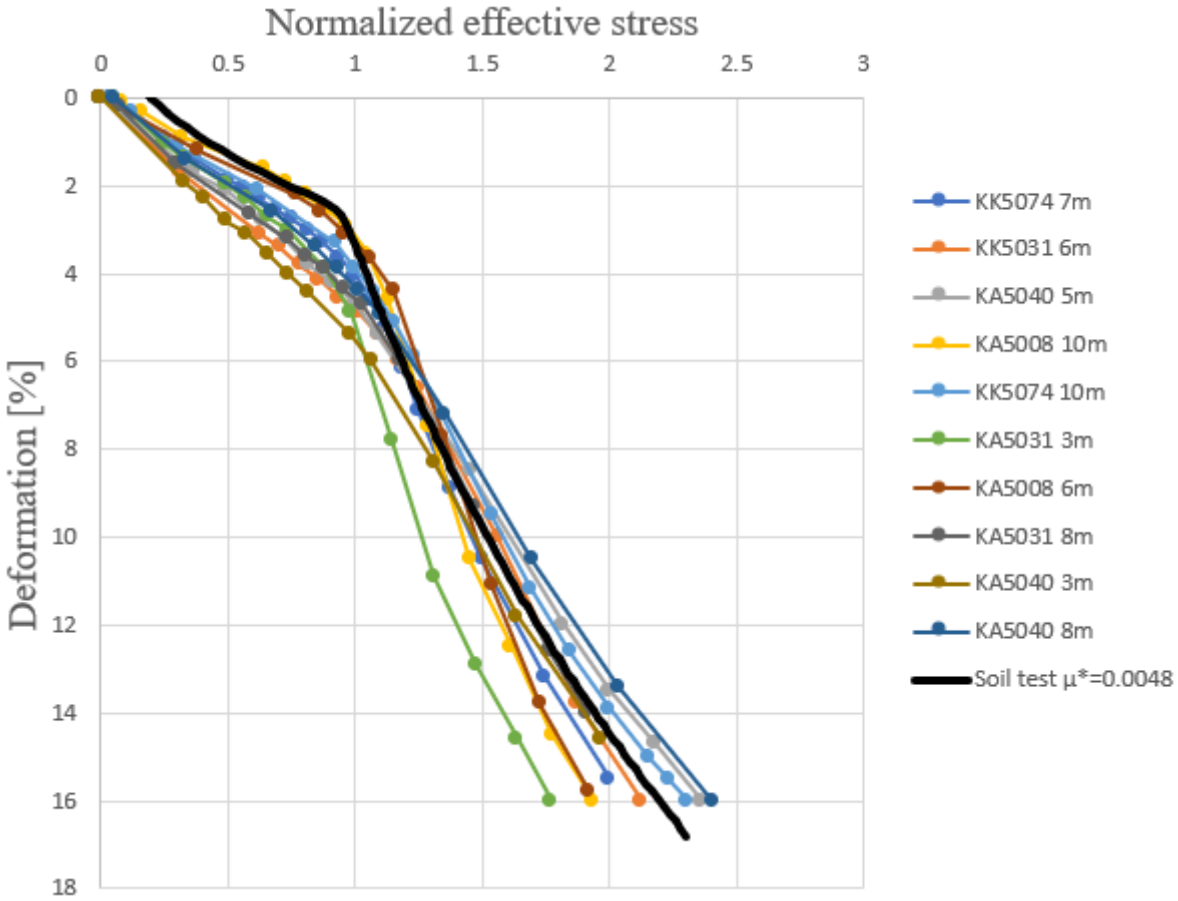

Figure A.9: Decision of μ for clay 1 with Plaxis soil test tool. The CRS-tests are normalized against σ'_c.*

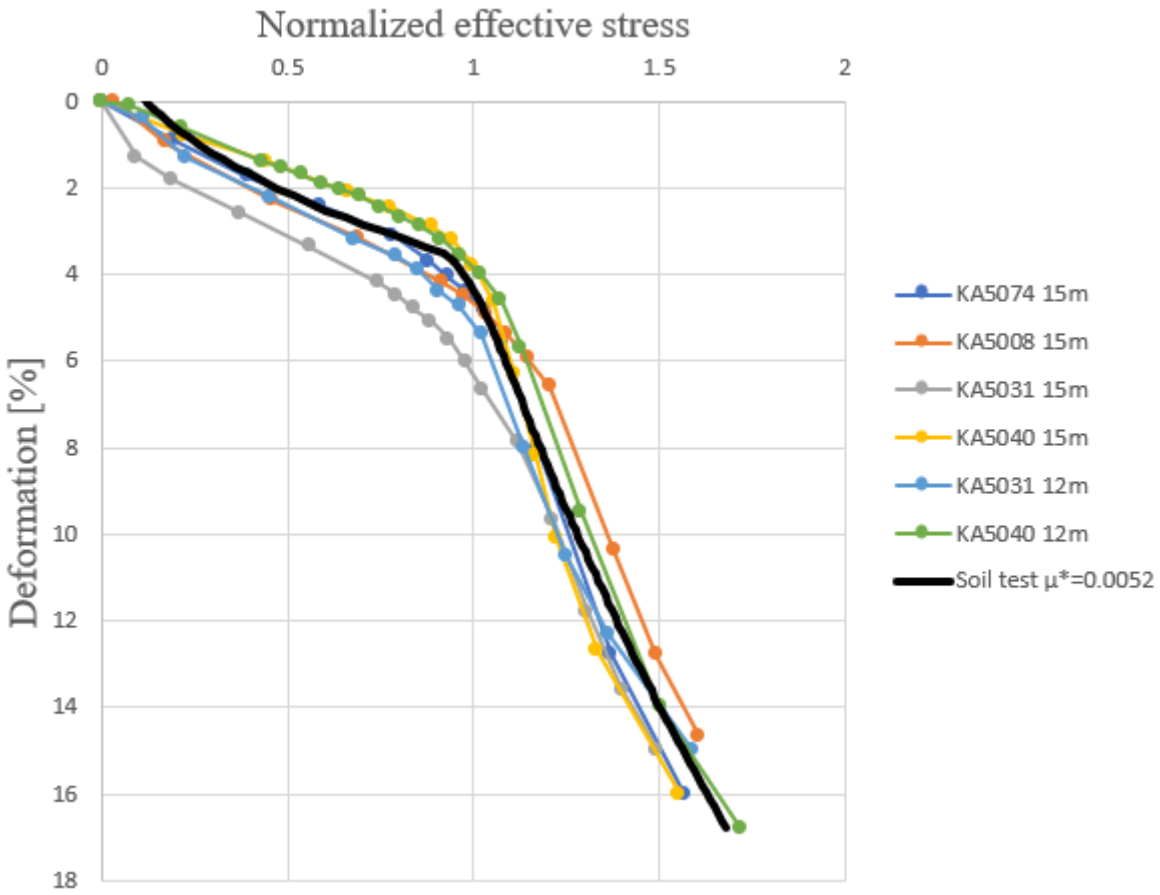

Figure A.10: Decision of μ for clay 2 with Plaxis soil test tool. The CRS-tests are normalized against σ'c.*

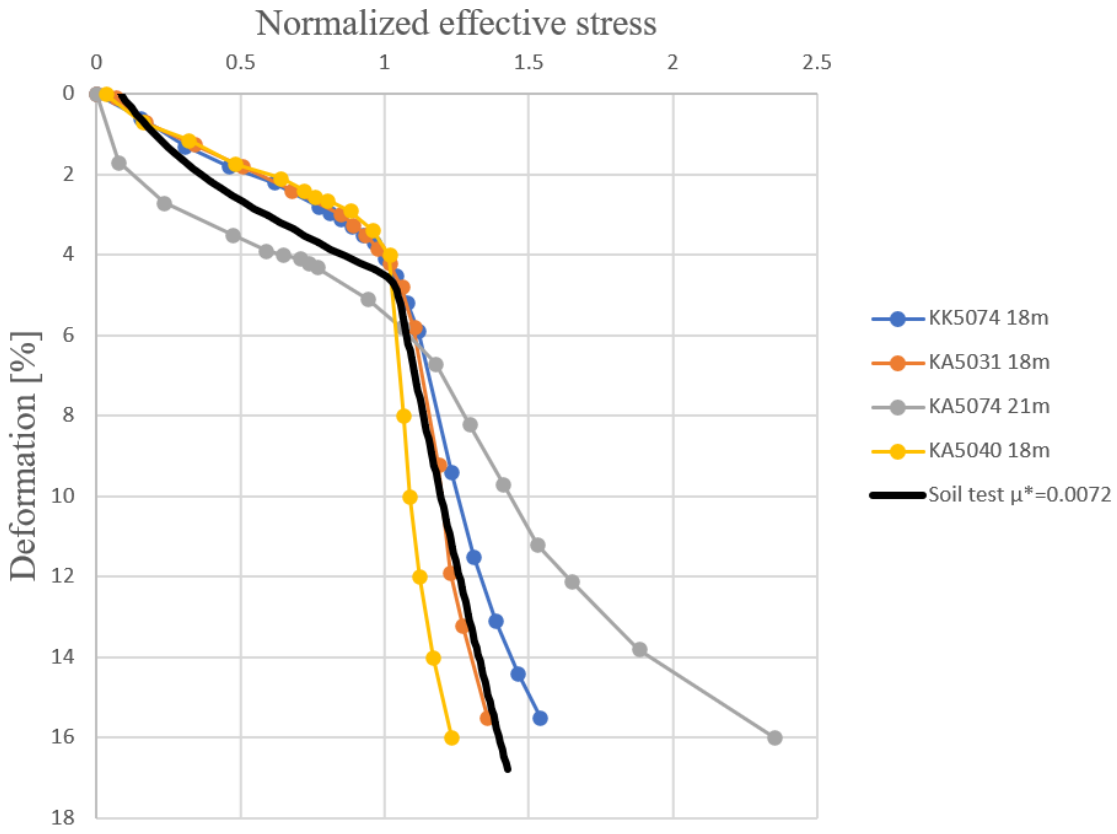

Figure A.11: Decision of μ for clay 3 and 4 with Plaxis soil test tool. The CRS-tests are normalized against σ'c.*

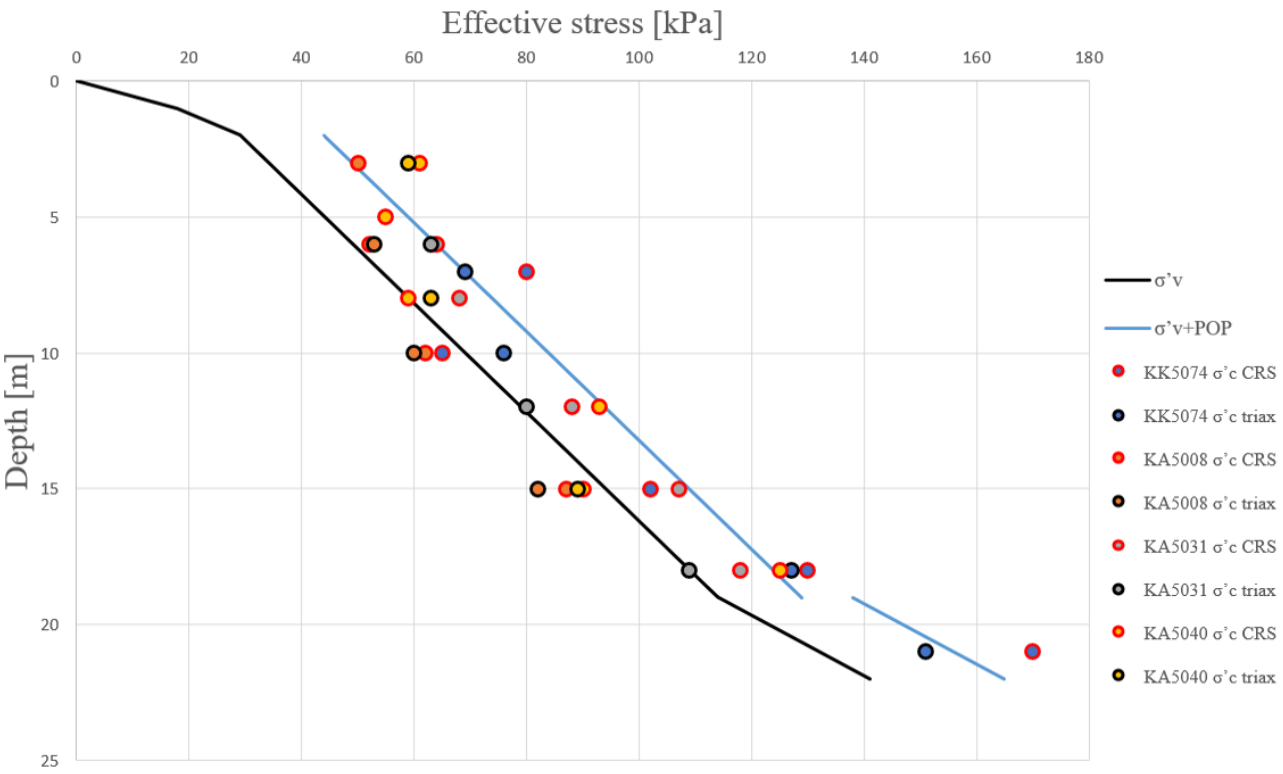

Figure A.12: Determination of the POP.

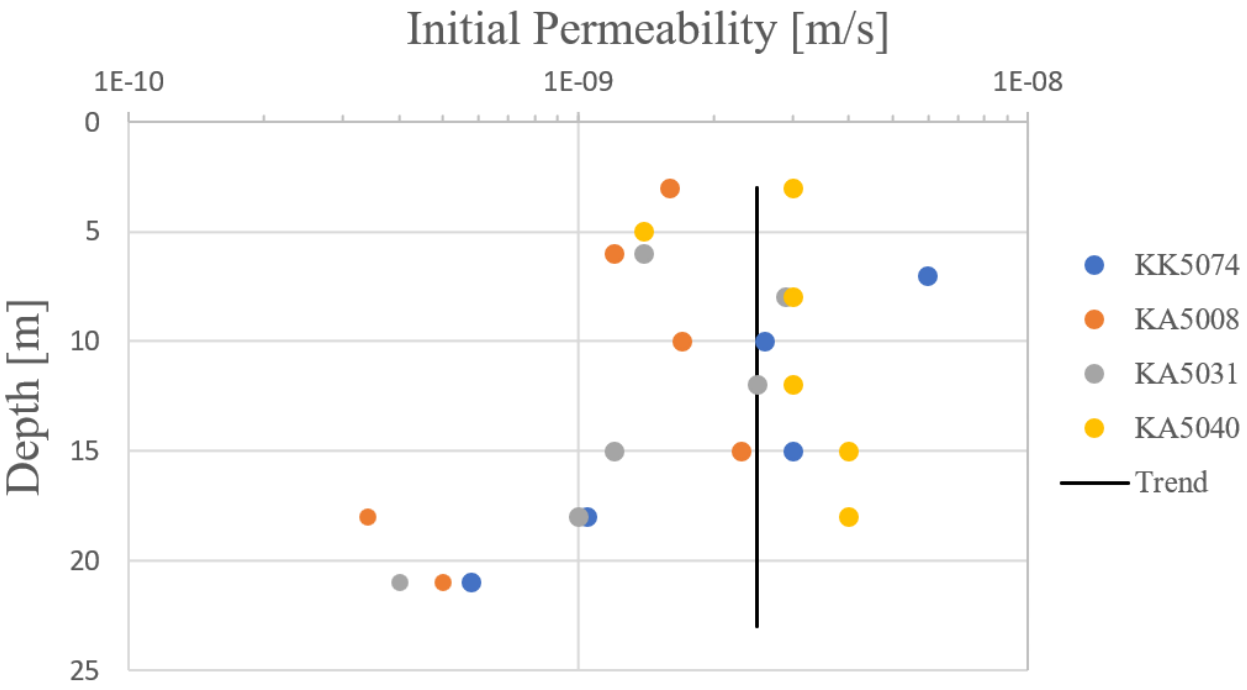

Figure A.13: Initial permeability of the clay.

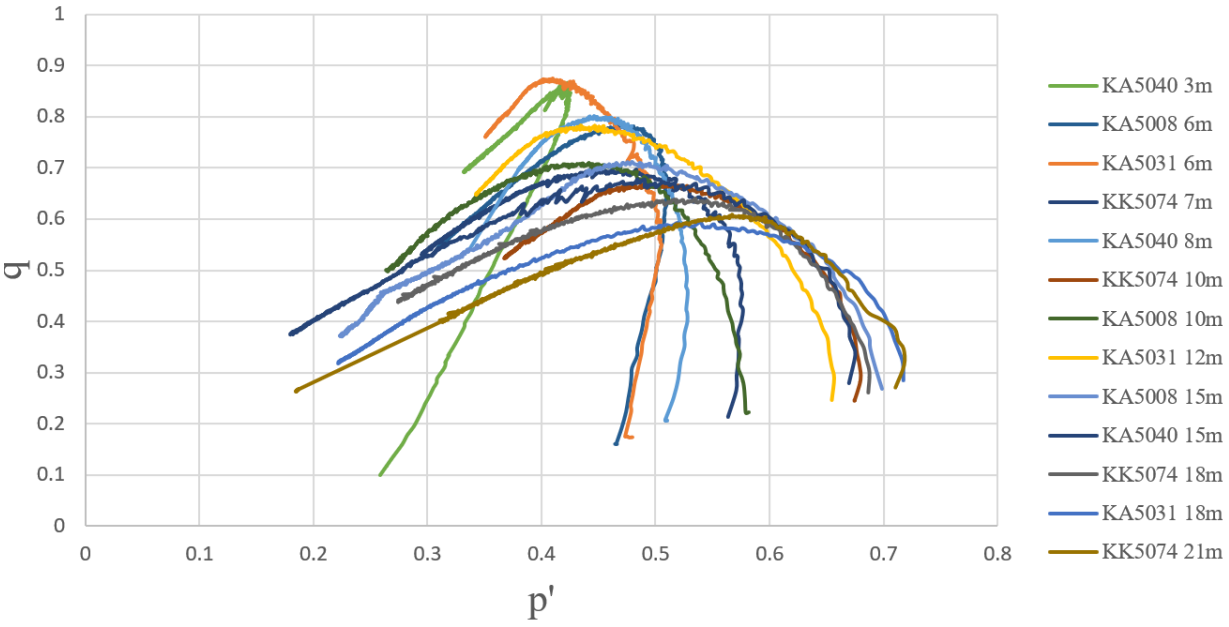

Figure A.14: Triaxial data normalized against σ'_c.

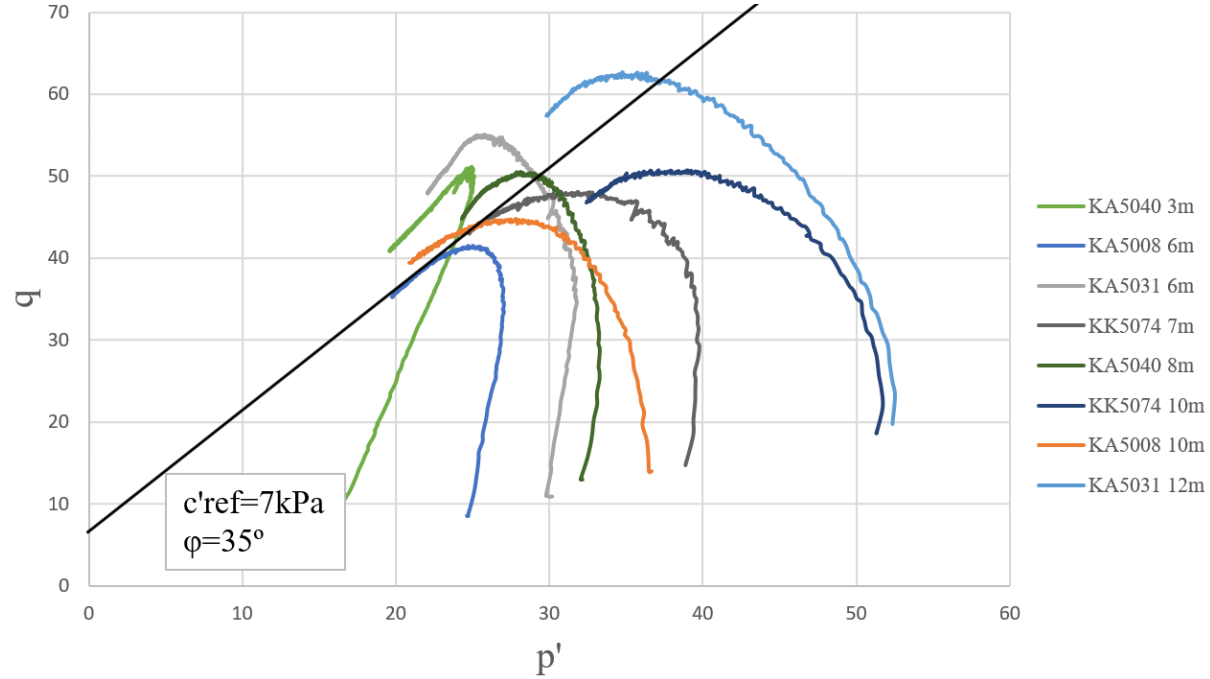

Figure A.15: Triaxial data with trendline for 3-12 m depth.

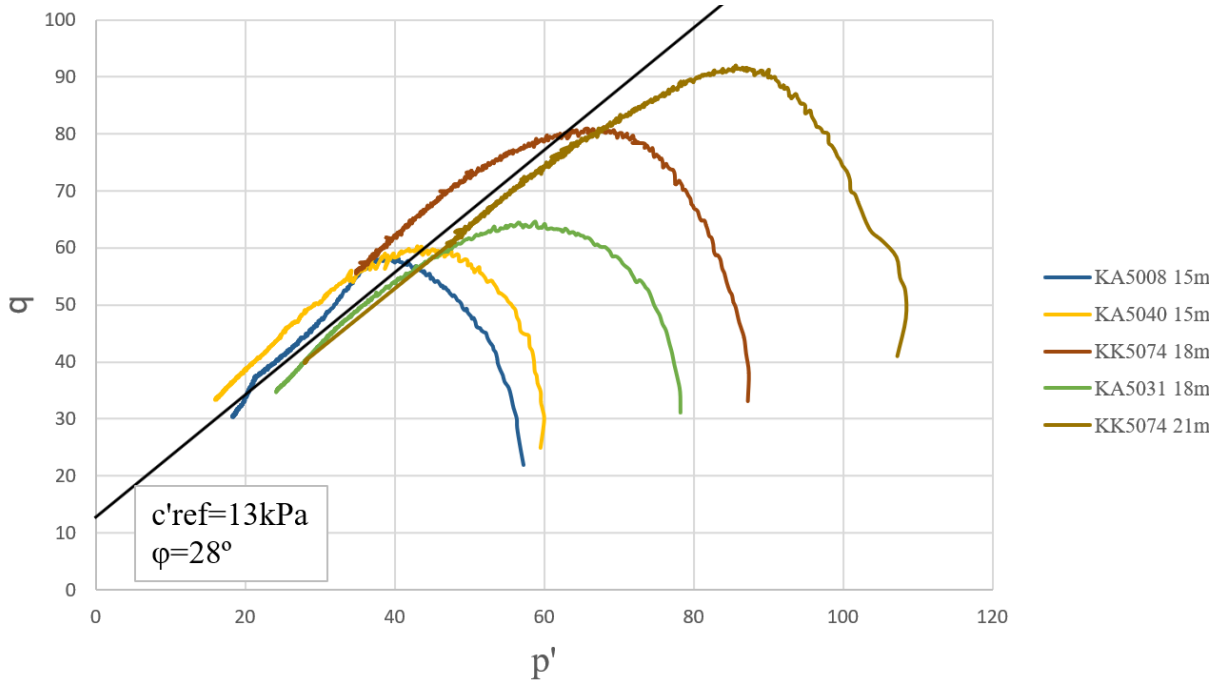

Figure A.16: Triaxial data with trendline for 15-21 m depth.

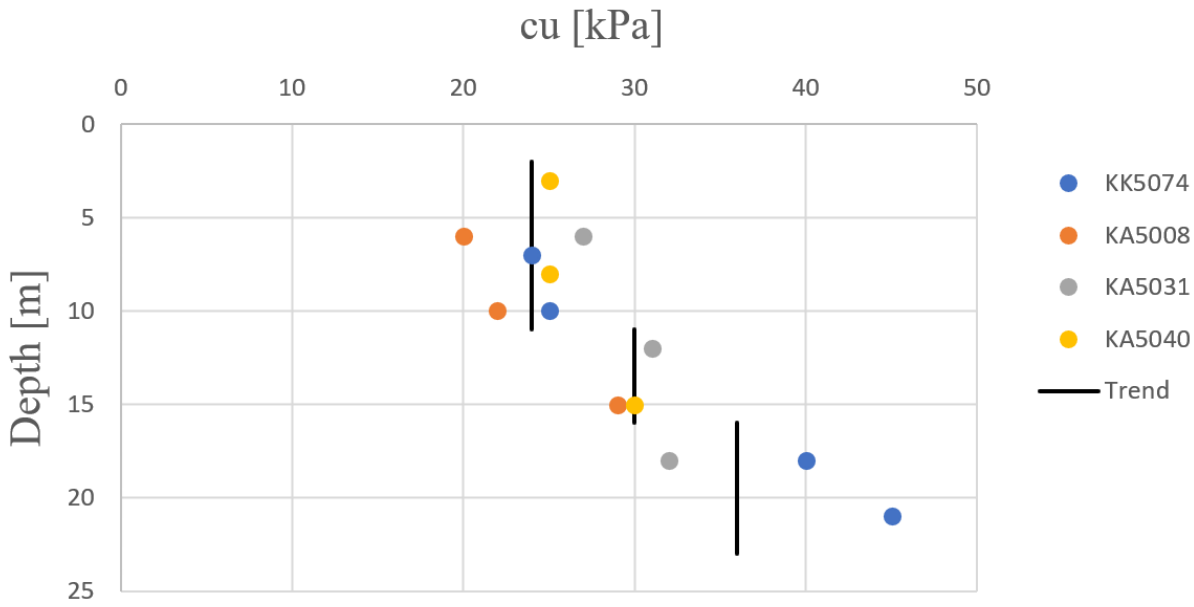

Figure A.17: Undrained shear strength from triaxial tests.

Appendix B: Results

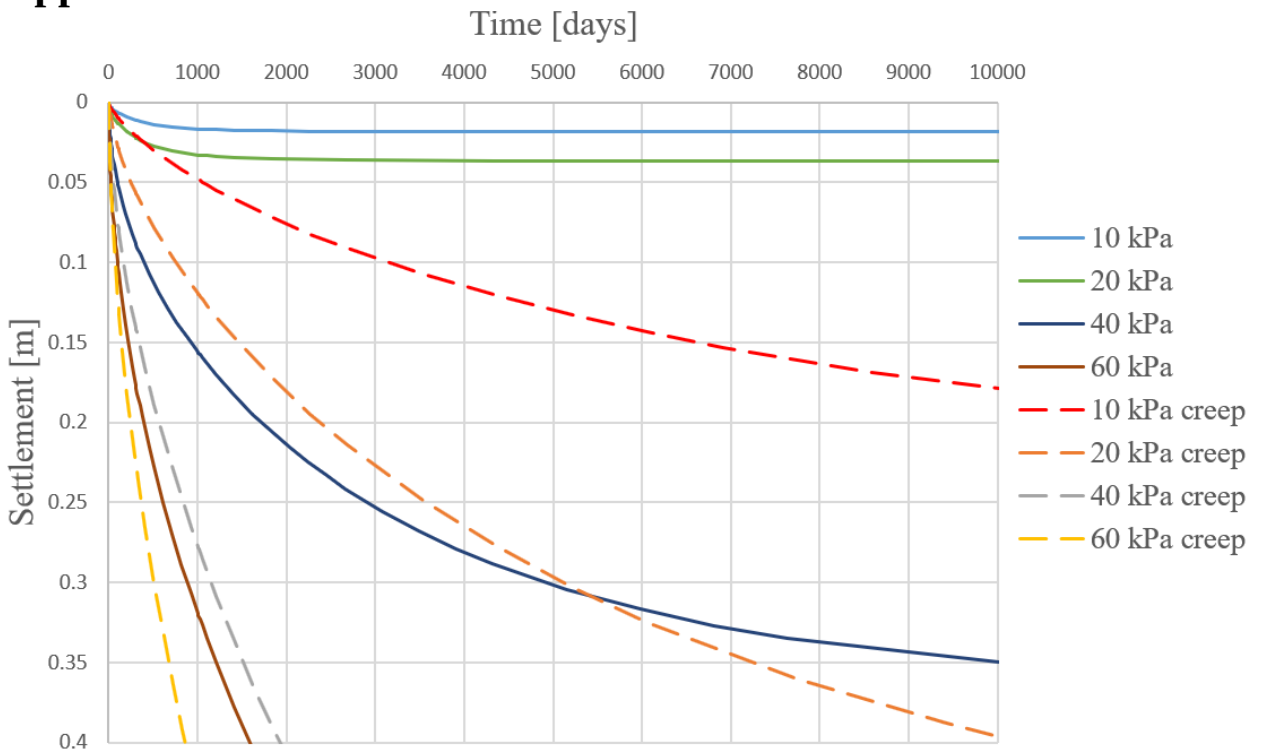

Figure B.1: Settlement development over 10 000 days for various pore pressure reductions. Zoomed in on the smaller settlements.

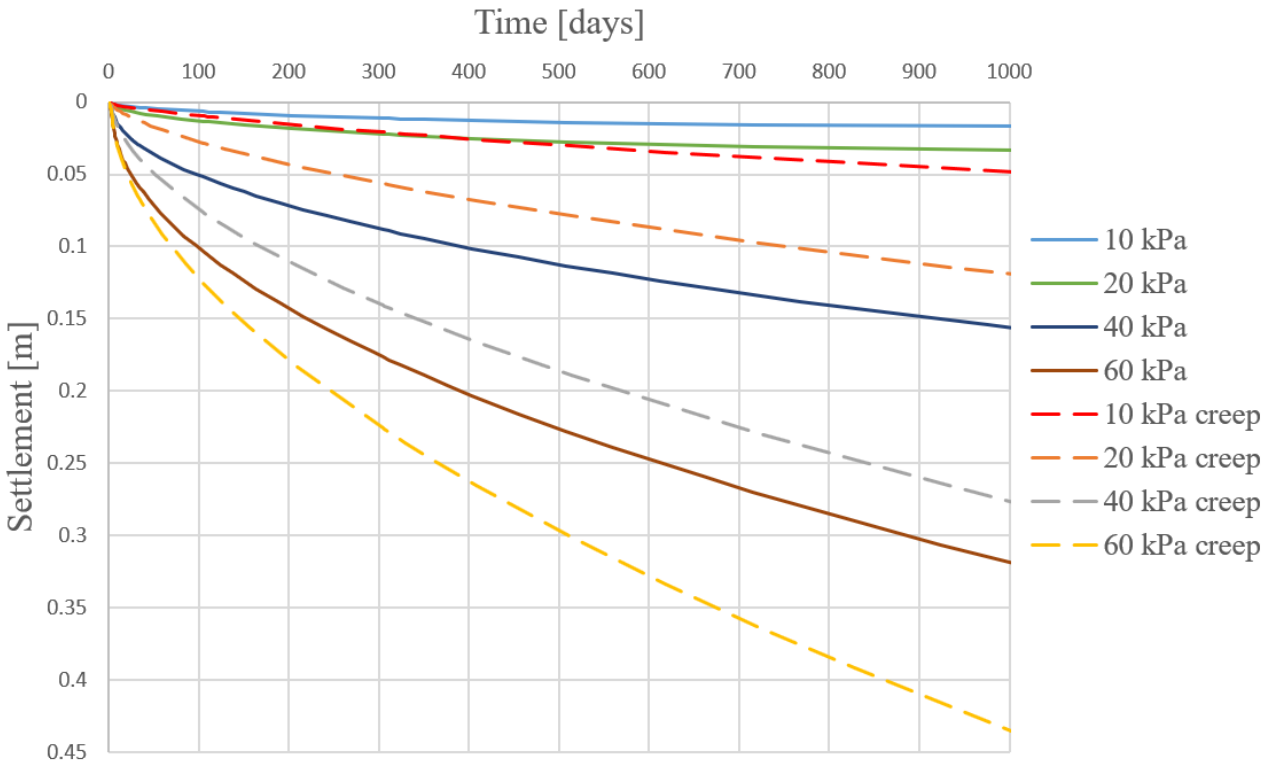

Figure B.2: Settlement development over 1000 days for various pore pressure reductions.

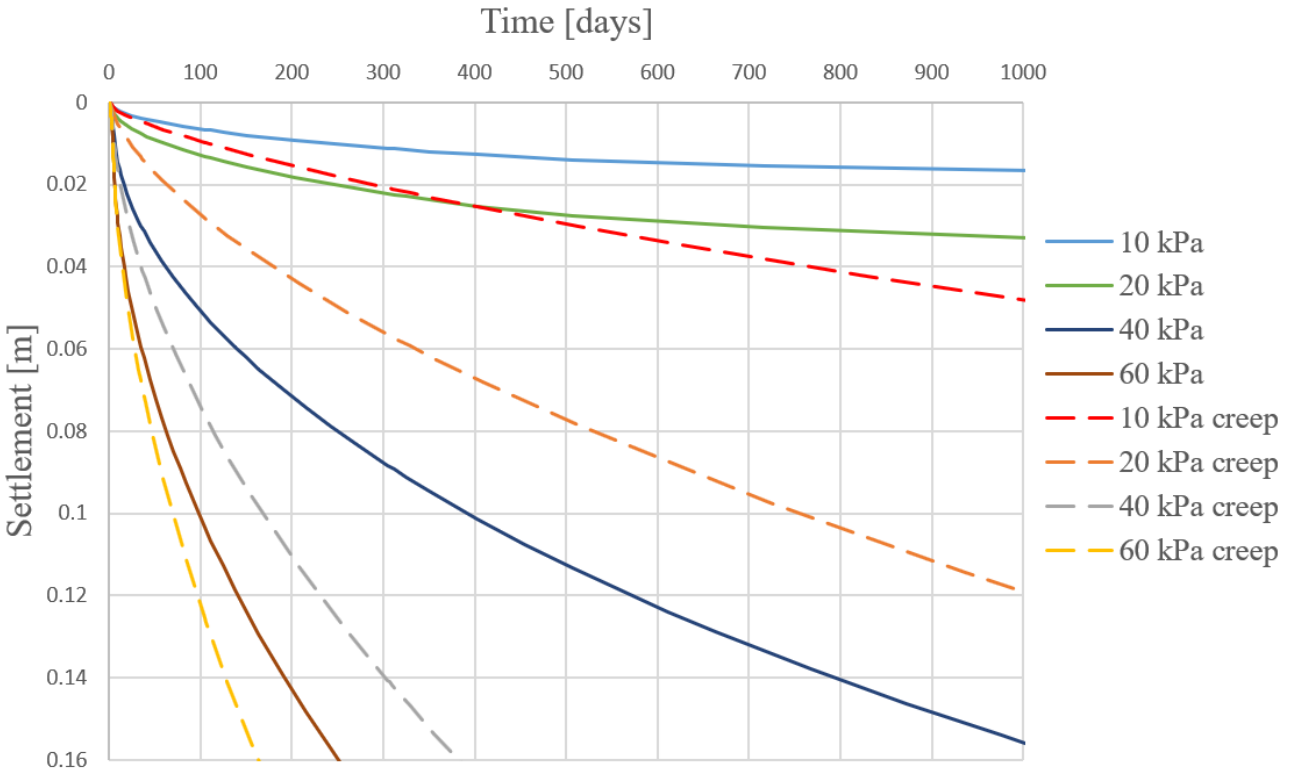

Figure B.3: Settlement development over 1000 days for various pore pressure reductions. Zoomed in on the smaller settlements.

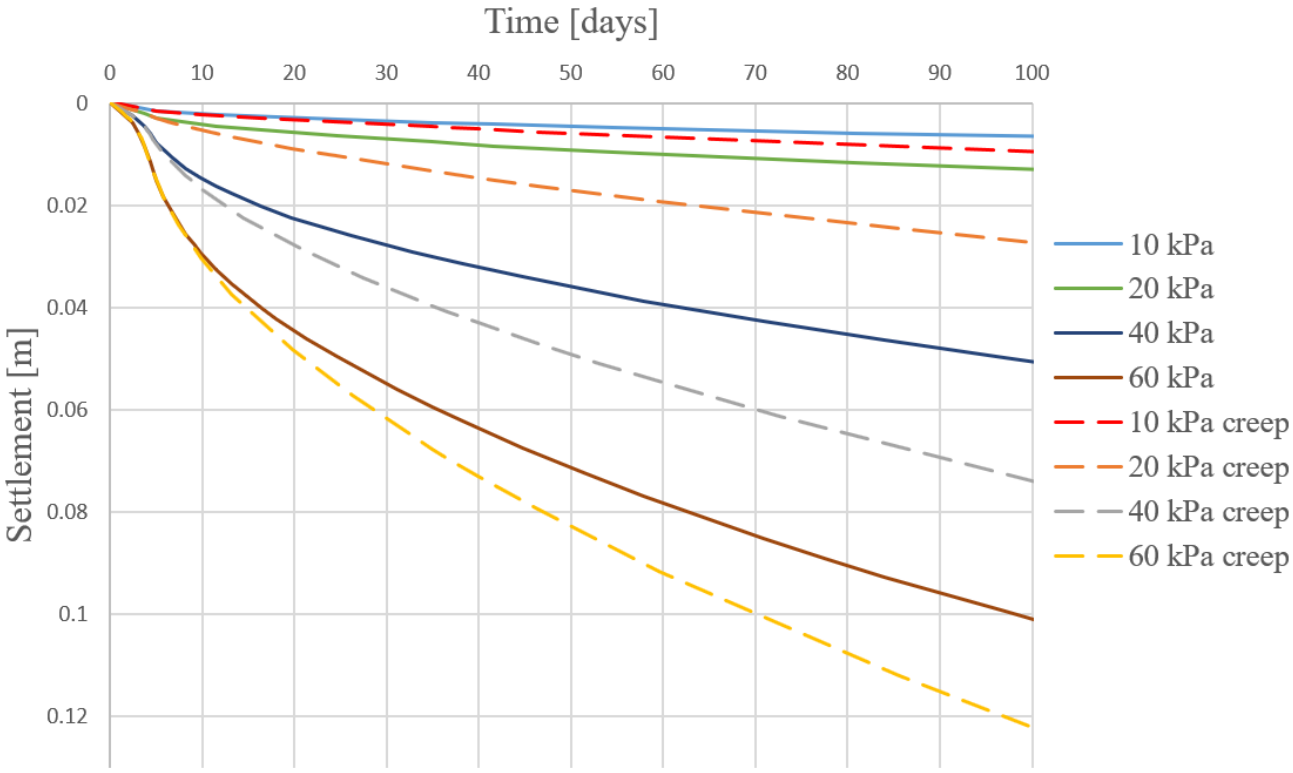

Figure B.4: Settlement development over 100 days for various pore pressure reductions.

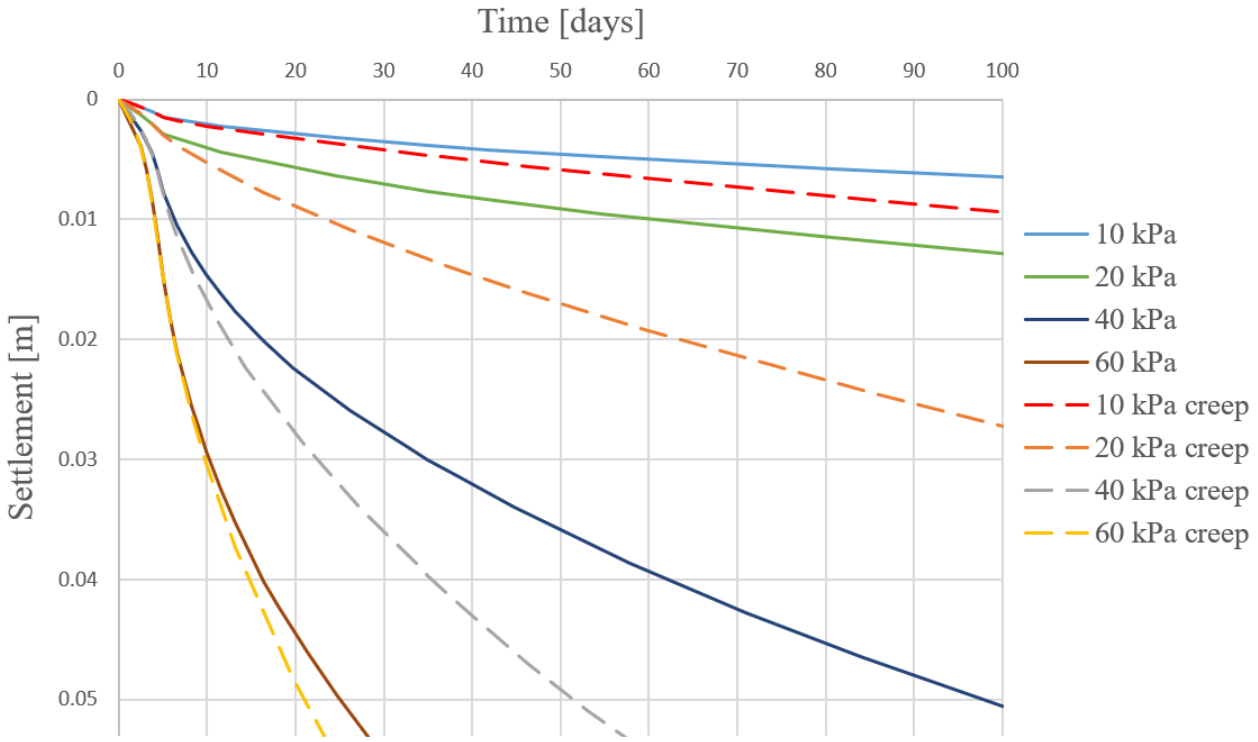

Figure B.5: Settlement development over 100 days for various pore pressure reductions. Zoomed in on the smaller settlements.

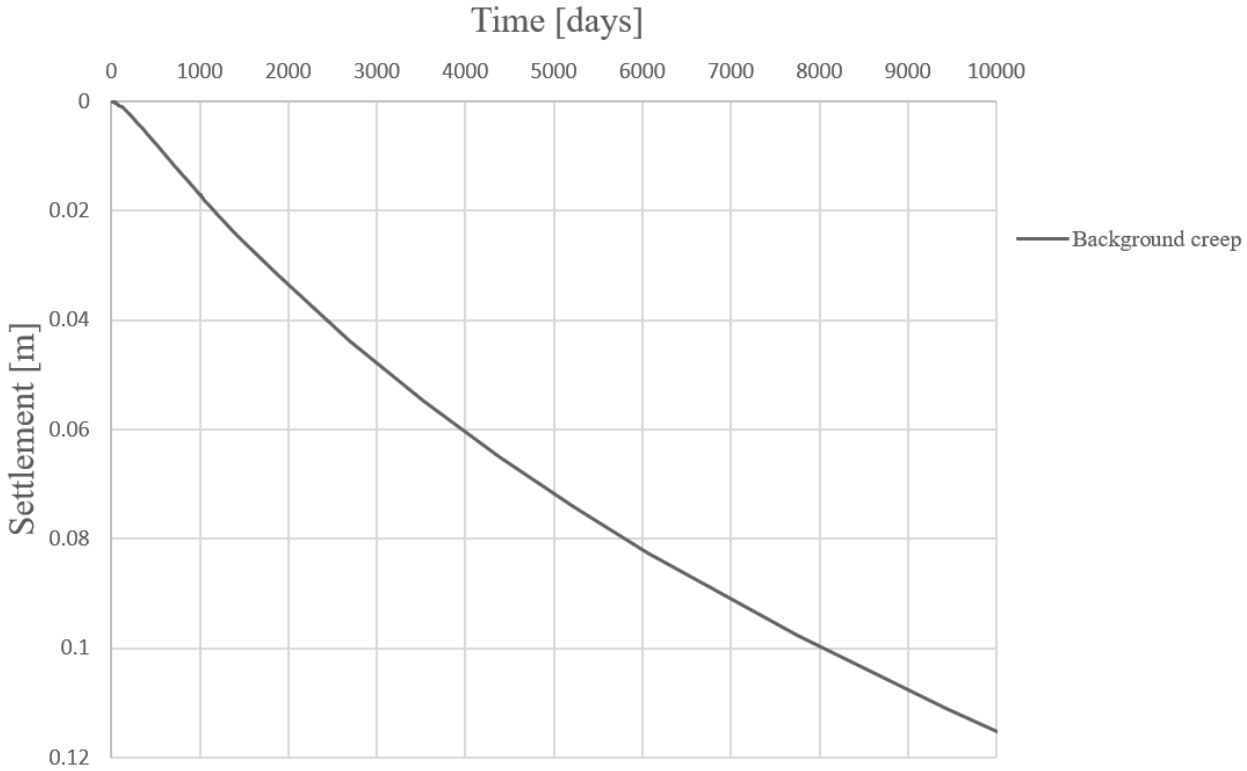

Figure B.6: Background creep over 10 000 days in the main analysis.

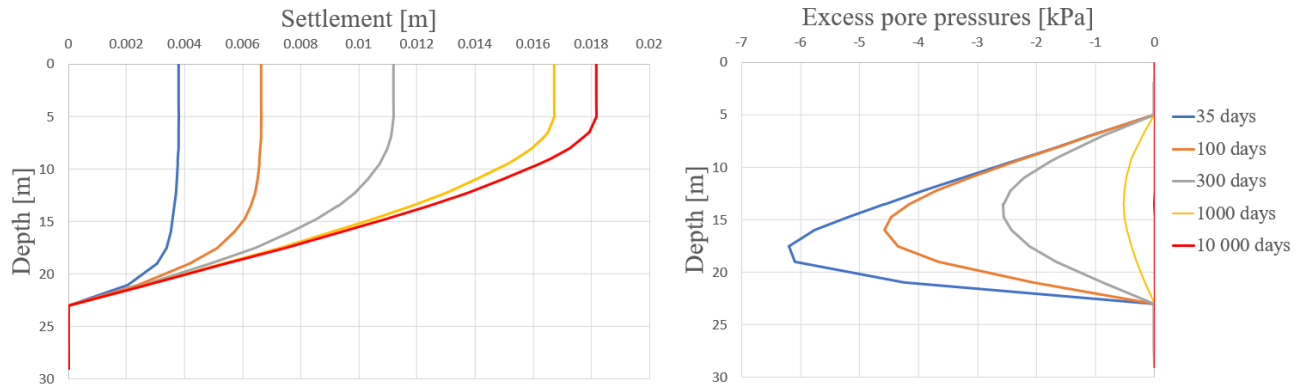

Figure B.7: Settlements and excess pore pressures for various times after a pore pressure reduction of 10 kPa without creep.

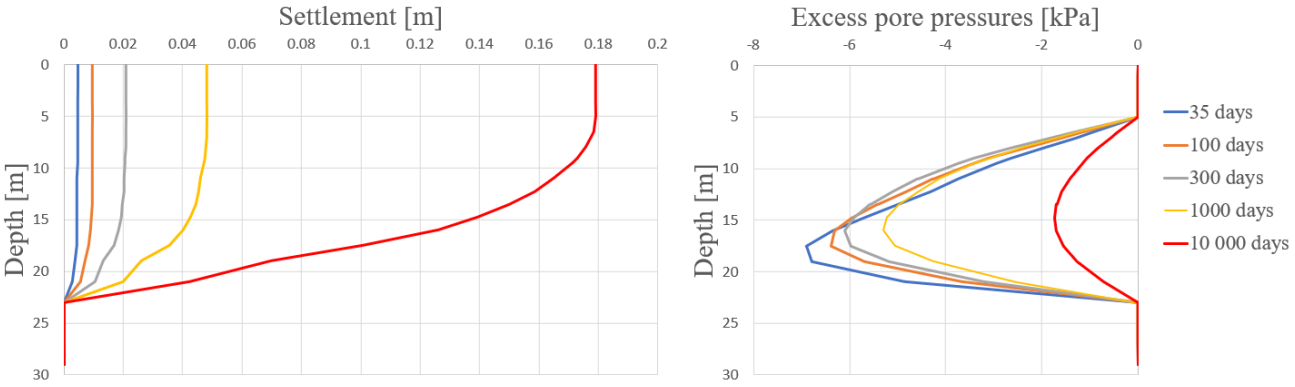

Figure B.8: Settlements and excess pore pressures for various times after a pore pressure reduction of 10 kPa with creep.

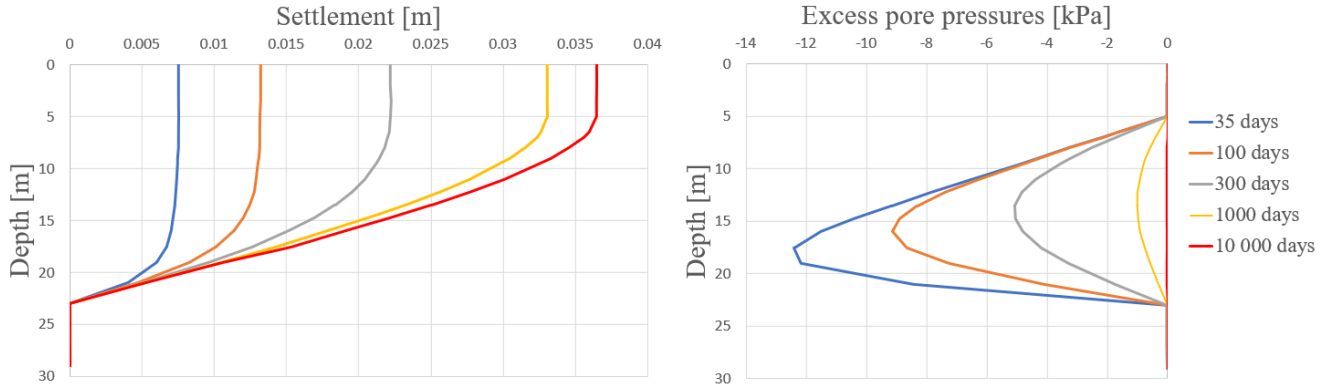

Figure B.9: Settlements and excess pore pressures for various times after a pore pressure reduction of 20 kPa without creep.

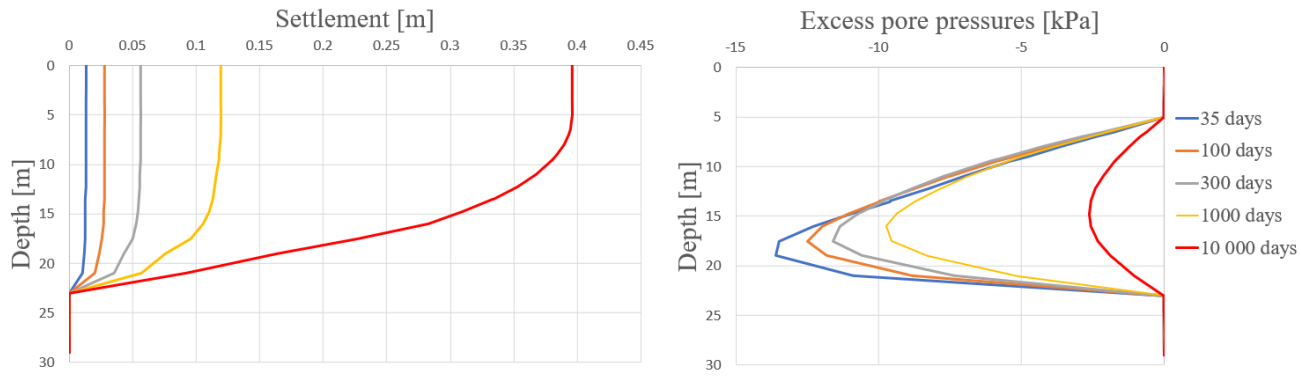

Figure B.10: Settlements and excess pore pressures for various times after a pore pressure reduction of 20 kPa with creep.

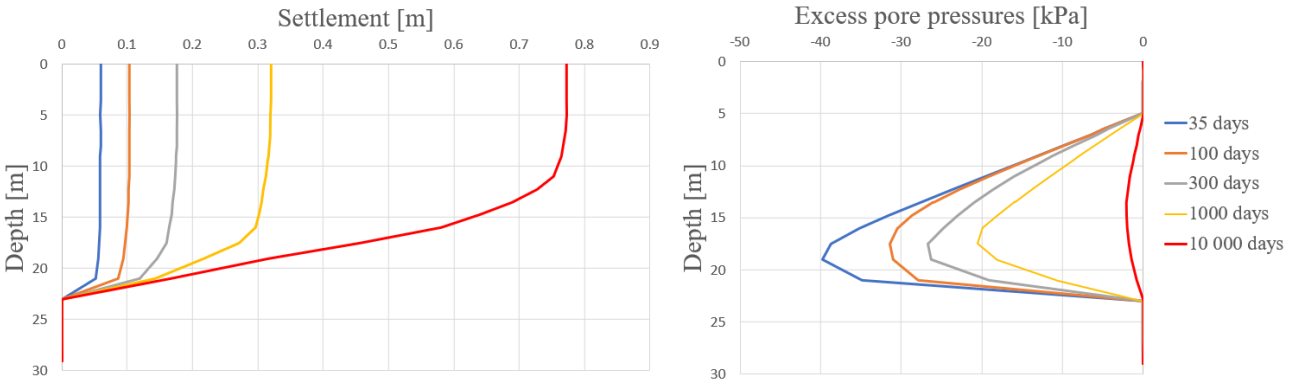

Figure B.11: Settlements and excess pore pressures for various times after a pore pressure reduction of 60 kPa without creep.

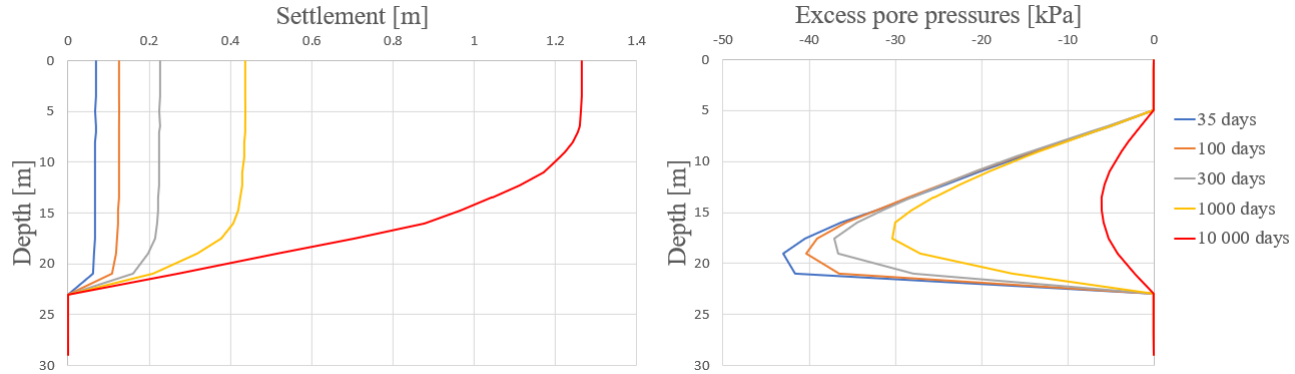

Figure B.12: Settlements and excess pore pressures for various times after a pore pressure reduction of 60 kPa with creep.

DEPARTMENT OF ARCHITECTURE AND
CIVIL ENGINEERING
DIVISION OF GEOLOGY AND GEOTECHNICS
CHALMERS UNIVERSITY OF TECHNOLOGY
Gothenburg, Sweden 2021
www.chalmers.se

CHALMERS
UNIVERSITY OF TECHNOLOGY